IMPROVING THE CURRENT DIAGNOSTIC STRATEGY FOR *BEAK AND FEATHER DISEASE VIRUS* IN PARROTS

Yuri Munsamy

January 2014

University of the Free State

Improving the current diagnostic strategy for *Beak and feather disease virus* in parrots

Yuri Munsamy

B.Sc. Hons (UFS)

Submitted in fulfilment with the requirements for the degree

MAGISTER SCIENTIAE

In the Faculty of Natural and Agricultural Sciences

Department of Microbial, Biochemical and Food Biotechnology

University of the Free State

Bloemfontein

South Africa

2014

Supervisor: Prof. R.R. Bragg

Co-supervisor: Dr. C.E. Boucher

DECLARATION

I declare that the dissertation hereby submitted for the qualification *Magister Scientiae* (Microbiology) at the University of the Free State is my own independent work and has not been previously submitted by me for a qualification at/in another University/faculty.

Furthermore, I concede copyright to the University of the Free State.

_____

Yuri Munsamy

ACKNOWLEDGEMENTS

- **The National Research Foundation (NRF)**: The financial assistance of the National Research Foundation (NRF) towards this research is hereby acknowledged. Opinions expressed and conclusions arrived at, are those of the author and are not necessarily to be attributed to the NRF.
- **Prof R.R. Bragg:** For giving me the independence to explore this project.
- **Dr C.E. Boucher**: For help with troubleshooting and constructive criticism.
- **Dr A.C. Hitzeroth**: For DNA extraction of some of the samples used in Chapter 3.
- **Dr J.F. Strydom, Dr M.J. du Plooy and the UFS101 Team**: For their support and encouragement.
- **Gips Seisho**: For help with navigating SPSS 21.0.
- **Jay Lee**: For all the lessons, that extended far beyond the lab.
- **Marisa Coetzee**: For the wake up calls at ungodly hours, pomodoro typing sessions and provision of a quiet typing haven!
- **My Family**: For instilling in me the importance of education and their unwavering support**.**

To all of you, thank you.

TABLE OF CONTENTS

LIST OF NON-SI ABBREVIATIONS

Abbreviation	Definition
Amp	Ampicillin
ATP	Adenosine triphosphate
BFD	Beak and feather disease
BFDV	*Beak and feather disease virus*
bp	Base pairs
BSA	Bovine serum albumin
DNA	Deoxyribonucleic acid
dNTP	Deoxynucleotidetriphosphate
ds	Double stranded
EDTA	Ethylenediaminetetra acetic acid
E. coli	*Escherichia coli*
HCl	Hydrogen chloride
HI	Haemagglutination inhibition
HRPO	Horse radish peroxidase
IPTG	Isopropyl β-D-^{1}-thiogalactopyranoside
Kan	Kanamycin
LB	Luria Bertani
MCS	Multiple cloning site
$MgCl_2$	Magnesium chloride
NaCl	Sodium chloride
N-terminus	Amino terminus

OD	Optical density
ORF	Open reading frame
ORF C1	Open reading frame C1 that codes for *BFDV* capsid (coat) protein
ORF V1	Open reading frame V1 that codes for *BFDV* replication-associated protein
PAGE	Polyacrylamide gel electrophoresis
PBS	Phosphate buffered saline
PCR	Polymerase chain reaction
RCR	Rolling circle replication
Rep	Replication-associated protein
SDS	Sodium dodecyl sulphate
Taq	*Thermus aquaticus* DNA polymerase
TAE	Tris acetate EDTA

INDICES

Index of Figures

Index of Tables

Index of Equations

CHAPTER 1 A REVIEW OF LITERATURE ON *BEAK AND FEATHER DISEASE VIRUS*

1.1 Introduction

Beak and feather disease (BFD), caused by *Beak and feather disease virus* (*BFDV*) was first described in 1975 in Australian cockatoos (Pass & Perry, 1984). It has since spread globally due to the bird trade (Ritchie & Carter, 1995). BFD has been recognised as the most significant infectious disease afflicting parrot species, although there is limited information available on infection rates and mortality for wild populations (McOrist *et al*., 1984; Pass & Perry, 1984). South African bird breeders suffer severe losses, approximating R24 million per annum (Heath *et al*., 2004; Rybicki *et al.*, 2005) as 10 to 20% of South African psittacine breeding-stocks succumb to the disease. Furthermore, *BFDV* threatens the survival of the endangered Cape parrot (*Poicephalus robustus*) and the vulnerable black-cheeked lovebird (*Agapornis nigrigenis*) (Heath *et al.*, 2004) [Figure 1.1].

A **B**

Figure 1.1. (A) Endangered Cape parrot (Boyes, 2013) and (B) Vulnerable black-cheeked lovebird (Tree of Life, 2008).

1.2 The *Circoviridae*

The causal agent of BFD is a member of the family *Circoviridae,* genus *Circovirus*. The only other formally recognised members belonging to the same genus *Circovirus* are *Porcine circovirus* type 1 (*PCV1*) and *Porcine circovirus* type 2 (*PCV2*) (Lukert *et al*.,1995), with

phylogenetic analysis of *PCV1* revealing it to be the closest relative to *Beak and feather disease virus* (Niagro *et al*., 1998). The plant virus families *Nanoviridae* and *Geminiviridae* are considered the closest relatives to the *Circoviridae*. It is proposed that a predecessor to *PCV1* and *BFDV* may have originated from a plant nanovirus that infected a vertebrate host and then recombined with a vertebrate-infecting RNA virus, presumably a calicivirus (Gibbs & Weiller, 1999).

1.3 *Beak and feather disease virus* characteristics

Virions of *BFDV* are icosahedral, non-enveloped and are between 14 to 16 nm in size (Figure 1.2). Circoviruses can be characterised by their small, single-stranded circular DNA. The capsid or coat protein, displays T=1 organisation comprising 60 subunits, arranged in 12 pentamer clustered units (Crowther *et al*., 2003).

There are three major structural proteins associated with the virus, having approximate molecular weights of 26.3, 23.7 and 15.9 kDa, respectively (Ritchie *et al*., 1989a). Morphologically and antigenically similar isolates comprise similar major viral proteins. *BFDV* is not able to grow *in vitro*, either due to its high *in vivo* tissue specificity or its specific growth requirements (Ritchie *et al*., 1989a).

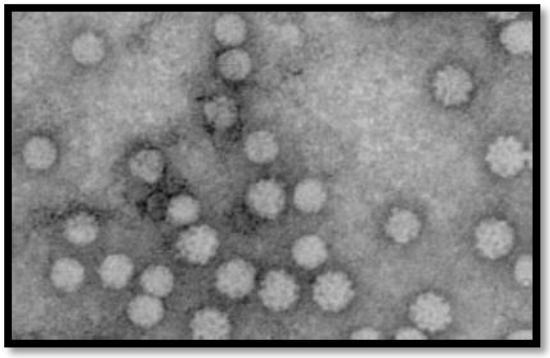

Figure 1.2. Electron micrograph of a negatively stained mixture of *Beak and feather disease virus* and *Chicken anaemia virus* particles. The larger, rough particles are *Chicken anaemia virus* and the smaller, smoother particles are *Beak and feather disease virus* (Crowther *et al*., 2003).

1.4 Genome organisation and viral proteins

BFDV contains a circular, single-stranded ambisense DNA genome with a characteristic stem loop structure similar to that of the geminiviruses, as can be seen in Figure 1.3 (Bassami *et al.*, 1998; Niagro *et al.*, 1998). Seven open reading frames (ORFs) are present,

with three ORFs situated on the virus sense strand (V1 to V3) and four ORFs located on the complementary-sense (C1 to C4) strand. The two major open reading frames, ORF V1 and ORF C1, are in opposing orientations and encode the putative replication-associated (Rep) and capsid proteins (CP), respectively, as illustrated by Figure 1.4 (Todd *et al*., 2001).

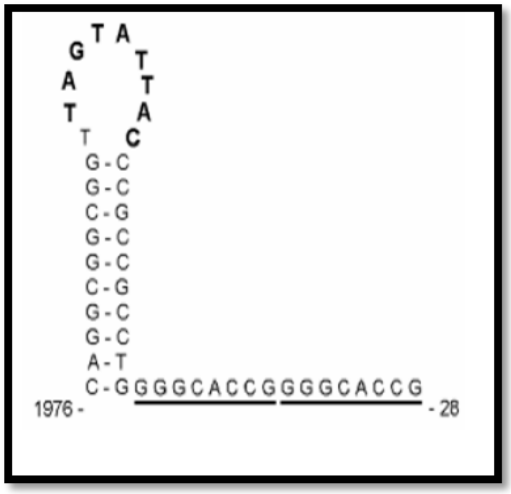

Figure 1.3. Stem-loop structure depicting the position of the conserved nonanucleotide motif (TAGTATTAC). (Bassami *et al*., 1998).

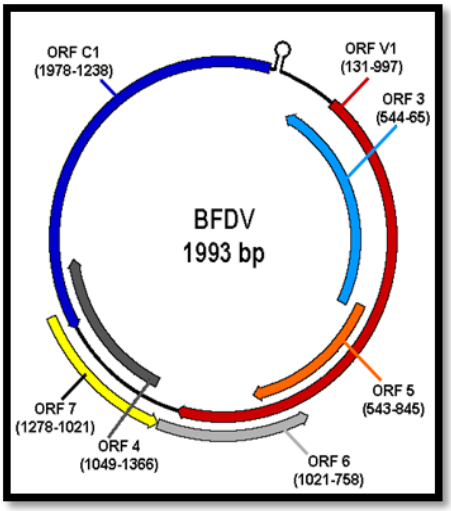

Figure 1.4. Schematic representation of the circular ss-DNA genome of *BFDV* and the seven ORFs (Modified from Bassami *et al*., 1998).

The function of the transcriptional product of the other ORFs is unknown. The gene products, Rep and CP, perform the most elementary functions of a virus, including copying and packaging of the viral genome. Aside from being the major structural component of the

viral particle, CP is also the main antigenic determinant of *BFDV* and is therefore a target of the immune system (Rybicki *et al*., 2005; Stewart *et al*., 2007).

Similar to other circoviruses, *BFDV* CP contains an arginine-rich basic N-terminus responsible for nuclear localisation (Niagro *et al*., 1998; Johne *et al*., 2004; Heath *et al*., 2006). The N-terminal residues are also responsible for binding viral DNA after entry into the cell, providing evidence that the *BFDV* CP likely functions to target the viral genome to the nucleus for replication (Heath *et al*., 2006; Patterson *et al*., 2012).

The intergenic region (IR) between the 5' ends of the two major ORFs contains a stem-loop structure (depicted in Figures 1.3 and 1.4) is located between nucleotide (nt) positions 1976-1993, flanked by the ORFs for C1 and V1 in the replicative form. The apex of the stem-loop contains a highly conserved nonanucleotide motif (TAGTATTAC). An octanucleotide repeat sequence (GGGCACCG) is located immediately downstream of the stem-loop structure (Bassami *et al*., 1998). Two potential TATA boxes were detected in the virion strand; the first (TATA) is positioned at nt 86-89, whilst the second (TATAAAA) is located at nt 680-686. Two polyadenylation signals are at nt 1019–1024 (CATAAA) and 1196-1201 (AATAAA) of the virion strand respectively, downstream of the stop codon for ORF1. The complementary strand also features a polyadenylation signal at nt 758–763 (AATAAA), located 1 nt downstream of the stop codon for ORF2 (Bassami *et al.*, 1998). The function of these TATA boxes remains unknown.

1.5 *BFDV* replication

BFDV, a model of efficiency, possesses a small genome with limited protein encoding capacities and is heavily dependent on the host-cell DNA replication machinery (Todd, 2000). It is thought to replicate in rapidly dividing tissues, with evidence suggesting that the liver is an important site of replication (Todd, 2000; Raidal *et al*., 1993a). Circular ss-DNA viruses replicate using rolling circle replication (RCR) (Niagro *et al*., 1998). RCR is thought to be initiated at the nonanucleotide motif (Ritchie *et al*., 2003) [Figure 1.3], as a loss in replicational function is observed when there are mutations of the first two nucleotides (Todd *et al*., 2001). The two octanucleotides (GGGGCACC) located downstream of the stemloop are thought to be the binding sites for circovirus replication associated proteins (Niagro *et al*., 1998) [Figure 1.3]. Conservation of both the amino acid sequence and the structural location demonstrates not only the significance of these motifs for RCR, but also most likely for the survival of these viruses. Additionally, the similarities in the positions of the RCR motifs support the hypothesis that *BFDV* evolved from a nanovirus.

Heath and co-workers (2006) deduced that *BFDV* CP transports the viral genome across the nuclear envelope before replication can occur. Once inside the nucleus of the host cell, the ssDNA genome serves as the template for the formation of a complementary strand of DNA, making a double-stranded DNA (dsDNA) intermediate, known as the replicative form (RF). The dsDNA RF forms the template for production of mRNA, with ORFs potentially on both the original virion strand (V) and also on the complementary strand (C) of the replicative intermediate (Biagini *et al.*, 2012; Ilyina & Koonin, 1992; Mankertz *et al.*, 1997; Mankertz *et al.*, 2004).

1.6 Genetic diversity

BFDV has a wide host range and varies in its clinical and pathological appearance. These differences were previously attributed to host factors; such as the presence or absence of cell surface receptors for virus attachment or major histocompatibility complex (MHC) presentation (Shearer, 2008), rather than antigenic or genetic variation of *BFDV* (Ritchie *et al.*, 1990). However, recent studies on the *rep* and capsid genes indicate a higher level of genetic diversity than what was initially suggested (Bassami *et al*., 2001). Although the deduced amino acid sequence of the CP of various isolates may differ by as much as 27% (Bassami *et al*., 2001); they appear to be antigenically similar in haemagglutination (HA) and haemagglutination inhibition (HI) tests (Ritchie *et al*., 1990). It is possible that certain genotypes may develop host specificity or strains may develop differences based on the geographical location from which they originate (Bassami *et al.*, 2001). Numerous observations confirm that different strains of *BFDV* may infect diverse bird species with varying clinical presentation or leave the bird asymptomatic, in a species- or subfamily-specific manner (de Kloet & de Kloet, 2004).

Southern African isolates exhibit a similar level of genetic diversity to that of Australian and New Zealand isolates and can be separated into eight lineages (Heath *et al*., 2004). These isolates cluster into three unique genotypes, having diverged from viruses found in various parts of the world (Heath *et al*., 2004). The level of divergence between African genotypes compared to that of isolates found globally concludes that the occurrence of *BFDV* in Africa is not due to a recent introduction.

The possibility exists that genetic diversity may arise through recombination events (Ritchie *et al*., 1989b; Heath *et al*., 2004). Simultaneous infection with different but related strains of *BFDV* has been observed in an African grey parrot (*Psittacus erithacus*) [de Kloet & de Kloet, 2004]. As the rate at which circoviruses evolve is unknown, it is unclear

as to whether birds may suffer from infection with multiple strains of *BFDV* or if different strains occur as a result of a mutation, resulting in non-pathogenic strains acquiring pathogenicity (de Kloet & de Kloet, 2004). However, the rate of occurrence for a mixed infection is probably fairly high as it is a prerequisite for recombination; even though evidence supporting this theory is limited (Heath *et al*., 2004).

1.7 Clinical presentation and pathology of BFD

Birds of varying age groups are considered susceptible to infection by *BFDV*, although juveniles, aged between hatching and three years, are thought to be more susceptible to acute BFD. This is due to host conditions rather than antigenic or genotypic traits of *BFDV* (Ritchie *et al.*, 2003). Older birds may overcome the infection to become carriers of the virus; and maternal antibodies have been shown to provide immunity to offspring (Ritchie *et al*., 1992).

This dermatological condition is irreversible, lasting between several months to several years (Pass & Perry, 1984; Jacobson *et al*., 1986). As *BFDV* is dependent on the hosts' machinery for replication, it is predominantly found in rapidly dividing cells (Todd, 2000) such as those of the epithelium (Latimer *et al*., 1991a). Consequently, the skin, feathers, beak, oesophagus and crop, as well as organs of the immune system such as thymus, cloaca, bursa of Fabricius and bone marrow are affected (Latimer *et al*., 1991a; b). Viral DNA has been detected mainly in the heart, intestine and liver, and less frequently in the testes, cloaca, upper respiratory and digestive tract (Rahaus *et al*., 2008). *BFDV* presents itself in the peracute, acute and chronic forms (Ritchie *et al*., 1989b; Schoemaker *et al*., 2000) with a characteristic feature of the disease in all species being abnormal feather development. Active follicles are targeted by *BFDV*; therefore a lack of powder down strongly suggests that the bird is currently infected with *BFDV*. The developing feathers will have a host of deformities including shortening, retention of a thick outer sheath, constrictions of the shaft and stress lines in the vane (Pass & Perry, 1984; Jergens *et al*., 1988).

Symptoms are most often associated with the feathers rather than with the beak (Ritchie *et al*., 1989b). Although species such as Sulphur-crested cockatoos (*Cacatua galerita*), Galahs (*Eolophus roseicapillus*), Little Corellas (*Cacatua sanguinea)* and Moluccan cockatoos (*Cacatua moluccensis*) are more susceptible to beak changes (Ritchie *et al*., 1989b) (See Figure 1.5 A; B).

The correlation between DNA sequence of *BFDV* strain and its ability to cause disease is unknown, as asymptomatic infections also occur (Rahaus & Wolff, 2003). Even though different genotypes exist, absolute specificity is not seen and the relationship between *BFDV*

strains, host species and pathogenicity is yet to be fully understood (de Kloet & de Kloet, 2004).

A **B**

Figure 1.5. (A) A Galah chronically infected with *BFDV* displaying gross clinical signs of beak fracture and (B) Two Sulphur-crested cockatoos chronically infected with *BFDV* displaying gross clinical signs of feather loss (Raidal *et al*., 2004).

1.7.1 Pathogenesis of BFD

The maximum incubation period in birds that are subclinically infected is still undetermined, but it is suspected to be years (Greenacre *et al*., 1992). The incubation period and the clinical signs vary depending on the age at which infection occurs, the stage of feather development at the time of infection, titre of the infecting virus, route of inoculation, virulence of the particular *BFDV* strain, the degree of immunocompetence of the host, and other genetic, physiologic, metabolic and / or environmental factors that alter host resistance to infection (Ritchie *et al*., 1989b; Latimer *et al*., 1991a).

Generally, neonates are considered more susceptible to infection than birds over 3 years old. However, older birds may develop infection following a heavy challenge (Jones, 2006). Latent carriers may also become clinical under conditions of stress. The incubation period between infection and development of disease in young birds with an undeveloped immune system may be as short as 14-28 days, with severe illness ensuing (Jones, 2006). In an experimental study, chicks that were inoculated with viral particles developed feather abnormalities within 25-40 days, post-inoculation (Ritchie *et al*., 1989b) (Figure 1.6).

Figure 1.6. Twenty-five-day-old budgerigar inoculated with purified *BFDV* at five days of age by oral and intracloacal routes. The bird exhibited slowed maturation and poor feather formation (Ritchie *et al*., 1989a).

Older birds typically show an incubation period of a few months, with the clinical signs being insidious and chronic. Disease progression is variable and carrier states are possible, during which asymptomatic birds may shed virus (Jones, 2006).

1.7.2 Immunosuppression

In later stages of the disease, rapid weight loss, severe anaemia, depression and immunosuppression are evident; with the latter occurring as a result of lymphoid tissue depletion (Ritchie *et al*., 1989a). In addition, extensive damage is seen in the lymphoreticular tissue of the bursa of Fabricius and the thymus (Latimer *et al*., 1991b).

Low concentrations of pre-albumin and hypogammaglobulinemia, as deduced by avian protein electrophoresis studies, support the demonstration of acquired immunosuppression (Ritchie *et al.*, 1989b; Wissman, 2006). Furthermore, a decrease in helper ($CD4^+$) and cytotoxic ($CD8^+$) T-cells is resultant of the virus targeting precursor T-cells (Schoemaker *et al*., 2000; Latimer *et al*., 1993). Consequently, birds usually succumb to secondary and often multiple infections, including gram-positive and gram-negative septicaemia, localised bacterial infections and fungal or parasitic infections. The birds may be susceptible to chlamydiosis, severe pulmonary aspergillosis and severe enteric cryptosporidiosis (Latimer *et al.*, 1991a). Secondary herpes virus infection, polyomavirus infection and adenoviral infection are commonly seen, with adenoviral infection being widespread and usually asymptomatic in African grey species (Doneley, 2003). Gross pathologic lesions are known to occur in internal organs, in addition to the changes normally associated with the beak and feathers of affected birds. However, these internal lesions are not always evident as they may stem from secondary infections (Latimer *et al*., 1991b).

1.7.3 Epidemiology

Thus far the transmission of the virus has not been fully elucidated. However, based on other avian circoviruses, it has been suggested that *BFDV* is transmitted both horizontally and vertically (Rahaus *et al*., 2008). *BFDV* is multi-systemic, based on observations of cytoplasmic inclusions within macrophages in the adrenal gland and pancreas, and nuclear inclusions within testicular germinal epithelium (Latimer *et al*., 1991a). Testicular infection implies that *BFDV* may be gonadotrophic. Infection of the ovary or oviduct suggests a route for the vertical transmission of virus (Latimer *et al*., 1991a). Pass and Perry (1984), suspected a vertical route of transmission, supporting observations made where chicks obtained from artificially-incubated eggs of a *BFDV*-positive hen consistently developed BFD after hatching (Maramorosch *et al.*, 2001). Nestlings (approximately four weeks of age) of *BFDV*-positive parents also tested positive for *BFDV* (Rahaus *et al*., 2008); reiterating the idea that *BFDV*-infected birds show signs of viraemia (Pass & Perry, 1984). Viral DNA was detected in 35.3% of non-embryonated and 20% of embryonated eggs, confirming that *BFDV* can be transmitted both horizontally and vertically (Rahaus *et al*., 2008). It has been reported that asymptomatic parents may produce offspring showing clinical signs of *BFDV*, suggesting that a carrier state exists with vertical or horizontal transmission and / or an existence of a genetic predisposition to the disease (Ritchie *et al*., 1989a). However, epidemiological studies indicate that it is more probable that exposure to the virus occurred through sources other than the parents (Ritchie *et al*., 1989a). Modes by which the disease may be transmitted horizontally include: inhalation of infected feather dust or dried faeces, or ingestion of contaminated faeces or crop secretions (Latimer *et al*., 1991b). It is speculated that humans are the main vehicles of disease transmission as the disease can be spread by handling a healthy bird after coming into contact with infected birds (Bragg, R. R., personal communication; 2013).

1.8 Diagnosis of beak and feather disease

Diagnosis is based upon the observation of various clinical symptoms. However BFD is difficult to diagnose based on clinical signs alone as feather abnormalities may be due to a host of causes, including infection by *Avian polyoma virus* (*APV*) (Ritchie *et al*., 1989b).

1.8.1 Histology

The presence of basophilic inclusion bodies in macrophages in the dermis, epidermis, beak, bursa of Fabricius, thymus, endothelial cells, Kupffer cells and oesophageal epithelial cells are characteristic of *BFDV* (Pass & Perry, 1984; Wylie & Pass, 1987). Basophilic to

amphophilic inclusion bodies were found in histological sections of feathers and follicular epithelium using haematoxylin and eosin-stains (Latimer *et al*., 1991a) (Figure 1.7). The feather and follicular epithelial cells house nuclear inclusions, which are glassy in appearance (Latimer *et al*., 1991a). Multiple cytoplasmic inclusions are located within the macrophages in feather epithelium, follicular epithelium, pulp cavity or the feather sheath and are globular in appearance (Latimer *et al*., 1991a).

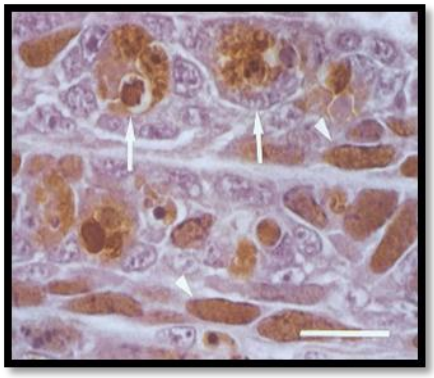

Figure 1.7. Intranuclear inclusions within epithelial cells (arrowheads) and cytoplasmic inclusions within macrophages (arrows) stain positively for *BFDV* antigen (Latimer *et al*., 1990).

BFDV infection cannot however be excluded based on the absence of inclusion bodies (Pyne, 2005). Similar basophilic inclusions have been observed with viruses like *APV* and *Adenovirus*, hindering diagnosis based solely upon histopathology. Hence, there is a great need for the development of additional diagnostic tests (Latimer *et al*., 1991b).

As *BFDV* cannot be cultivated in tissue or cell cultures or in embryonated eggs (Todd, 2000); diagnosis must be confirmed by detection of either viral antigen or viral nucleic acid (Latimer *et al*., 1991b; Ritchie *et al*., 1992).

1.8.2 Polymerase chain reaction (PCR) and quantitative real-time PCR (qPCR)

A universal PCR test was developed for detection of *BFDV* DNA (Ypelaar *et al*., 1999) and has since been modified (Ritchie *et al*., 2003). The oligonucleotide primers hybridise within the ORF V1 (Rep) of the *BFDV* genome, and allow for the detection of clinically infected as well as latently infected birds (Rybicki *et al*., 2005). However, conventional PCR methods are not quantitative and do not distinguish non-specific products of similar sizes since the products are detected by gel electrophoresis (Katoh *et al*., 2008). Post-PCR processing therefore makes conventional PCR time-consuming and labour-intensive (Aslanzadeh, 2004;

Borst *et al*., 2004). Conversely, quantitative real-time PCR (qPCR) simultaneously amplifies and detects the target DNA in the same, closed reaction vessel (Bustin *et al*., 2005). Furthermore, the increased speed attributed to qPCR assays may be due to shortened ramp rates (Mackay *et al*., 2007).

qPCR assays are highly sensitive and specific, thus allowing detection of asymptomatic infections with simultaneous quantification of the amount of virus present in a sample (Shearer *et al*., 2009a). This indication of the viral titre can be used to determine the clinical relevance of the infection. Although conventional PCR can be used quantitatively through a competitive PCR setup, the analytical range is limited (Claas *et al*., 2007). In qPCR, the threshold cycle (C_T values) determines the DNA copy numbers, which correlates to the copy number of the infecting agent present in the sample. In contrast to conventional PCR, real-time PCR does not rely on the final amount of amplicon (Claas *et al*., 2007). Therefore, qPCR is able to detect viral DNA in birds that test negative by standard PCR, highlighting the sensitivity of such assays (Bonne, 2009). As real-time PCR assays exhibit low inter and intra-assay variability (Abe *et al*., 1999; Locatelli *et al*., 2000; Schutten *et al*., 2000), they may eventually replace conventional PCR methods as the gold standard for the diagnosis of *BFDV* infection (Katoh *et al*., 2008).

1.8.3 Haemagglutination (HA) and haemagglutination inhibition (HI) assays

BFDV demonstrates the ability to agglutinate red blood cells, allowing for the development of haemagglutination (HA) and haemagglutination inhibition (HI) assays for the virus and antibody responses to infection, respectively (Raidal & Cross, 1994a). Virus is detected in affected feathers and antibodies in blood, serum, plasma or yolk (Ritchie *et al*., 1991; Raidal *et al*., 1993a;; Sanada & Sanada, 2000).

The suitability of the HA and HI tests as serological tools are complicated by differences in agglutinating ability of *BFDV* for different species as well as amongst individuals of the same species (Sanada & Sanada, 2000). However, no substantial difference in haemagglutinating ability was observed amongst individual African grey parrots (Kondiah, 2004). The HA assay has been shown to be ineffective in identifying carriers of the disease as it does not detect latent or incubating *BFDV* infection.

Although *BFDV* can be purified from feather follicle tracts for the development of HA and HI assays (Studdert, 1993), this method requires persistently infected birds and inadequate amounts of virus are usually obtained, limiting the use of this technique (Kondiah, 2004). In

addition, the HA and HI assays are limited by the possibility of genetic and antigenic diversity of *BFDV* (Raidal *et al*., 1993b; Johne *et al*., 2004).

1.8.4 Enzyme-linked immunosorbent assay (ELISA)

An indirect ELISA using recombinant CP as antigen, for the detection of *BFDV*-specific antibodies has been developed. The secondary antibody used in this assay was directed against immunoglobulin G (IgG) from an African grey parrot (Johne *et al*., 2004), however the cross-reactivity between IgG of different species is unknown (Shearer *et al*., 2009a). In another indirect, competitive ELISA, using recombinant CP as antigen no cut-off value was assigned to the assay, impeding its use as a diagnostic test (Kondiah, 2008).

A direct, competitive ELISA affords a more cost-effective and efficient alternative to the indirect, competitive ELISA (Shearer *et al*., 2009a). Only one other direct, competitive ELISA has been described for measuring the immune status of psittacine species to *BFDV* (Shearer *et al*., 2009a).

The advantages of a direct, competitive ELISA include its use as a non-invasive diagnostic test and the ability to screen multiple samples simultaneously. So far, the main hindrance in the development of an ELISA has been the inability to produce large amounts of standardised serological diagnostic test antigen, which is safe to use.

1.9 Control of BFD

The ability of *BFDV* to haemagglutinate is unaffected by incubation at 80 °C for 30 minutes, as can be observed in Figure 1.8 (Raidal, 1994), thus demonstrating a similar heat sensitivity to that of *CAV* and *PCV*, although at higher incubation temperatures the titre declined. This environmental stability is attributed to *BFDV* being a non-enveloped virus, thus it hampers the total disinfection of aviaries (Department of Environment and Heritage, Australian Government; 2006).

The potential for disease is intensified by overcrowding, which is often the case when housing captive birds. Biosecurity forms the basis of disease control and consists of implementation of external measures to avoid the entry of pathogens into a farm; and internal measures, when the pathogen is already present (FAO Animal Production and Health Paper No. 169. Rome, FAO. Food and Agriculture Organization of the United Nations, 2010).

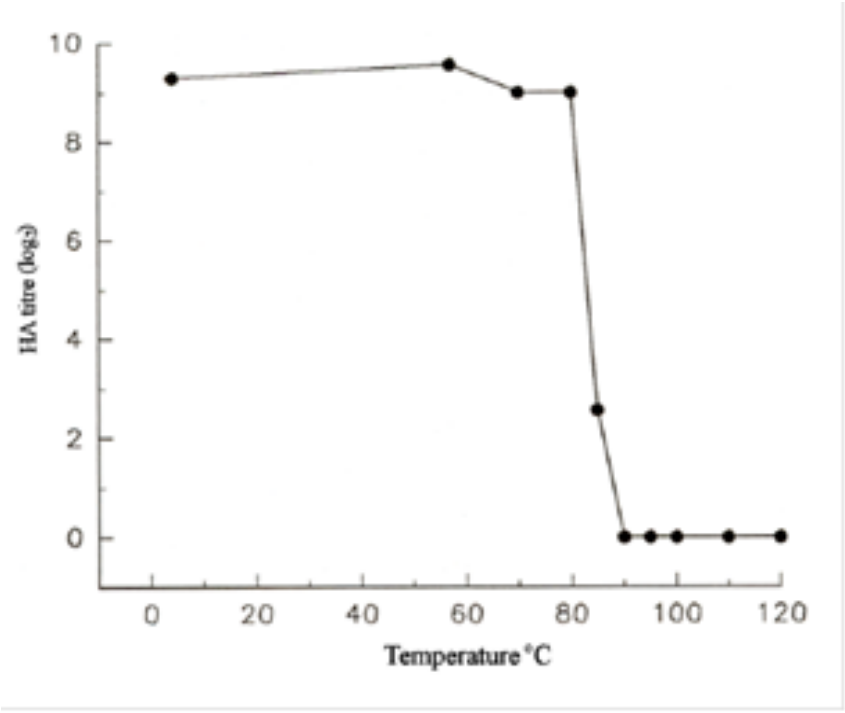

Figure 1.8. The effect of incubating *BFDV* for 30 minutes at various temperatures on viral titre (Raidal, 1994).

The following methods should be employed to ensure effective biosecurity:

1. Disinfection

Disinfectants are only effective when applied to a surface that has been cleared of debris and macroscopic organic matter for the recommended minimum time, usually 5-10 minutes, but up to 30 minutes for some disinfectants.

Inactivation of pathogens occurs more readily when proper disinfection protocols are executed.

The efficacy of disinfectants on the virus is difficult to assess unless a system of cultivating the virus has been established. However, based on the closely-related virus, *PCV*-2, it was ascertained that, classes of disinfectants able to reduce viral titre would include: oxidising agents, quaternary ammonium compounds, phenols and alkalis. In contrast, ethanol, chlorhexidine and iodine based disinfectants showed no significant reduction in viral titre of *PCV*-2, and are hence not expected to be effective against *BFDV* (Royer *et al*., 2001).

2. Segregation

The majority of parrot breeders do not protect their flocks with a quarantine policy. Their facilities are visited by other breeders and they themselves visit other aviaries. Birds are

taken to exhibitions and returned to the aviary without going through a quarantine period. Newly acquired birds are similarly introduced directly into the aviary. Some breeders do however put quarantine policies in place, but it is usually without a technical basis and therefore they tend to be ineffective (Department of Environment and Heritage, Australian Government; 2006).

Restricting exposure to infected birds or viral-contaminated environments, as well as an improved combination of monitoring and quarantine, is necessary to reduce the risk of infection (Department of Environment and Heritage, Australian Government; 2006).

Birds of unknown health status should be quarantined and subjected to diagnostic testing prior to introduction into a healthy population. The proposed quarantine period should be based on the detection of antigen and antibody for *BFDV*. Since the time of infection is usually unknown, it is usually not possible to place a maximum time on the incubation period. However, a 63 day quarantine period is recommended, with testing for *BFDV*, at day 0, day 28 and day 56, leaving a week for results to be delivered (Department of Environment and Heritage, Australian Government; 2006).

Breeders, their personnel and facilities are the weakest links, when trying to curb the spread of *BFDV*. If the concepts of hygiene, modes of transmission and epidemiology of the disease are fully understood, the greatest part of disease control in a captive bird facility will have been accomplished (Department of Environment and Heritage, Australian Government; 2006).

1.10 Vaccine development

There is a substantive need for a vaccine to efficiently control *BFDV* (Todd *et al*., 2001; Kondiah, 2008).

An inactivated vaccine is able to confer partial immunity to the bird against challenge with purified *BFDV* (Raidal *et al*., 1993a). Inactivated virus can be recovered from diseased birds and may be used in the production of inactivated vaccines for the control of *BFDV* infection (Ritchie *et al.*, 1992; Raidal & Cross, 1994b). There are ethical questions surrounding obtaining virus from persistently infected birds. Moreover, this method of obtaining virus results in low yields, is expensive, and is time consuming. It is therefore not deemed feasible for the large-scale production of a vaccine, in order to keep up with the demand of the South African breeding market. In addition, inactivated vaccines may represent the threat of residual infectivity (Rybicki *et al*., 2005).

Vaccine development has been hindered by the inability to cultivate the virus. DNA and recombinant-based vaccines are promising alternatives, with the potential to be effective vaccines (Johne *et al*., 2004). Subunit and DNA vaccines, based on viral protein production by recombinant DNA-based expression have been developed (Kondiah, 2008; Bonne *et al*., 2008). Since only a part of the virus is present, there is no threat of introducing infectious material upon vaccination (Rybicki *et al*., 2005).

Baculovirus-expressed *BFDV* CP was shown to be immunogenic in Long-billed Corellas (*Cacatua tenuirostris*) and was proposed to be a suitable candidate vaccine for the prevention of BFD (Bonne *et al*., 2009). Transient viraemia was evident in vaccinated birds as opposed to an extended period of viraemia in non-vaccinated birds suggesting that vaccination may be useful in the prevention of persistent viraemia and virus shedding. Although viral replication was reduced by the vaccination, it could not completely prevent *BFDV* replication within the host (Bonne *et al*., 2009). Currently, there is no commercially available vaccine and research is now focused on providing an economically viable treatment option.

1.11 Conclusion

Despite the increasing volume of research on *BFDV* in recent years, gaps remain in the clinical and molecular pathogenesis of *BFDV*. High levels of genetic diversity may contribute to varying clinical presentation and to difficulties that may arise during molecular diagnosis of the virus. Serological test development is hindered by a lack of a suitable cell / tissue culture system in which to grow the virus. Improving how *BFDV* is currently diagnosed would see a reduction in the economic losses that bird breeders incur. Furthermore, endangered species such as the Cape Parrot would be assured a greater chance of survival.

CHAPTER 2 INTRODUCTION TO THE PRESENT STUDY

2.1 Problem identification

The international legal trade and illegal trafficking of exotic parrots has facilitated the spread of *BFDV*, so that it now has a global presence (de Kloet & de Kloet, 2004). Captive birds are at a higher risk of contracting infections, due to the proximity of various bird species that would not normally be in contact in the wild (Rahaus & Wolff, 2003). Consequently, *BFDV* poses a serious concern for bird breeders, leading to great financial losses. Factors contributing to the spread of the disease are: poor bio-security and the release of captive birds that are carriers of the virus, into the wild. In recent years there has been a significant increase in the prevalence of *BFDV* in South Africa (Kondiah *et al*., 2006), emphasising the significance of increased surveillance and development of standardised, sensitive and rapid diagnostic assays. In the absence of rigorous testing programmes, there is a risk of selling or exporting birds that are infected with *BFDV*.

Initially, the main criteria behind the implementation of DNA-based detection assays were either due to the failure of conventional microbiological diagnostics, as the microorganism is unculturable, or due to a lack of suitable serological tests (Claas *et al*., 2007). Molecular diagnostics have now become an irreplaceable tool in the diagnosis of infectious diseases (Yang & Rothman, 2004). Furthermore, the on-going search for new nucleic acid based techniques that can be applied to the diagnosis of infectious diseases has driven this technology forward. Currently, *BFDV* DNA can be detected by a universal polymerase chain reaction (PCR) (Ypelaar *et al*., 1999). However, diversity of *BFDV* genotypes may result in PCR not being able to detect all isolates even when conserved primers are used (Bassami *et al*., 2001; Ritchie *et al*., 2003; Heath *et al*., 2004; Johne *et al*., 2004). The interpretation of results obtained by PCR is dependent on whether the PCR is always reliable in amplifying all strains of the virus (Khalesi, 2007). Furthermore, in the absence of clinical symptoms, PCR may be unreliable in diagnosing infection (Kondiah, 2004). This may be due to the bird having a high enough antibody titre, to clear virus from the system (Ritchie *et al*., 1992). A quantitative real-time PCR was developed and now serves as a more sensitive means of viral detection and quantification and may reduce the amount of time needed for accurate diagnosis (Katoh *et al*., 2008; Shearer *et al*., 2009b).

Before proceeding to serological diagnosis of *BFDV*, it becomes necessary to examine protein expression systems. Due to the inability to culture *BFDV*, investigation into the antigenic diversity that exists amongst *BFDV* strains, vaccine development and

establishment of serological tools are reliant on recombinant technology. The coat protein of the virus is immunogenic and can be used as a standardised serological diagnostic test antigen and in vaccine development.

Bacterial expression of both the truncated form and full *BFDV* coat protein (CP) has been successful and the antigenic properties of the expressed proteins were tested by ELISA (Johne *et al*., 2004; Kondiah, 2008; Patterson *et al*., 2012). Although yeast systems have been used frequently in expression of recombinant proteins, they have been shown to be largely inefficient, as low levels of expression are observed (Sambrook & Russel, 2001). Attempted expression of the full length CP in *Yarrowia lipolytica*, strain Po1g, was unsuccessful (Kondiah, 2008). However, a baculovirus expression system using Fall Armyworm (*Spodoptera frugiperda*) insect cells as an expression host was successfully applied in the expressing of the full length recombinant CP (Heath *et al*., 2006; Stewart *et al*., 2007). Stewart and co-workers deduced that the resultant protein is similar to the native virus in morphology, haemagglutinating activity and the ability to react with anti-*BFDV* antibody in an ELISA. The full-length CP and a truncated CP were transiently expressed in tobacco (*Nicotiana benthamiana*) as fusions to elastin-like polypeptide (ELP), for use as a subunit vaccine (Duvenage *et al*., 2013).

Ideally, using the CP as an antigen for serological diagnosis, in addition to the results obtained with molecular-based tests will provide information on the progress of the infection and the immune status of the bird (Khalesi *et al*., 2005).

A competitive ELISA for the detection of anti-*BFDV* antibodies in parrot sera is advantageous as it is a more sensitive and specific diagnostic test for detection of antibodies against *BFDV* (Shearer *et al*., 2009a). A mass flock screening test that is able to detect antibodies against *BFDV* would be advantageous in decreasing result turn-around time in diagnosis.

As far as genetic variance is concerned, *BFDV* shows high sequence diversity (Bassami *et al*., 2001). However, its contribution to antigenicity is not known. Although different serotypes of *BFDV* have not yet been identified (Khalesi *et al*., 2005); the possibility of antigenically-distinct subgroups of *BFDV* should be included during the design of serological diagnostic tests (Hattingh, 2009).

In improving the current diagnostic strategy for *BFDV*, one can limit the spread of the virus and identify possible control strategies. Furthermore, in understanding *BFDV* genetics, the prevention of the extinction of endangered psittacine species, such as the Cape Parrot is conceivable.

After an extensive literature study, a number of research questions arose, including:

- Is there a difference between PCR and real-time PCR as molecular diagnostic tools and can they be used to accurately diagnose infection?
- Can *BFDV* CP be heterologously expressed, for use in downstream serological test development?
- Can recombinantly expressed *BFDV* CP be used to develop a rapid agglutination test to accurately detect exposure to *BFDV*?
- Can a reliable and reproducible competitive ELISA using recombinantly expressed CP be developed to diagnose *BFDV* infection?

2.2 Aim and Objectives

Aim:

The overall aim of the study was to improve diagnostics of *BFDV* infection in parrots, using molecular and serological diagnostic tests.

Objectives:

1. To evaluate polymerase chain reaction (PCR) and quantitative real-time polymerase chain reaction (qPCR) as diagnostic tools for *BFDV*.
2. To recombinantly express *BFDV* CP using a bacterial expression system.
3. To develop serological diagnostic tests for *BFDV* using recombinantly expressed *BFDV* CP.

CHAPTER 3 AN EVALUATION OF POLYMERASE CHAIN REACTION AND REAL-TIME POLYMERASE CHAIN REACTION AS DIAGNOSTIC TOOLS FOR *BEAK AND FEATHER DISEASE VIRUS*

3.1 Background Information

Beak and feather disease (BFD) caused by *Beak and feather disease virus* (*BFDV*) is a dermatological condition afflicting parrot species, thereby causing severe monetary losses (Heath *et al*., 2004). The disease has been spread by the close contact of birds due to the global trade of pet birds (de Kloet & de Kloet, 2004). Molecular diagnostics has had a great impact on detection of *BFDV*, due to the fact that it is not culturable (Ypelaar *et al*., 1999). So far, however, there has been little discussion about whether the mere detection of virus is suitable for diagnosis, or whether the amount of virus is a better indication of clinical status. Quantitative tests such as haemagglutination assays are difficult to standardise, thus it is vital that a more sensitive as well as standardised method of quantifying viral load is found. There is an obvious role for real-time PCR in the specific and sensitive detection of this virus (Katoh *et al*., 2008). Quantitative real-time PCR serves as a means of viral detection, characterisation of infection as well as elucidating viral excretion (Shearer *et al*., 2009b). In this study, the comparison of PCR and a highly sensitive quantitative real-time PCR assay, based on the ORF V1 (encoding the Rep protein) is reported. The assay makes use of absolute quantification to report the specific number of viral copies, in relation to a quantified and characterised standard. Sequencing of PCR products and phylogenetic analyses was performed in order to investigate possible genetic diversity that has been described in literature (Ritchie *et al*., 2003; de Kloet & de Kloet, 2004; Heath *et al*., 2004; Raue *et al*., 2004; Kondiah *et al*., 2006).

3.2 Materials and methods

3.2.1 Sample collection and DNA extraction

Blood samples sent to the University of the Free State (Veterinary Biotechnology Laboratory) for diagnostics for the presence of *BFDV* were pre-selected with regard to: (i) the species of birds, and (ii) the presence or absence of clinical disease. Species included in this study: Budgerigar (*Melopsittacus undulates*), Galah (*Eolophus roseicapilla*), Indian ringneck

(*Psittacula krameri*), African grey (*Psittacus erithacus*), Cape Parrot (*Poicephalus robustus*), Alexandrine parakeet (*Psittacula eupatria*), Brown-headed Parrot (*Poicephalus cryptoxanthus*), Grey-headed parrot (*Poicephalus fuscicollis*) and Orange-winged Amazon (*Amazona amazonica*).

Blood samples were also obtained from birds housed at the University of the Free State, under Ethics approval number NR06/2013. The blood was spotted from the brachial vein onto sterilised filter paper and dried overnight (Riddoch *et al*., 1996; Albertyn *et al*., 2004). The blood spot was cut out from the filter paper strip, taking care to avoid contact, to minimise carryover contamination. The scissors used was disinfected between samples with Virukill avian®.

Total genomic DNA was extracted by means of silica adsorption, using the QIAamp DNA Mini Kit (QIAGEN) according to the Dried Blood Spot protocol in the manufacturer's instruction booklet.

The blood spot was placed in a 1.5 ml microcentrifuge tube with addition of 180 µl of Buffer ATL. Buffer ATL is a tissue lysis buffer for the use in purification of nucleic acids. The tube was incubated at 85 °C for 10 minutes (min), after which, it was briefly centrifuged. Proteinase K (20 µl) was added, the sample mixed by vortexing and incubation carried out at 56 °C for one hour, to allow for denaturation of nucleases and other protein contaminants. Buffer AL (200 µl), a cell lysis solution, was added and the sample incubated at 70 °C for 10 min, followed by brief centrifugation.

A total of 200 µl of absolute ethanol was added to the sample and it was briefly mixed and centrifuged, to precipitate the DNA from the extracted material. The sample was carefully applied to a QIAamp Spin Column (in a collection tube) and the column centrifuged (Eppendorf Centrifuge 5417R) at 6 000 x *g* (8 000 revolutions per min [rpm]) for one min. Under conditions of low pH and high ionic strength, DNA molecules will strongly bind to silica allowing DNA to be captured onto the silica filter. The ethanol reduces the activity of water by formatting hydrated ions, leading to the silica surface and DNA becoming dehydrated. Thus, it becomes energetically favourable for DNA to adsorb to the silica filter. Buffer AW1 (500 µl) was added to the column, centrifuged at 6 000 x *g* for one min and the filtrate, including residual salts, was discarded. After placing the column in a clean collection tube, 500 µl of Buffer AW2 was added, centrifuged at 20 000 x *g* (13 000 rpm) for 3 min and the filtrate, including residual alcohol, was discarded. The column was placed back in the collection tube and centrifuged at 20 000 x *g* for one min to eliminate buffer carryover. After rinsing of the silica filter, the column was placed in a clean 1.5 ml microcentrifuge tube and 30 µl of sterile Milli-Q water (Millipore) was added and it was incubated at room temperature

(RT) for 5 min. DNA was eluted due to the low ionic state of the Milli-Q by centrifuging at 6 000 x *g* for 1 min and the eluted DNA was stored at -20 °C until required for PCR and real-time PCR.

3.2.2 Diagnosis of *BFDV* by Polymerase Chain Reaction (PCR)

Diagnostic primers (Table 3.1), based on ORF V1, encoding the Rep protein were described by Ypelaar and co-workers (1999) and modified by Kondiah (2004).

Table 3.1. Primers used to amplify part of ORF V1 (Rep) in the *BFDV* genome.

Assay	Primer Identity	Sequence	Size	Position	Tm (°C)
PCR	PBF F1	5'-AACCCTACAGACGGCGAG-3'	18	182-189	56.9
	PBF R1	5'-GTCACAGTCCTCCTTGTACC-3'	20	879-898	54.7
Real-time PCR	BFDV rep F	5'-TGTCGCTATTGGTCGGTTC-3'	19	571-589	62
	BFDV rep R	5'-TATTTAGTTCCGGGCTGCTC-3'	20	742-761	62

The reactions were assembled as in Table 3.2 in a 50 µl reaction with the primer pair, PBF F1 and PBF R1 according to the parameters detailed in Table 3.3. The elongation time is dependent on the expected amplicon size and was calculated on a time of 45 s / kb amplicon.

Table 3.2. Reaction components used in PCR to amplify the *BFDV* rep gene.

Reaction components	Volume (µl)
DNA template	5
200 µM dNTPs	1
Each 10 µM primer	1 each
10X ThermoPol Reaction Buffer	5
$MgCl_2$	1
1.7 U *Taq* DNA Polymerase (New England Biolabs)	0.37
Milli-Q water	35.63
TOTAL:	50

Table 3.3. Thermocycling (Vacutec G-storm) was carried out as per the following parameters.

Step	Temperature	Time	Cycles
Initial denaturation	94 °C	2 min	
Denaturation	94 °C	30s	x 30
Annealing	57 °C	30s	
Elongation	72 °C	90s	
Terminal elongation	72 °C	2 min	
Hold	4 °C	5 min	

Amplification products were visualised by gel electrophoresis (Sambrook & Russel, 2001), with a 1% w/v agarose gel (Seakem) dissolved in TAE buffer [0.1 M Tris, 0.05 M EDTA (pH 8.0) and 0.1 mM glacial acetic acid]. The gels contained 10 $mg.ml^{-1}$ ethidium bromide and were run at a constant voltage of 90 V for 30 min. Gels were analysed using the Biorad Gel Doc™ EZ Imager system. For reference, the molecular ladder, GeneRuler™ Express DNA Ladder (Fermentas) was used.

Positively amplified fragments were selected for sequencing and were purified using the Illustria™ GFX PCR DNA and Gel Band Purification Kit (GE Healthcare) according to the protocol for purification of DNA from PCR mixtures, in order to remove any remaining PCR primers, enzyme and unincorporated dNTPs that may interfere with the sequencing reactions.

The PCR mixture was placed in a microcentrifuge tube and 500 µl of Capture buffer type 3 added. The contents were mixed by inversion and transferred to the GFX Microspin™ column. In the presence of the chaotropic buffer, the DNA is dehydrated allowing for a salt bridge of positive ions to form between the negatively charged silica filter and the negatively charged DNA. The DNA backbone is then under conditions of high salt concentration.
It was centrifuged at 16 000 x *g* for 30 s (Eppendorf Centrifuge 5417R). The flow-through was discarded, the GFX Microspin™ column placed back in the collection tube and 500 µl of Wash buffer type 1 added to the column, for removal of excess waste particles. It was centrifuged at 16 000 x *g* for 30 s and the GFX Microspin™ column transferred to a clean microcentrifuge tube. A volume of 30 µl of Elution buffer type 4 (10 mM Tris-HCl, pH 8.0), a low salt solution, was added directly to the centre of the column membrane; the sample incubated at RT for 1 min, and purified DNA recovered by centrifuging at 16 000 x *g* for 1 min. The purified DNA was quantified with a NanoDrop™ 1000 Spectrophotometer v3.7 (Thermo Scientific) and stored at -20 ˚C until further use.

3.2.3 DNA sequencing and phylogenetic analyses of *BFDV* isolates

Bi-directional PCR sequencing was performed with the amplification primers on the PCR products generated, using the BigDye® Terminator v3.1 Cycle Sequencing kit (Applied Biosystems). The sequence reaction is carried out in both directions with both forward and reverse primers. The reaction was carried out in a 10 µl volume, consisting of DNA template (10-40 ng/µl), 0.5 µl premix (containing Tris-HCl, $MgCl_2$, fluorescently-labelled dNTPs and Ampli*Taq* DNA polymerase, concentrations not supplied; Perkin Elmer), 1 µl of either PBF F1 or PBF R1 (3.2 pmoles) and 2 µl of sequencing buffer (composition not supplied, Perkin Elmer) and Milli-Q made up to the final volume of 10 µl. The reactions were thermocycled (Vacutec G-storm) for 35 cycles at 94 °C for 10 s, 50 °C for 5 s and 60 °C for 4 min.

Post-reaction cleanup was performed with EDTA/Ethanol precipitation to remove unincorporated dye terminators and salts. The sequencing reaction was mixed with 10 µl sterile Milli-Q water, 5 µl 125 mM EDTA (pH 8.0) and 60 µl of 100% ethanol. The reactions were vortexed and precipitated at RT for 15 min, then centrifuged at 4 °C for 15 min at 20 000 x *g* (Eppendorf 5417R). The supernatant was completely aspirated, making sure that the cell pellet was not disturbed. A wash step was carried out, with the addition of 120 µl of 70% ethanol to the tubes, followed by centrifugation at 4 °C for 5 min at 20 000 x *g*. The supernatant was aspirated and the wash step repeated. The samples were dried in a Speedvac Concentrator (SAVANT) and stored at 4 °C before being sent in for sequencing, at the University of the Free State, Department of Microbial, Biochemical and Food Biotechnology.

Sequencing was performed with a capillary sequencer, 3130xl ABI Genetic Analyzer (Applied Biosystems). Sequence chromatograms were analysed using CLC Main Workbench 6 and compared with known *BFDV rep* sequences in the GenBank Database using a nucleotide-nucleotide Basic local alignment search tool (BLAST) (Altschul *et al*., 1997). Multiple sequence alignment was performed with Clustal Omega software hosted by the European Bioinformatics Institute (http://www.ebi.ac.uk/Tools/msa/clustalo/).

Table 3.4. Table indicating the sample identity of the parrots infected with *BFDV*, used in the phylogenetic analysis. The location of the bird was noted as well as the species, if known.

Sample identity	Location	Species
016/12	Wolmaranstad, North-West Province	Unknown
019/12	Wolmaranstad, North-West Province	Unknown
025/12	Wolmaranstad, North-West Province	Unknown
029/12	Wolmaranstad, North-West Province	Unknown
090/12	Kimberley, Northern Cape	Unknown
095/12	Worcester, Western Cape	*Psittacula eupatria* (Alexandrine parakeet)
096/12	Worcester, Western Cape	*Psittacula eupatria* (Alexandrine parakeet)
097/12	Bloemfontein, Free State	*Psittacula eupatria* (Alexandrine parakeet)
098/12	Unknown	*Poicephalus robustus* (Cape Parrot)
112/12	Unknown	Indian ringneck (*Psittacula krameri)*

Table 3.4. gives the sample identities of the parrots used in the phylogenetic analysis; the location of the bird was noted as well as the species, if known. The evolutionary history was inferred using the Neighbour-Joining method (Saitou & Nei, 1987). The evolutionary distances were computed using the Maximum Composite Likelihood method (Tamura *et al*., 2004) and are in the units of the number of base substitutions per site. The analysis involved 10 nucleotide sequences. All positions containing gaps and missing data were eliminated. There were a total of 515 positions in the final dataset. Evolutionary analyses were conducted in MEGA5 (Tamura *et al*., 2011).

3.2.4 An evaluation of PCR and a quantitative real-time PCR assay with melt curve analysis

3.2.4.1 Primer design

Oligonucleotide primers (Table 3.1) were designed and analysed using the 'Real-time PCR Tool' at http://eu.idtdna.com/scitools/Applications/RealTimePCR/ using default settings. Complete genome and partial sequences of *BFDV* (29 sequences) were retrieved from GenBank (accession numbers are available in Appendix A) and were aligned to identify the conserved regions using Clustal Omega software (http://www.ebi.ac.uk/Tools/msa/clustalo/). Primers BFDV rep F and BFDV rep R (Whitesci) were designed to obtain a 115 bp amplicon. The region chosen was highly conserved for viral quantification purposes. The considerations stated in Table 3.5. were kept in mind during primer design.

Table 3.5. Primer design rules in real-time PCR (Nitsche, 2007).

Design rule	Reason
Amplicon should be short (100-300 bp)	Increases PCR efficiency
Primer-dimers and secondary structures should remain below a binding energy of 5 kcal/mol	Increases PCR efficiency

The specificity of the primers was analysed *in silico* with BLAST (www.ncbi.nlm.nih.gov) to examine for homology with the *Beak and feather disease virus* genome.These results can be viewed in Appendix B and C.

3.2.4.2 Optimisation with thermal gradient

The primer concentrations and annealing temperatures were optimised using a Vacutec G-storm thermocycler. The optimal annealing temperatures were found by means of a thermal gradient, deviating 5 °C within the theoretical melting temperature determined [Range: 50-60 °C]. Thermocycling (Vacutec G-storm) was carried out with the primer pair designed for real-time PCR, BFDV rep F and R primers (Table 3.1.).

The PCR reaction was heated at 94 °C for 5 min, then 0.34 µl (1.7 units) of *Taq* DNA polymerase was added to each reaction tube. Thermocycling (Vacutec G-storm) then continued as stated in Table 3.6

Table 3.6. Thermocycling (Vacutec G-storm) was carried out as per the following parameters for optimisation of *BFDV rep* primers.

Step	Temperature	Time	Cycles
Initial denaturation	94 °C	2 min	
Denaturation	94 °C	30s	x 30
Annealing	50-60 °C	45s	
Elongation	72 °C	90s	
Terminal elongation	72 °C	2 min	
Hold	4 °C	5 min	

3.2.4.3 Conventional PCR reaction

In order to compare real-time PCR with conventional PCR, samples were tested using the PBF primers, listed in Table 3.1. The reactions using the PBF primers were set out according to Table 3.2 and were thermocycled according to Table 3.3.

3.2.4.4 Construction of standard plasmid for real-time PCR

To generate a standard curve for the real-time reaction, a 717 bp *BFDV* PCR product, using the PBF oligonucleotide primers (Table 3.1) was cloned into the pGEM-T Easy vector (Promega). The resulting plasmid was used to transform *E. coli* Top 10 competent cells and circular plasmid DNA was manually extracted. For the purposes of brevity, the cloning method followed is elaborated on in Chapter 4, Section 4.2.6.1. All DNA concentrations were measured using the NanoDrop ND-1000 Spectrophotometer from NanoDrop Technologies. The plasmid DNA (A260/280 ratio of 1.66) was stored at -20 °C, until further use. Serial 10-fold dilutions of plasmid DNA were used in the amplification reactions.

3.2.4.5 Amplification with real-time PCR assay

The real-time PCR was performed in the Roche Applied Science LightCycler® 2.0 (Germany) with SYBR® Green I detection and melt curve analysis. The procedure was optimised with regard to concentrations of primers (volume of 5 µM concentration: 1.0 µl; 0.8 µl; 0.6 µl; 0.4 µl; 0.2 µl), magnesium chloride concentration (3 mM, 4 mM, 5 mM) and annealing temperature (55, 57 and 58 °C).

The optimised reaction was carried out in a 20 µl final reaction volume containing 4 µl of kit-supplied master mix (containing DNA polymerase, SYBR® Green I dye, buffer, mixed dNTPs and 3 mM $MgCl_2$), 0.8 µl of each forward and reverse primer (5 µM), 1 µl DNA template, and distilled water to a final volume of 20 µl.

To determine the reaction sensitivity and limit of detection of the assay, 10-fold serial dilutions of prepared positive control DNA (Section 3.2.4.4), ranging from 50 ng/ µl to 5 x 10^{-3} ng/ µl were tested.

In order to quantify viral load in the samples tested, known-copy-number DNA standards were generated using serial dilutions of the prepared positive control DNA (Section 3.2.4.4), and were included in each run for viral quantification, also serving as the positive control. The sample was diluted to an initial concentration of 50 ng/µl and then serially diluted to give a range of concentrations, with the lower limit being 0.05 ng/µl, thus providing an accurate measurement over a variety of starting amounts. The standard curve dilution points were set up in triplicate.

Negative (DNA extracted from a *BFDV*-negative bird) and no template controls were included in each run. The thermocycling conditions used are represented in Figure 3.1.

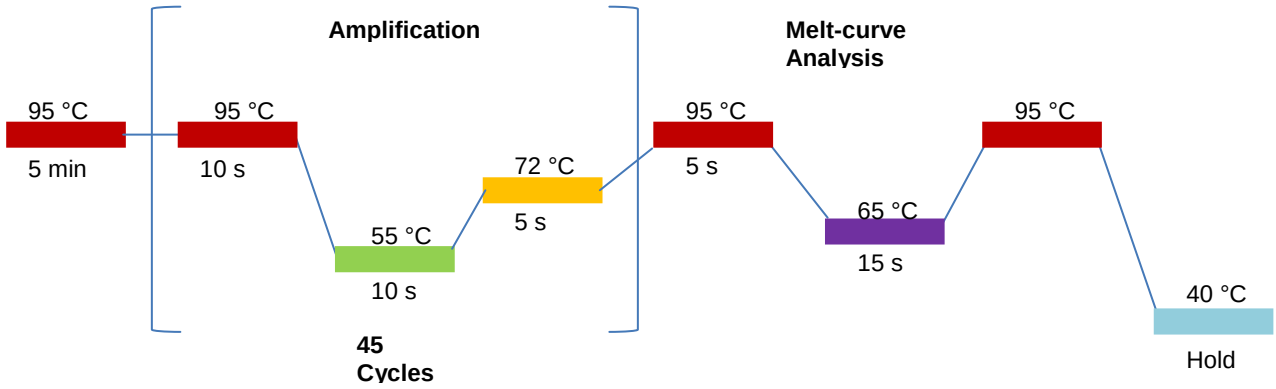

Figure 3.1. Thermocycling conditions used in real-time assay, to detect a 115 bp product.

3.2.4.6 Melt curve analysis of the PCR product

Melt curve acquisitions were conducted by heating the PCR product at 95 °C for 5 s, followed by cooling to 65 °C for 15 s and subsequent heating to 95 °C at a linear transition rate of 0.1 °C/s with continuous fluorescence recording while the temperature was increasing. SYBR® Green I was released upon denaturation, which resulted in a decreasing fluorescence of the signal. The software calculated the T_m. The temperature was then decreased to 40 °C at a ramp rate of 20 °C/s and held at this temperature for 30s.

3.2.4.7 Calculation of viral copy numbers

The software calculated the threshold cycle (C_T), or more correctly, the crossing point (C_p); defined as the number of PCR cycles where the fluorescence generated from the

amplification plot crosses a defined fluorescence threshold. A graph plotting the second derivative of the melt curve was displayed. The standard curve was drawn up by plotting the C_p values of the known-copy-number standards against time, using the software on the LightCycler®. The copy numbers are presented in Table 3.7, the full calculation of copy numbers can be found in Appendix E.

Table 3.7. Copy number of plasmid DNA used in real-time standard curve.

Concentration of plasmid DNA (ng/ µl)	**Copy number**
50 ng/ µl	3.33×10^{20} copies
5 ng/ µl	3.89×10^{19} copies
0.5 ng/ µl	4.28×10^{18} copies
5 x 10^{-1} ng/ µl	3.38×10^{17} copies
5 x 10^{-2} ng/ µl	3.33×10^{20} copies
5 x 10^{-3} ng/ µl	3.89×10^{19} copies

The slope is determined by linear regression and is represented by equation 3.1:

$$\mathrm{E} = 10^{(-1/\mathrm{slope})}$$

Equation 3.1. The calculation of the slope of the standard curve; from the slope the PCR efficiency can be determined.

The number of copies per µl can be calculated using equation 3.2.

$$\underline{\mathrm{DNA\ (copy)} = 6.02\times10^{23}(\mathrm{copy/mol}) \times \mathrm{DNA\ amount(g)}}$$
$$\mathrm{Plasmid\ length + insert\ length(bp)} \times 660(\mathrm{g/mol/dp})$$

Equation 3.2. The number of copies per µl.

3.3 Results

3.3.1 Diagnosis of *BFDV* by polymerase chain reaction (PCR)

Birds housed at the animal housing facility at the University of the Free State, were tested sporadically for *BFDV* and these birds often tested negative (Figure 3.2), even though they

were *BFDV* positive when they first arrived at the animal housing facility. The bird identified as 053 initially showed clinical symptoms, which later cleared up; whilst the bird identified as A2 showed progressive increase in clinical symptoms throught this study.

The full sample identities of birds tested from all over South Africa, can be found in Appendix D. PCR analysis of these parrot blood samples showed that 73% of birds tested were *BFDV* positive (See Figure 3.3). Table 3.8 gives a summary of PCR results obtained from this study. One of the Bloemfontein breeders submitted samples for testing, however, the birds were obtained from all over South Africa. In addition to definitive bands of approximately 717 bp, indicative of *BFDV rep* amplification, smears were also often obtained as can be seen in Figure 3.3. A (006/12); B (093/12, 095/12, 096/12, 097/12) & C (051/12; 061/12; 063/12).

Table 3.8. A summary of PCR results and the location, if known, of parrots tested from farms around South Africa (SA). Appendix D gives detailed results obtained by PCR.

Location	PCR Results		
	-	+	Grand Total
Bloemfontein		1	1
Bloemfontein (Birds from all over SA)		10	10
Kimberley		1	1
Wolmaranstad	29	50	79
Worcester		6	6
Unknown location		10	10
Grand Total	29	78	107

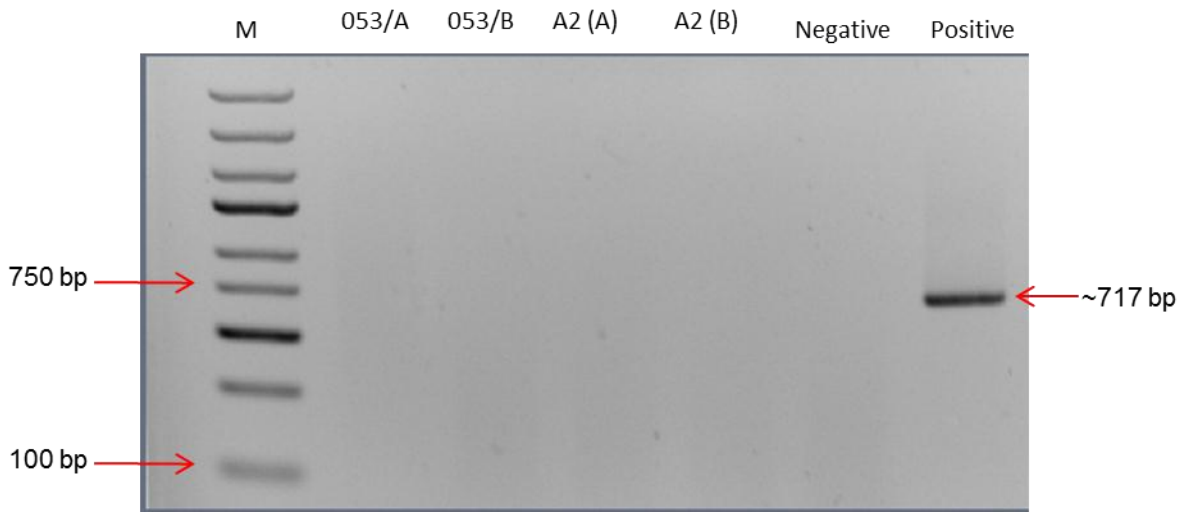

Figure 3.2. A 1% w/v agarose gel visualised under UV illumination of PCR amplification of the *rep* gene of *BFDV* from blood samples obtained birds housed at the University of the Free State, showing negative PCR results. Amplicons of approximately 717 bp were obtained during amplification of the positive control. The GeneRuler Express DNA Ladder (Fermentas, USA) was used as a reference (Lane M).

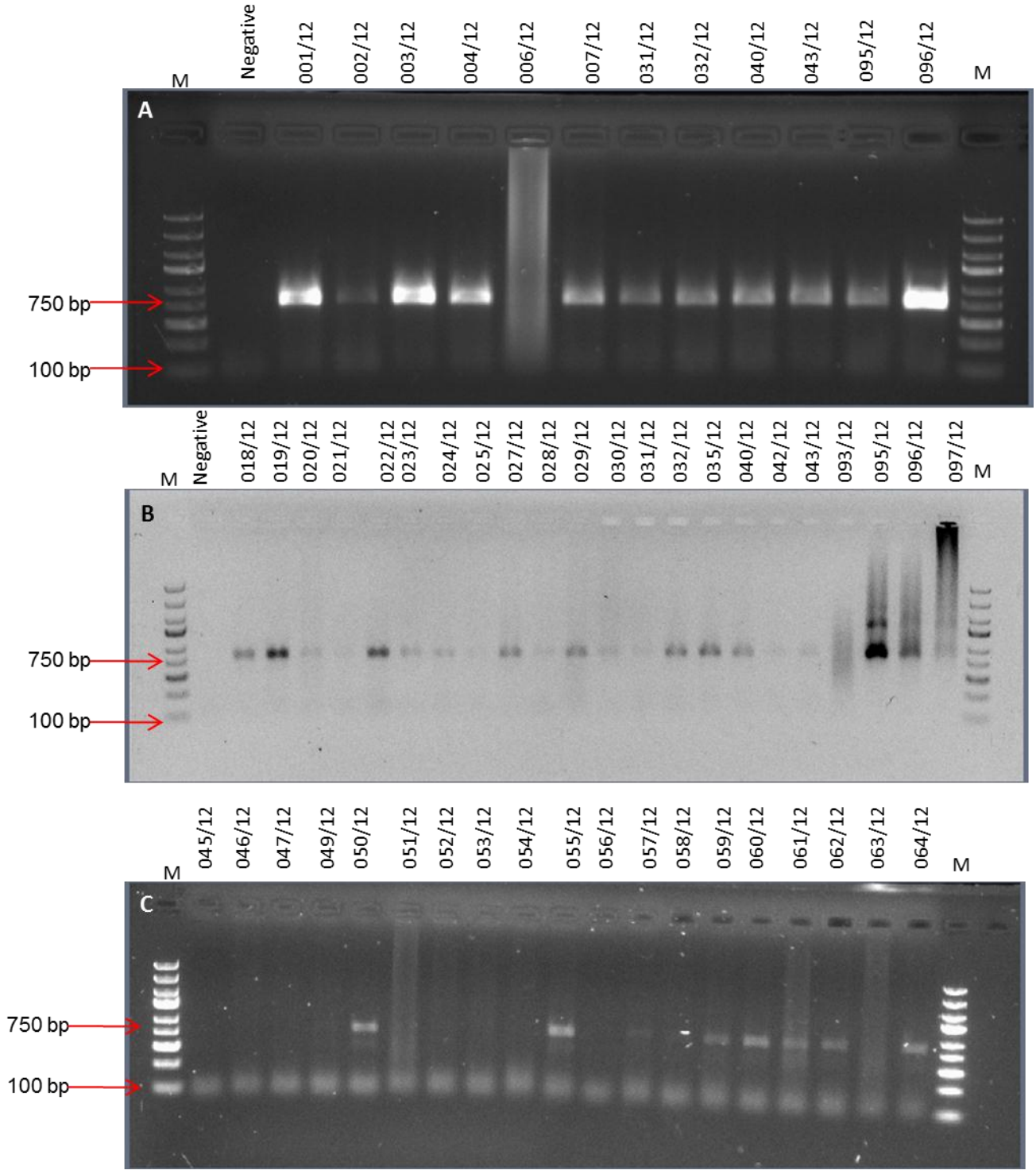

Figure 3.3. A 1% w/v agarose gel visualised under UV illumination indicating PCR amplification of the *rep* gene of *BFDV* from blood samples obtained from farms around South Africa. Amplicons of approximately 717 bp were obtained during amplification. The GeneRuler Express DNA Ladder (Fermentas, USA) was used as a reference (Lane M). Samples from gel A, B and C were run concurrently, and included the same negative control (not shown on Gel C).

3.3.2 Phylogenetic analysis of *BFDV* isolates

The nucleotide sequences of ten *BFDV* isolates obtained from diverse psittacine species at different geographical locations in South Africa were determined and aligned with six previously published sequences (Kondiah *et al*., 2006). The Neighbour-Joining method was used to infer evolutionary history (Saitou & Nei, 1987) and is shown in Figure 3.4.

Relationships are presented as an unrooted tree with branch lengths being proportional to the estimated genetic distance between samples, with the sum of branch lengths equalling 0.11245093. The evolutionary distances were computed using the Maximum Composite Likelihood method (Tamura *et al*., 2004) and are in the units of the number of base substitutions per site. The scale bar represents the % nucleotide difference, thus there is 0.5% nucloetide difference amongst the sequences.

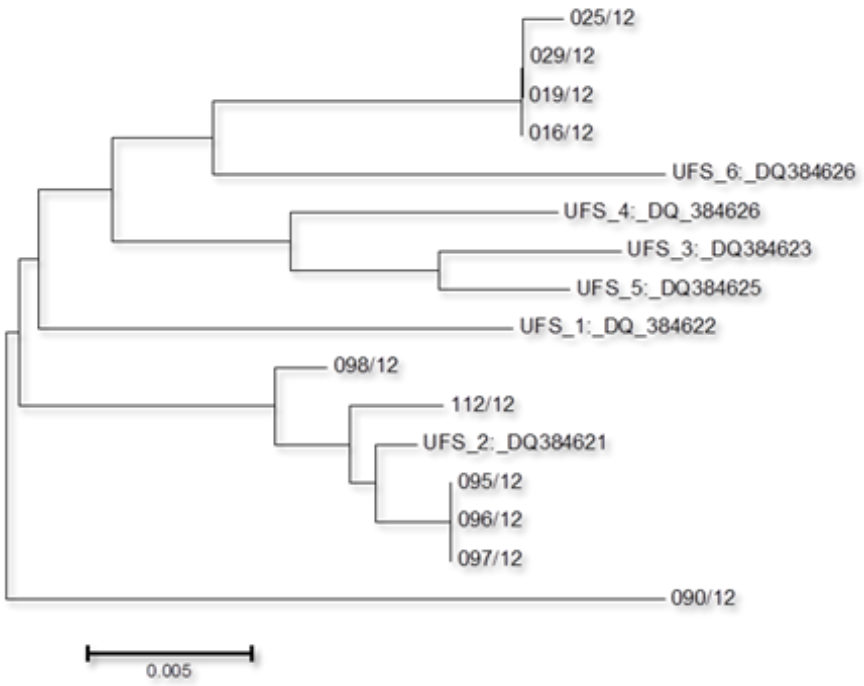

Figure 3.4. Evolutionary relationships of taxa. The evolutionary history was inferred using the Neighbour-Joining method. The optimal tree with the sum of branch length = 0.11245093 is shown using ORF V1 sequences from farm samples as well as the isolates described by Kondiah (2008). The tree is drawn to scale, with branch lengths in the same units as those of the evolutionary distances used to infer the phylogenetic tree.

The sample identity, location and species if known, of the samples used in the phylogenetic analysis is shown in Table 3.8. Analysis was completed on 515 bp of *BFDV* rep sequences. Samples obtained from the farm in Wolmaranstad (016/12, 019/12 and 029/12), appeared to be the same virus, whilst 025/12, also from Wolmaranstad, is closely related. Samples 095/12 and 096/12 were obtained from the same farm in Worcester, which were both

Alexandrine parakeets. They are identical to sample 097/12 from Bloemfontein, which is also an Indian ringneck. 112/12 was also obtained from an Indian ringneck; however, the location is unknown. This sample also clustered closely to other ringneck samples.

090/12 and UFS 6:_DQ384625 have accumulated mutations at a faster rate than the other samples, as seen by their longer branch lengths. Thus, 090/12 from Kimberley shows the greatest genetic diversity.

3.3.3 An evaluation of PCR and a quantitative real-time PCR assay with melt curve analysis

3.3.3.1 Conventional PCR reactions

Faint bands were obtained by PCR (Figure 3.5), with 128/13 and 131/13 representing samples from the same bird at two different time points. Smears can also be seen in sample 127/13.

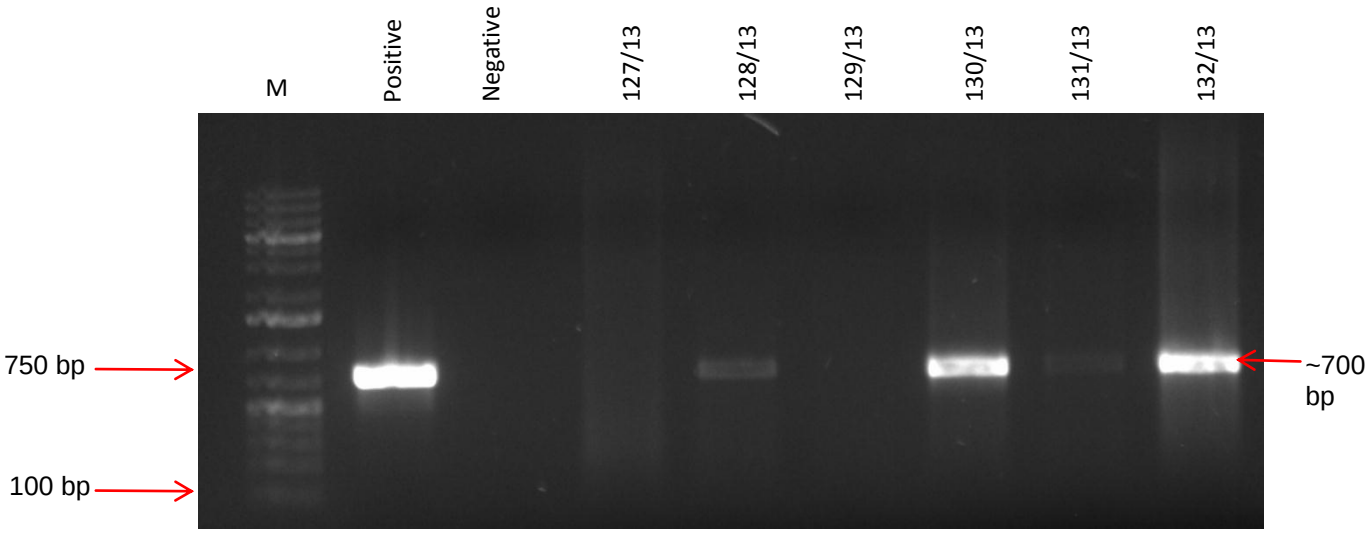

Figure 3.5. A 1% w/v agarose gel visualised under UV illumination indicating PCR amplification of the *rep* gene of *BFDV* from blood samples. Amplicons of approximately 717 bp were obtained during amplification and were both of strong and faint intensities. The GeneRuler DNA Ladder mix (Fermentas, USA) was used as a reference (Lane M). Samples 128/13 and 131/13 were obtained from the same bird at two different time points

Ten samples were tested using the PBF primers and showed that samples 048/14 and 044/14 were positive, as seen in Figure 3.6

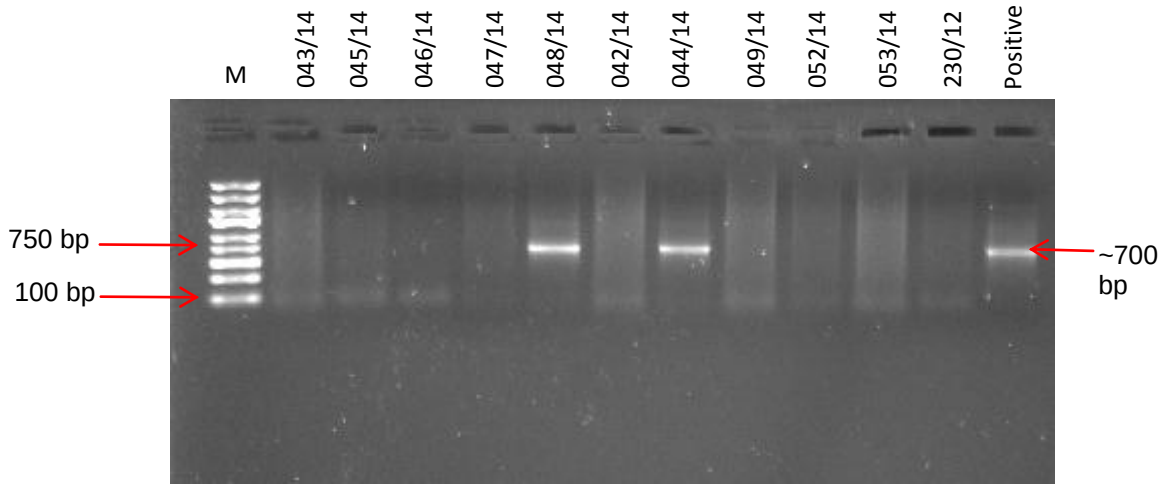

Figure 3.6. A 1% w/v agarose gel visualised under UV illumination indicating PCR amplification of the *rep* gene of *BFDV* from blood samples. Amplicons of approximately 717 bp were obtained during amplification, using the PBF primers. Sample 230/12 represents the negative control. The GeneRuler Express DNA Ladder (Fermentas, USA) was used as a reference (Lane M).

3.3.3.2 Amplification with real-time PCR assay

The real-time PCR was optimised with regard to annealing temperature and showed that amplification was obtained at 57 °C; however the optimal amplification temperature was 55 °C. Various concentrations of primers were tested and the optimal amount of primer was found to be 0.8 µl of a 5 µM concentration (represented by the blue line in Figure 3.7).

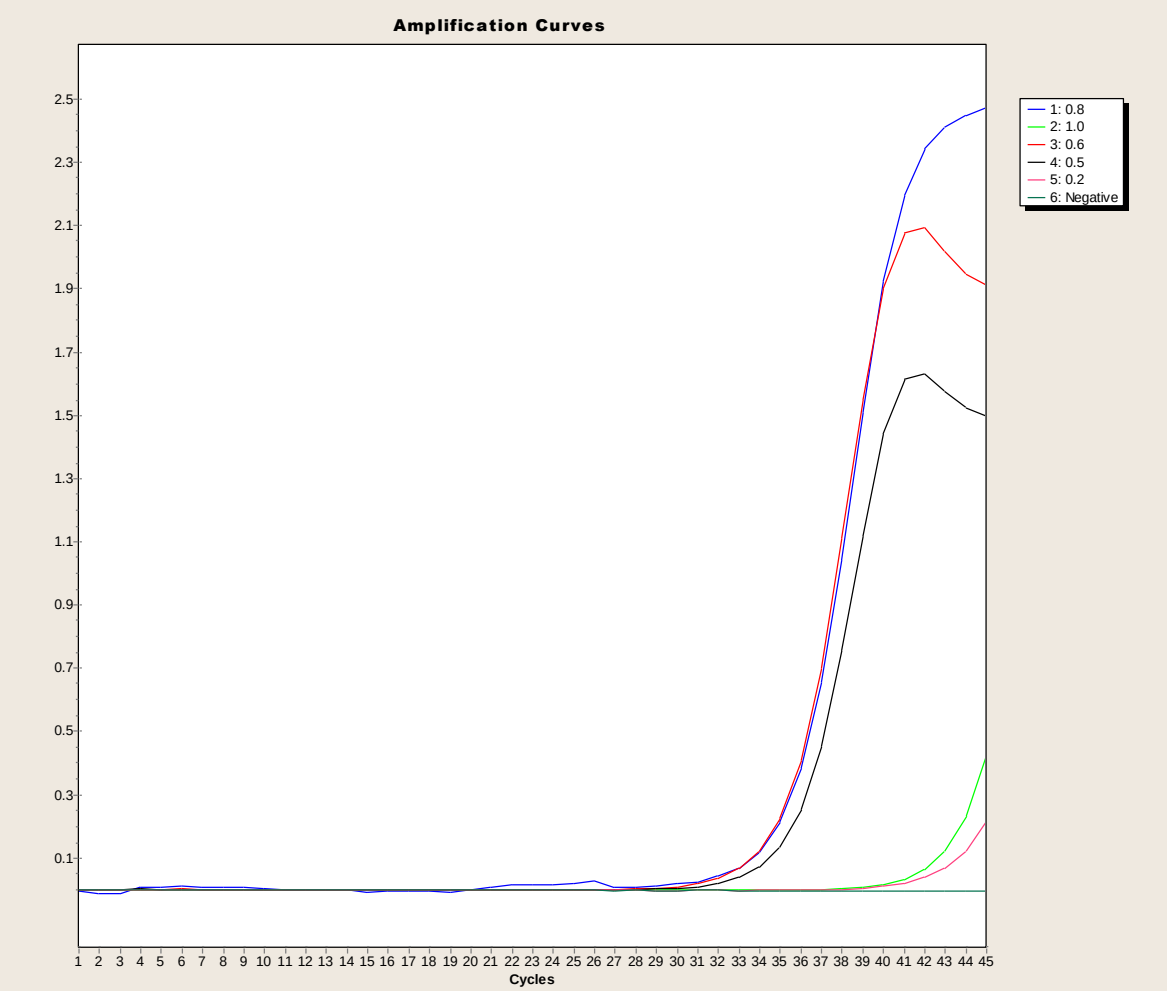

Figure 3.7. Plot of fluorescence versus cycle number showing primer concentration optimisation in real-time PCR

The reactions were optimised with regards to magnesium chloride concentration; it was found that the reaction did not require additional magnesium chloride as the premix already contained a sufficient concentration, as seen by the Plot 1 (blue) in Figure 3.8.

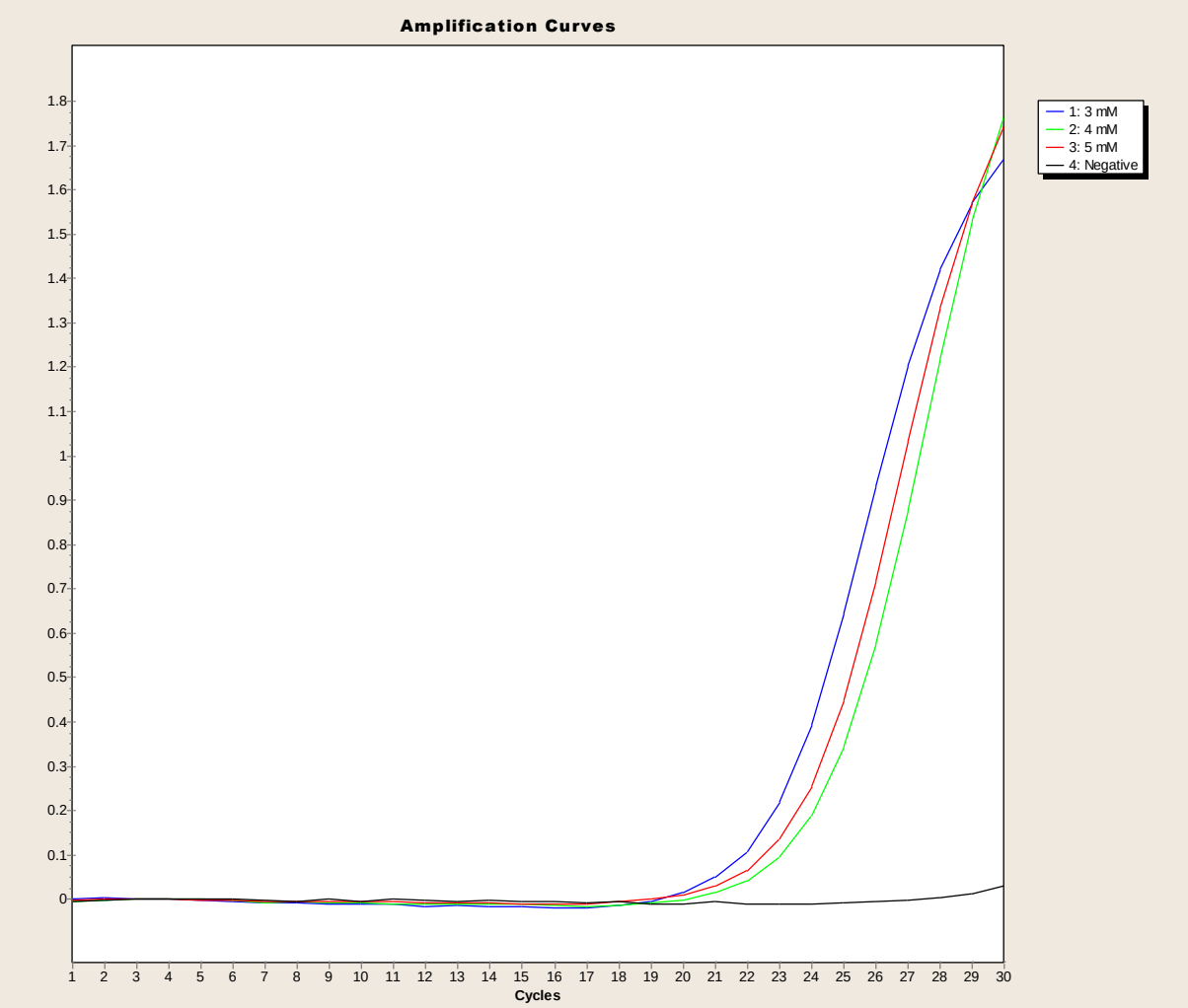

Figure 3.8. Plot of fluorescence versus cycle number showing magnesium chloride concentration optimisation in real-time PCR

The optimised real-time PCR was then performed with the qPCR primers on a sample that tested faintly positive with conventional PCR, using PBF primers (Figure 3.5). Sample 168/13 and gave a definitive positive amplicon of ~115 bp as seen in Figure 3.9. The conventional diagnostic PCR is run at 30 cycles normally, which may not give sufficient time to amplify viral DNA that is present at low concentrations. The real-time PCR is however run between 40-45 cycles and therefore a bright positive band is obtained.

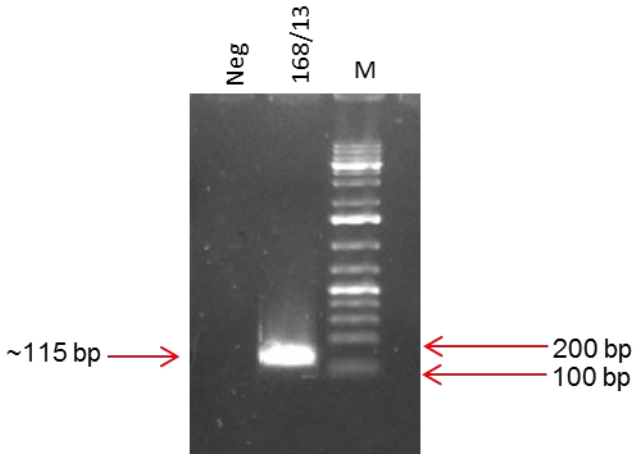

Figure 3.9. Sample 168/13 was tested by real-time PCR, using the qPCR primers. An amplicon of approximately 115 bp was obtained. The GeneRuler DNA Ladder mix (Fermentas, USA) was used as a reference (Lane M).

In order to make a direct comparison with the conventional diagnostic PCR, the real-time PCR was run at 30 cycles, testing 10 samples (Figure 3.10). Table 3.8. shows a comparison of results obtained by PCR and real-time PCR. Samples 048/14 and 044/14 were positive with both PCR (Figure 3.6) and real-time PCR; whilst sample 042/14 was negative by both PCR and real-time PCR. Interestingly, samples 045/14, 046/14, 047/14 and 049/14 were negative by PCR but positive by real-time PCR. Three samples (043/14, 052/14 and 053/14) were negative by PCR but were Uncertain in real-time PCR.

Table 3.8. A comparison of results obtained by PCR and real-time PCR.

Sample Identification	**PCR (**PBF primers)	**Real-time PCR** (qPCR primers)
043/14	-	Uncertain
045/14	-	+
046/14	-	+
047/14	-	+
048/14	+	+
042/14	-	-
044/14	+	+
049/14	-	+
052/14	-	Uncertain
053/14	-	Uncertain

Thermocycling for 30 cycles allows for amplification of only strongly positive samples. The C_p of the samples tested were over 25 cycles, explaining the lack of amplification even by PCR (Figure 3.6). Therefore, increasing the number of cycles may result in amplification of the samples that were called “Uncertain”.

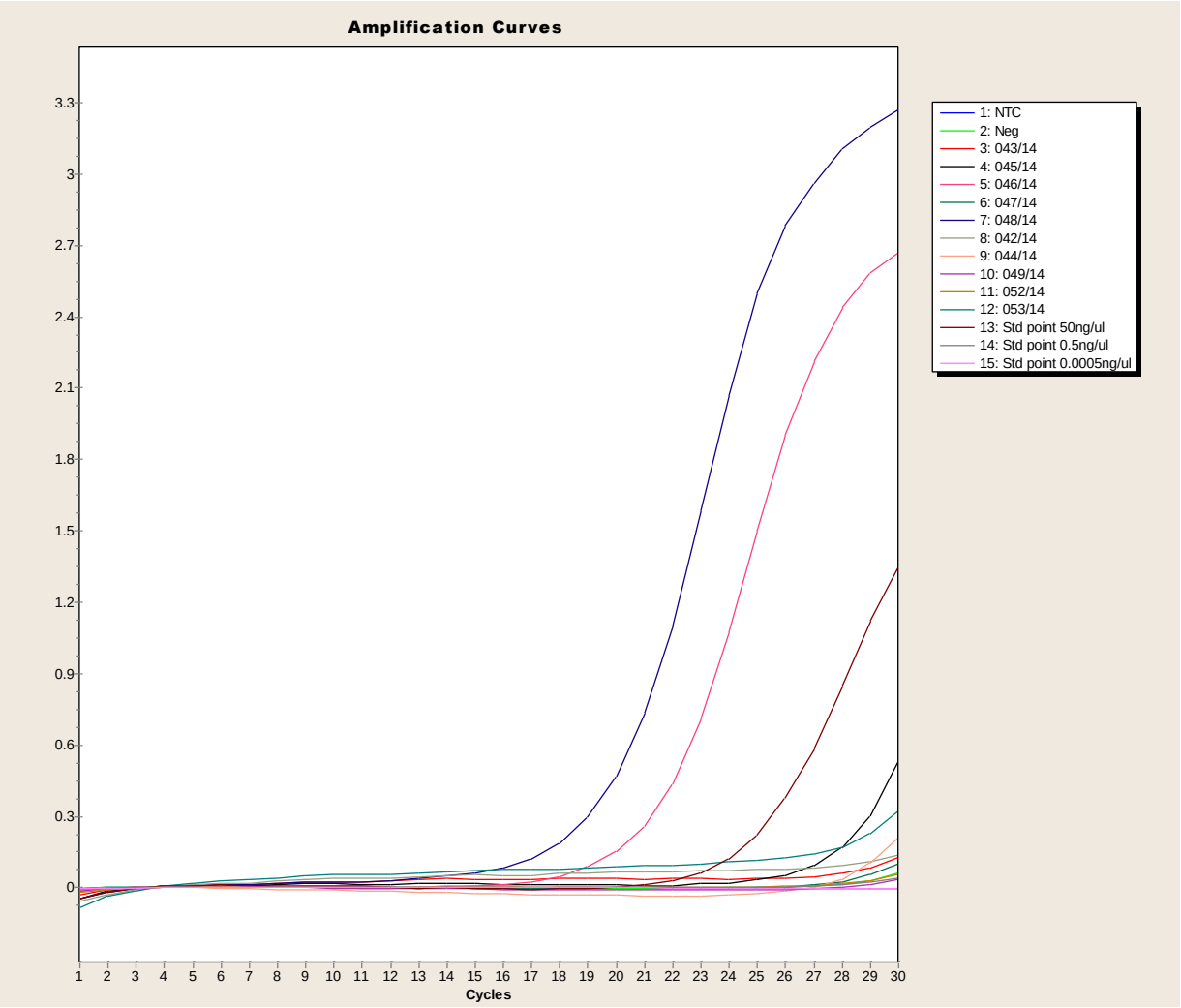

Figure 3.10. Plot of fluorescence versus cycle number showing real-time PCR detection of *BFDV* DNA in blood samples of 10 psittacine birds. The reaction was thermocycled for 30 cycles.

Thermocycling was carried out on 8 samples for 40 cycles and it allowed for amplification of all samples (Figure 3.11). These samples were also subject to melt curve analysis and viral quantification.

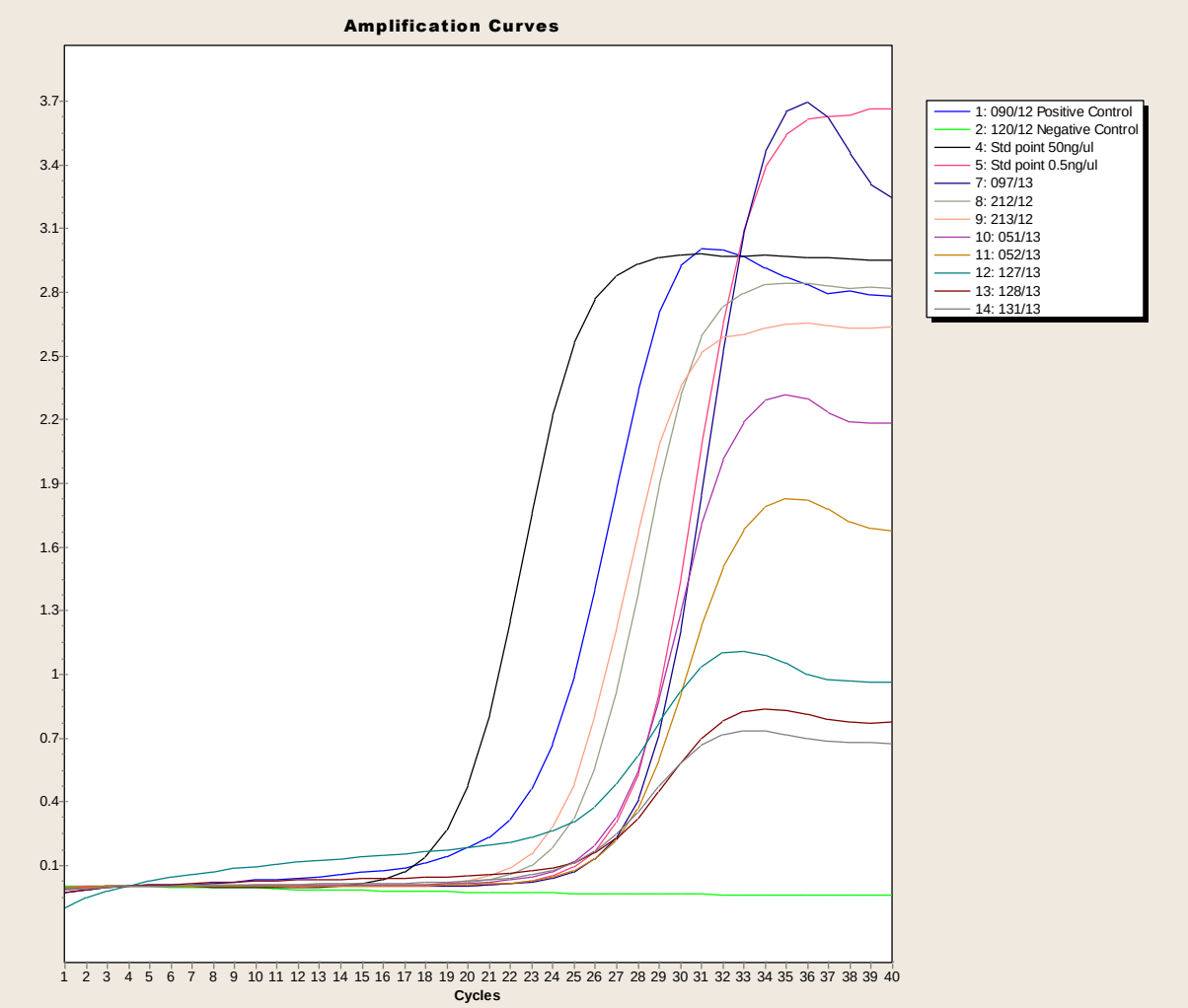

Figure 3.11. Plot of fluorescence versus cycle number showing real-time PCR detection of *BFDV* DNA in blood samples of 8 psittacine birds. The reaction was thermocycled for 40 cycles.

3.3.3.3 Melt curve analysis of the PCR product

To ensure that the optimised signal was specific, a melt curve analysis was performed and is depicted in Figure 3.12. The SYBR® green I technique is based on the detection of double-stranded DNA and is non-specific in its interaction. The expected melting point of the *BFDV* PCR product, depending on its size (115 bp) and guanosine cytosine (GC) content, is approximately 85 °C. Melting points ranged from between 85-87 °C. These melting points are in agreement with the melting point predicted for the PCR product and demonstrated by the positive control (85.19 °C). Sample 097/13 (81.52 °C) and sample 051/13 (80.51 °C) displayed melting temperatures far from the theoretically determined temperature and may be non-specific products or genetically diverse variants of *BFDV*.

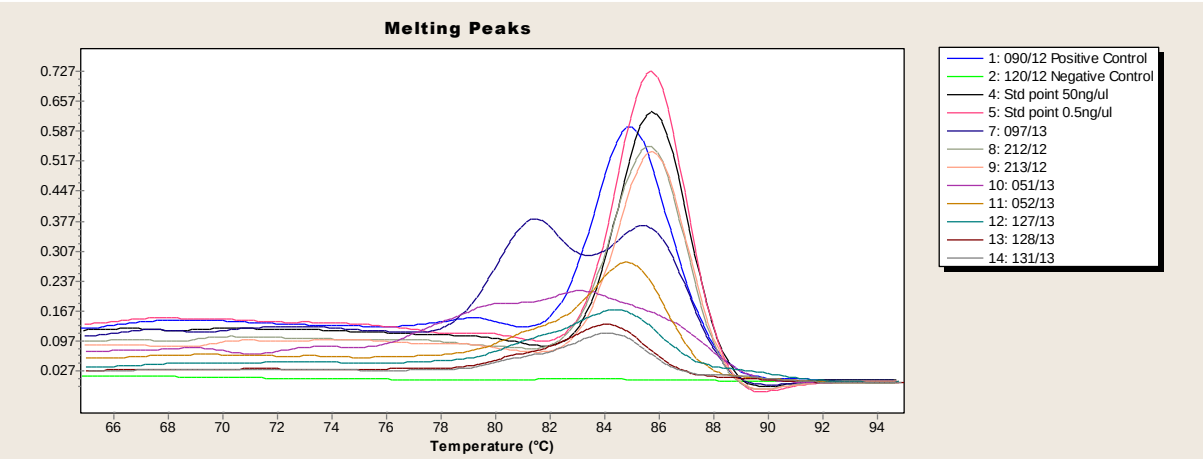

Figure 3.12. Melt curve analysis of the amplification products. The plot of the negative derivative (-dF/dT) of the melt curves versus temperature is present. Expected melting temperatures were around 85 °C, with the positive sample being 85.19 °C.

3.3.3.4 Calculation of viral copy numbers

The generated standard curve, in Figure 3.13, covered a linear range of four orders of magnitude, providing measurement over a variety of starting amounts. The efficiency of the real-time PCR amplification was determined to be 1.92. The equation of the line is:

y= -3.8439x + 28.091, as determined in Microsoft Excel.

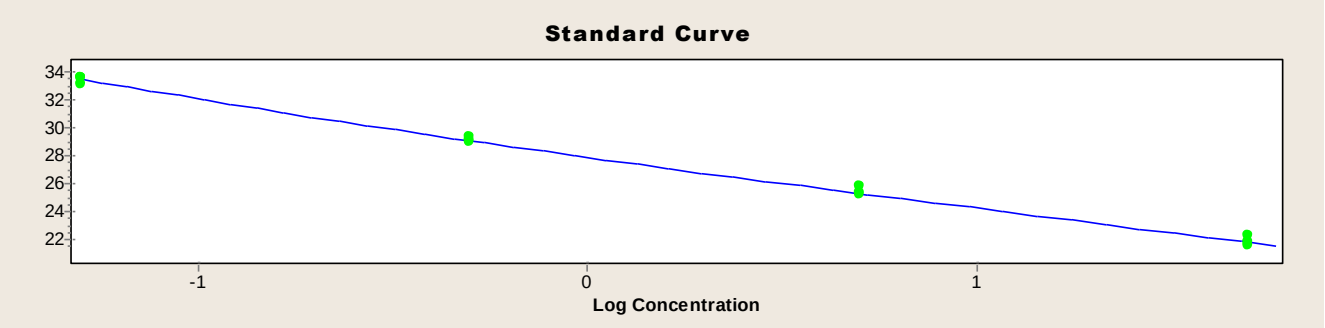

Figure 3.13. C_p values obtained with a 10-fold dilution series of a standard are plotted against the log value of the copy number.

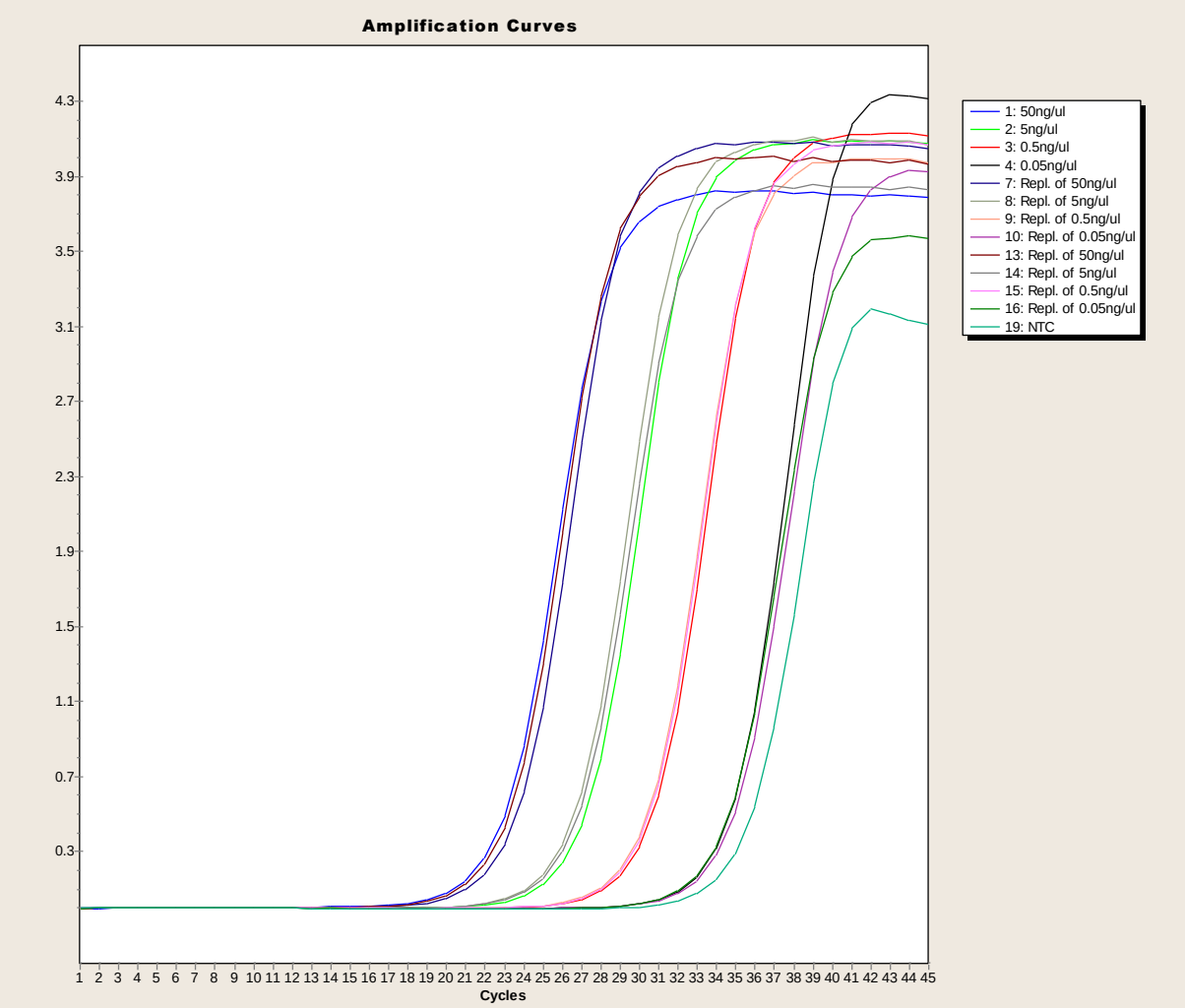

Figure 3.14. Amplification plot of the standard curve.

The no template control (NTC) was positive; with a C_p past 35 cycles, which is even later than the lowest dilution point's C_p. Melt curve analysis (Figure 3.15) of the standard curve samples shows that the product obtained in the NTC is not the same as the product of the standard samples, as the melting temperature is lower than that of the standard. However, two curves were obtained for the NTC and the initial curve may be attributed to the formation of primer dimers. The latter curve may be a contaminant; however it is present in low concentrations. The primers were purified by the manufacturer; however, no additional purification was requested, which may contribute to the non-specificity observed.

The lower limit of detection is 0.05 ng/µl (3.38×10^{17} copies); therefore standard point's 5×10^{-2} ng/ µl and 5×10^{-3} ng/µl were omitted from the plot.

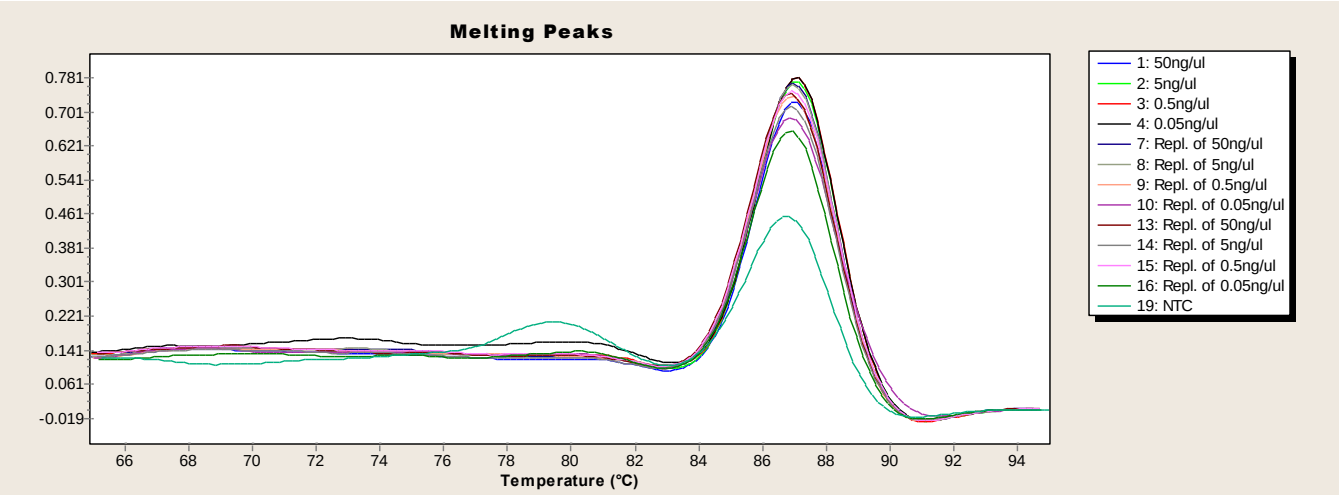

Figure 3.15. Melt curve analysis of the amplification products of the standard curve. The plot of the negative derivative (-dF/dT) of the melt curves versus temperature is present.

Table 3.9. Results obtained with real-time PCR, showing product melting temperatures and sample viral load. Viral load was calculated according to Equation 3.2. *Relative to known standards.

Sample identity	Call Target	Results				
		C_p	Score	Tm 1 (°C)	Tm 2 (°C)	Viral load (copies/µl)*
090/12- **Positive control**	Positive	22.26	5.00	85.19	__	2.609×10^{20}
120/12- **Negative control**	Negative	__	-5.00	__	__	__
Std point 50 ng/ µl	Positive	18.18	5.00	87.25	__	3.33×10^{20}
Std point 0.5 ng/ µl	Positive	26.45	5.00	87.36	__	4.28×10^{18}
097/13	Positive	26.93	5.00	81.52	__	1.59×10^{19}
212/12	Positive	23.89	5.00	85.78	__	9.823×10^{19}
213/12	Positive	23.01	5.00	85.89	__	1.66×10^{20}
051/13	Positive	25.63	5.00	80.51	85.13	3.46×10^{19}
052/13	Positive	25.93	5.00	__	85.03	2.17×10^{18}
127/13	Positive	24.20	3.55	84.56	__	8.16×10^{19}
128/13	Positive	24.90	5.00	84.18	__	5.36×10^{19}
131/13	Positive	24.11	5.00	84.23	__	8.61×10^{19}

3.4 Discussion

The effective control and treatment of *Beak and feather disease virus* requires access to rapid, reliable and sensitive diagnostic tests. Diagnosis based on histopathology lacks specificity, thus difficulties arise with diagnosis of *BFDV* infection (Latimer *et al*., 1991a). Direct culture of the virus is not possible due to the unavailability of suitable cell or tissue lines (Todd, 2000).

This study aimed to answer whether a difference exists between PCR and real-time PCR as molecular diagnostic tools and whether both techniques can be used to accurately diagnose infection.

Breeders perform routine diagnostics on birds before selling a bird or before introducing a new bird into the collection, as well as when *BFDV* infection is suspected. Therefore, clinical symptoms may not always be observed at the time of testing. The diagnostic PCR test for *BFDV* makes use of oligonucleotide primers designed on *rep* (ORF V1), as it displays a higher degree of conservation than the CP gene (ORF C1) (Ypelaar *et al*., 1999; Kondiah, 2004). DNA samples of *BFDV* were obtained from blood samples from infected parrots located on farms around South Africa. A 717 bp band was indicative of viral DNA being amplified (Figure 3.2. A., C.). A collection of birds of various species housed at the UFS, suspected of being BFD positive, also formed part of this study.

The use of dried blood spots in this study offered a convenient method of sample collection, transportation and testing, especially for bird breeders who collected samples themselves and sent it to the Veterinary Biotechnology laboratory (UFS) for testing. However, there have been varying reports as to whether blood, feather or cloacal samples should be used in the detection of *BFDV* (Ritchie *et al*., 1991; Pass & Perry, 1984; Hess *et al*., 2004; Shearer, 2008). Ritchie and co-workers (1991) argued that the use of blood samples neglects faecal excretion as a major route of virus transmission. It has also been suggested that the virus may persist in feathers and epithelial cells, especially in the absence of clinical signs and is actively shed (Pass & Perry, 1984). Positive *BFDV* infection was most often diagnosed in feather and cloacal samples, especially from birds without clinical signs of infection; whereas positive *BFDV* infection was not diagnosed as frequently in blood samples (Hess *et al.,* 2004). In contradiction, blood samples rendered more sensitive PCR results than feather samples by Shearer (2008).

Variability in PCR results was seen, where positive amplicons were detected at certain points and later, the birds tested negative. Two Amazon parrots [053/A; 053/B; A2(A); A2(B)] tested in 2011 were *BFDV* negative, as depicted in Figure 3.2. However, the bird identified as A2 tested positive by PCR in 2013 (Refer to Chapter 5, Table 5.3.). This is in accordance with results obtained by Kondiah (2004), where it was speculated that negative results were obtained when the virus was absent from the bloodstream and most likely residing in the organs. Crowther (1995) proposed that, as the disease state progressed to chronicity, less free viral DNA would be present due to increased antibody production. This is especially true for older birds where clinical symptoms are absent. Hence, it could conceivably be hypothesised that anomalous PCR results may be due to *BFDV* being present in low viral copy numbers.

Weak positive results were also obtained, as seen in Figure 3.3 B. A likely explanation may be the presence of genetic diversity in the *rep* gene. The conventional PCR test has been

the gold standard for detection of *BFDV* thus far and it was developed under the assumption that only one strain of *BFDV* exists (Ypelaar *et al*., 1999). However, extensive genetic diversity has been detected in *BFDV* isolates from a number of psittacine birds (Bassami *et al*., 2001; Ritchie *et al*., 2003; Raue *et al*., 2004). Furthermore, a cockatiel-specific *BFDV* has been discovered (Shearer *et al*., 2008) but the diagnostic PCR test described by Ypelaar and co-workers (1999) failed to detect this specific isolate. Sequence variation has always been, and will most likely always remain an issue of significant concern in PCR assays and may limit the use of PCR as a diagnostic technique (Heath *et al*., 2004; Johne *et al*., 2004).

From the previous discussion, it can be seen that managing the negative effect that *BFDV* has on the breeding industry, requires an understanding of how the virus evolves. Therefore, phylogenetic analysis of *BFDV rep* sequences obtained from breeding farms around South Africa was conducted using the distance-based method, Neighbour-Joining. The branch lengths are proportional to the number of nucleotide changes between the sequences (Tamura *et al*., 2004). However, it does not require that all lineages have diverged by equal amounts (Saitou & Nei, 1987).

The samples obtained from the farm in Wolmaranstad may likely all be infected with the same or a closely related virus. The birds may have been housed in close proximity to each other and therefore they could be infected by the same virus. Analysis of samples 095/12; 096/12 (Alexandrine parakeet) and 097/12 (Indian ringneck), shows that these birds are infected with the same strain of virus. The samples 095/12 and 096/12 are both from Worcester, however sample 097/12 is from Bloemfontein. These samples belong to birds within the same genus (*Psittacula*), pointing to slight evidence of specificity which needs further investigation with whole genome sequences. Circoviruses are known to be host-specific or to exhibit a narrow host range (Todd *et al*., 2005). The occurrence of species-specific lineages of viruses has been observed in previous studies (Ritchie *et al.*, 2003; de Kloet & de Kloet, 2004; Heath *et al.*, 2004; Hess *et al*., 2004; Raue *et al.*, 2004). However, even though genotypes exist, absolute specificity is not guaranteed; as reported by Khalesi *et al* (2005), where *BFDV* isolated from lorikeets did not show absolute exclusivity.

Strains may also develop differences based on the geographical location from which they originate (Bassami *et al.*, 2001). In an MSc study by Kondiah (2004), it was found that although six *BFDV rep* sequences, UFS 1 – 6, were closely related to other *BFDV* isolates, these isolates exhibited a high level of genetic diversity amongst themselves. Variation in restriction digest profiles of *BFDV* isolated from budgerigars around South Africa, showed

genetic variation, thus suggesting a correlation between regional distribution and genetic variation (Albertyn *et al*., 2004). However, in this study, sample 090/12 from Kimberley, clustered separately and did not share a close homology to any of the isolates obtained from Bloemfontein, which is in close proximity to Kimberley.

The sequences analysed in this study showed a 0.5 % nucleotide substitution percentage (Figure 3.4). This is a fairly low substitution percentage, meaning that the sequences analysed are highly conserved. Most genetic variation is considered neutral, however a single nucleotide polymorphism (SNP) in and around *rep* may have an effect on Rep protein expression or function if a few key amino acids are substituted.

Differences in pathogenicity, observed by Shearer (2008) were attributed to neutral mutations, as opposed to natural selection (Shearer, 2008). Circoviruses are provided with a greater means of exploring the available sequence space than would be observed with mutation alone (Heath *et al*., 2004). In a study on *Porcine circovirus* type-2 (*PCV*-2) *rep*, genetic diversity was attributed to random mutations, recombination and purifying selection (Biagini *et al*., 2001). Hence, the same phenomenon may be observed with *BFDV rep* (Biagini *et al*., 2001; Heath *et al*., 2004).

In this study, analysis was based on a 515 bp fragment of *rep*, which reveals very little when taking the evolutionary history of the whole genome into consideration. The various methods used to analyse sequences of *BFDV* isolates may severely compromise the value of the phylogenetic analyses, as analysis of genomic fragments ignores the effect of recombination (Posada & Crandall, 2001). Given the number of species of parrots, it is not surprising that there is genetic diversity and all parrot species are thus assumed to be susceptible to infection by *BFDV*. Even though strains or serotypes have not been definitely identified at this stage, high levels of recombination may possibly lead to eventual differentiation into strains/serotypes, as seen in related circoviruses. In future, phylogenetic analysis would be based on the full genome sequences of isolates, and include a recombination analysis to determine how virus strains are interacting.

Before proceeding to examine results obtained by real-time PCR, it is necessary to explain the primer design for the real-time PCR assay. The sequences used in real-time PCR primer design include the reference sequence (Niagro *et al*., 1998), South African sequences and a sequence from New Zealand. Due to the conserved region used, these primers may also be able to amplify isolates from other countries as seen in the BLAST results (Appendix C).

To determine the optimum annealing temperatures before conducting real-time PCR; conventional PCR was carried out at annealing temperatures in a range of 50-60 °C. The

annealing temperature was determined to be 55 °C, as the expected products were amplified in all reactions of *BFDV* and no extra products were observed. This temperature was then tested with real-time PCR and was determined to be optimal.

In real-time PCR, the initial phase of the amplification plot (Figure 3.7; 3.8; 3.10), the fluorescent signal is below the detection limit of the signal detector. However, in the second stage, the signal increases as the ratio of polymerase to PCR product decreases. Finally, product ceases to grow exponentially and the signal is roughly linear and finally reaches a plateau. Positive reactions were defined by the cycle during amplification, for which the target of interest (~115 bp of ORF V1) is first detected, rather than the measurement of the amount of the PCR product that is accumulated at the end of the PCR reaction.

The amplification efficiency of the reaction was calculated as 1.92 with the use of a standard curve. In addition, it permitted the calculation of the copy number of the unknown target, relative to that of the standard curve. The lower limit of detection was determined as 3.38×10^{17} copies, as SYBR® Green I can only produce accurate quantification results as long as the target amount is not close to the detection limit of the assay (Queipo-Ortuno *et al*., 2005). Copy numbers of between 2.17×10^{18} and 3.33×10^{20} copies/µl were detected indicating that the birds had very high levels of viral particles.

Comparing PCR and real-time PCR results, evidence arose in this study to show that real-time PCR may be more sensitive and specific than PCR for detecting *BFDV* in blood spots. This is due to *BFDV* being detected in samples that tested negative in conventional PCR (Figure 3.6).

It can be hypothesised that the differences may have been due to low copy number or genetic variance. Alternatively, the differences observed may also be explained by the fact that the real-time PCR machine used, had a higher ramp rate than the conventional PCR machine, allowing for more specific primer binding. In the case of genetic variation, a higher ramp rate may allow for more accurate amplification of the target region.

Melt curve analysis performed with real-time PCR showed melting temperatures of between 80.51 °C and 85.98 °C. The temperature at which a DNA strand separates when heated can vary over a wide range, depending on the sequence, length of the strand and GC content. Melting temperatures can vary for products of the same length but different GC distribution. Even single-base differences can result in melting temperature shifts (Roche Applied Science, 2010). The differences in melting temperature were not expected as the primers were designed on a highly conserved fragment of the *rep* gene. Therefore, it can be

hypothesised that these differences in melting temperatures may be as a result of genetic diversity.

During melt-curve analysis, most of the melting temperatures fell within the same range; except for that of sample 051/13 (80.51 °C). Therefore, it can be suggested that this was a non-specific product; however alignment of qPCR primers and the whole *BFDV* genome shows that the primers do not bind non-specifically in the genome (Appendix B, C).

A melting curve with a double peak was observed with the same sample (051/13) and may suggest the presence of two varying sequences. Simultaneous infection with different but related strains of *BFDV* has been observed previously (de Kloet & de Kloet, 2004). The rate at which circoviruses evolve is not known, therefore it is unclear whether birds may suffer simultaneous infection with multiple strains of *BFDV* or if different strains occur as a result of a mutation; where, a non-pathogenic strain gains pathogenicity (de Kloet & de Kloet, 2004). However, Heath and co-workers (2004) suggested that the frequency at which a mixed infection occurs must be fairly high, as a mixed infection is a prerequisite for recombination; even though limited evidence exists for the occurrence of mixed infections. Even though this assay was designed on the most conserved region of *rep*, genetic variance was still evident and may likely be resultant of immune pressure (Lefeuvre *et al*., 2009). Genetic variation is of significant concern when developing PCR assays, but it may have a particularly negative effect in quantitative assays. It may be that the primers preferentially amplify certain strains which would have an implication on viral load quantification. Therefore, depending on how well the primers bind, certain virus strains would appear to have lower or higher viral loads (Mackay *et al*., 2007).

Further work therefore needs to be done in fully characterising *BFDV* genetics, so that the genetic variation of *BFDV* is reflected in the primer design. In order to specifically detect genetic variants of *BFDV*, it may be necessary to design probes that allow rapid detection of SNPs in the *BFDV* sequence in real-time or infection with multiple strains; as opposed to the use of conventional sequence data analysis to provide such information.

Real-time PCR assays have been described previously for *BFDV*; based on the CP gene (Raue *et al*., 2004) and *rep* (Katoh *et al*., 2008; Shearer *et al*., 2009b). Raue and co-workers (2004) described genetic diversity within the CP gene, thus showing the possibility of genotypes in a non-quantitative real-time PCR assay with melting point analysis. Real-time PCR with melting point assay and quantification, based on *rep* showed that blood, feather, tissue and faeces are all suitable for diagnosis but it could not be determined which tissue was the most appropriate for sampling (Katoh *et al*., 2008). Vaccine efficacy was determined by real-time PCR with melting point and quantification in a study by Shearer and co-workers

(2009a). This assay showed that environmental contamination from feather dander was responsible for detection of viral DNA in the blood of all non-vaccinated birds.

Overall, this study indicated that PCR alone is not a reliable diagnostic tool, as birds may test positive at certain points and at later stages, test negative. Although PCR is said to detect *BFDV* infection in birds with clinical signs as well as latently infected birds; non-replicating DNA may still be present in the blood. Thus, a positive PCR result does not indicate that the bird is currently infected by the virus, but that viral DNA is detected in the sample, which may be remnants of viral particles that have been phagocytosed. Reinfection of birds that have been previously exposed to the virus may still occur, with Kundu and co-workers (2012) proposing that the mechanism for this was rapid evolution and selection.

There has been a shift from conventional PCR to real-time PCR in clinical diagnostic settings (Claas *et al*., 2007); therefore, real-time PCR may be valuable in the diagnosis of *BFDV* and may change how *BFDV* is currently identified in diagnostic laboratories.

This study offered some insight into the limitations that currently exist with the molecular diagnosis of *BFDV* and further highlights the need for standardised diagnostic tests. A question that needs to be asked, is whether the presence of viral DNA is sufficient to make a diagnosis? PCR is not a quantitative test and thus does not give much information as to the extent of viral infection. Diagnosis of infection, whether active or latent, is still important for the implementation of good biosecurity measures. However, bird breeders test their birds on tend to abandon implementation of good biosecurity measures as soon as negative PCR results are obtained. These breeders do not take the history of the bird's exposure to the virus into consideration. Therefore, PCR alone may not be a suitable diagnostic tool and it should rather be used in a two-step testing regime that involves serological testing.

CHAPTER 4 BACTERIAL EXPRESSION OF RECOMBINANT *BEAK AND FEATHER DISEASE VIRUS* COAT PROTEIN

4.1 Introduction

Beak and feather disease virus (BFDV) is recognised as a threat to endangered psittacine birds globally; with the highest impact being on birds in Australia, Indonesia, New Zealand and South Africa (Stewart *et al*., 2007). In addition, the virus hampers breeding programs and causes huge monetary losses (Heath *et al*., 2004; Stewart *et al*., 2007). *BFDV* is not able to be cultured *in vitro*, either due to its high *in vivo* tissue specificity or its specific growth requirements (Todd, 2000). The inability to cultivate the virus in tissue / cell culture has hindered the development of a vaccine and reliable diagnostic tests as well as studies into the genetics, antigenicity and pathogenicity of the virus.

BFDV ORF C1, encoding the putative coat protein (CP) with a molecular mass of 31 kDa, is a major structural component of the virus (Ritchie *et al*., 1989a). The CP, being the immuno-dominant antigen of the virus, is responsible for haemagglutinating activity and induction of a protective immune response (Niagro *et al*., 1998; Kondiah, 2008; Shearer, 2008). *BFDV* is a genetically variant virus, with the CP showing a higher rate of genetic diversity than the gene for the replication-associated protein (Rep) (Heath *et al*., 2004). The majority of variation has been shown to occur within specific areas of the CP. Variation may represent a mechanism by which the virus evades the immune system, or may be the result of host-virus interactions specific to individual species (Shearer, 2008).

Currently, there is a great need for *BFDV* antigen for use in diagnostics as well for vaccine development. The development of antibody-detecting diagnostics is heavily reliant on recombinant-based technologies as *BFDV* remains unculturable (Johne *et al*., 2004). Recombinant technology allows for the production of immunogenic CP in large quantities by means of bacterial, eukaryotic and / or insect cell expression systems. Both full-length (Bonne *et al*., 2009; Heath *et al*., 2006; Stewart *et al*., 2007; Kondiah, 2008; Duvenage *et al*., 2013) and truncated (Heath *et al*., 2004; Johne *et al*., 2004; Duvenage *et al*., 2013) forms of the CP have been produced by means of various expression systems.

The use of a bacterial system is advantageous because bacteria can be grown and genetically manipulated fairly easily and inexpensively, whilst a high level of expression is attainable (Sambrook & Russel, 2001). However, a limitation of prokaryotic expression systems is that the codon usage in *Escherichia coli* (*E. coli*) displays a codon bias, in which certain codons are favoured during translation (Kane, 1995; Rocha, 2004; Sharp *et al*., 2005). In general, the more codons that a gene contains that are rarely used in the expression host, the less likely it is that the heterologous protein will be expressed at high levels. Low expression levels are exacerbated if the rare codons appear in clusters or in the N-terminal part of the protein (Gustafsson *et al*., 2004).

Figure 4.1. Synthesised *Beak and feather disease virus* CP gene sequence, based on the complete genome sequence of *Beak and feather disease virus* isolate AFG3-ZA, deposited in Genbank (Accession number: AY450443). Coloured codons indicate codons that are rarely used by *E. coli*. The arginine codons, AGA, AGG and CCC are rarely found in *E. coli* genes but are commonly found in eukaryotes. Percentage (%) represents the average frequency this codon is used per 100 codons (Maloy *et al*., 1996).

While attempting to express the full length *BFDV* CP in *E. coli*, Johne and co-workers (2004) found that an accumulation of arginine residues in the amino-terminal region of the coat protein was responsible for a low expression rate. However, after deletion of the first 38 amino acids, the protein was readily expressed with relatively high efficiency. Although the function of the amino-terminal region is unknown, it was speculated that positively charged amino acids could be involved in packaging of viral DNA into the capsid. This assumption was made on the basis that corresponding regions within the capsid proteins of *Chicken anaemia virus* (*CAV*) and *Porcine circovirus* (*PCV*) have the same function

(Todd *et al*., 2001). As a result, the amino-terminus of the CP would be located within the capsid, and thus may not contribute to the protective antibody response. Therefore, an option would be to truncate the CP gene at the N-terminal region. However, rare codons are seen throughout the synthesised *BFDV* CP gene sequence (Figure 4.1.) and may result in translational stalling, premature translation termination, translation frameshifting and amino acid misincorporation (Kurland & Gallant, 1996).

In order to recombinantly express *BFDV* CP using a bacterial expression system, an expression strategy was devised, involving the use of the plasmid pRARE that encodes tRNA genes for all of the problematic rarely used codons. This plasmid contains tRNA genes coding for Arg, Ile, Gly, Leu and Pro, but not for Arg (CGA/CGG). The use of pRARE would therefore circumvent the need to synthesise codon optimised genes (Novy *et al*., 2001).

Before proceeding to express the *BFDV* CP, it will be necessary to examine the protein for antigenic determinants. Prediction of antigenic determinants may be of great value in the design of diagnostics and treatment options (Larsen *et al*., 2006). *In silico* antigenic predictions have shown that genetic variance could contribute to antigenic differences (Hattingh, 2009). This is in spite of reports of genetic diversity, that the virus is supposedly antigenically conserved as it does not display evidence of different serotypes using HI assay techniques (Ritchie *et al*., 1990; Raidal *et al*., 1993b; Khalesi *et al*., 2005; Stewart *et al*., 2007).

4.2 Materials and Methods

4.2.1 Summary of experimental procedure

The bacterial strains and plasmids used in the study are listed in Table 4.1. An overview of the methodological approach to the study is represented by Figure 4.2.

Table 4.1. List of plasmids used in this study.

Plasmid	Description	Selection	Source
pGEM®T Easy	Linear vector with T overhangs for subcloning of *Taq* polymerase-amplified DNA.	Amp	Promega
pSMART-HCKan	Linearised and dephosphorylated high-copy number vector for efficient blunt cloning of unstable sequences.	Kan	Lucigen

E. coli BL21(DE3) was the proposed expression host. Dr J. van Marwijk (University of the Free State) isolated the pRARE plasmid from Rosetta-gami and transformed it into *E. coli* BL21(DE3).

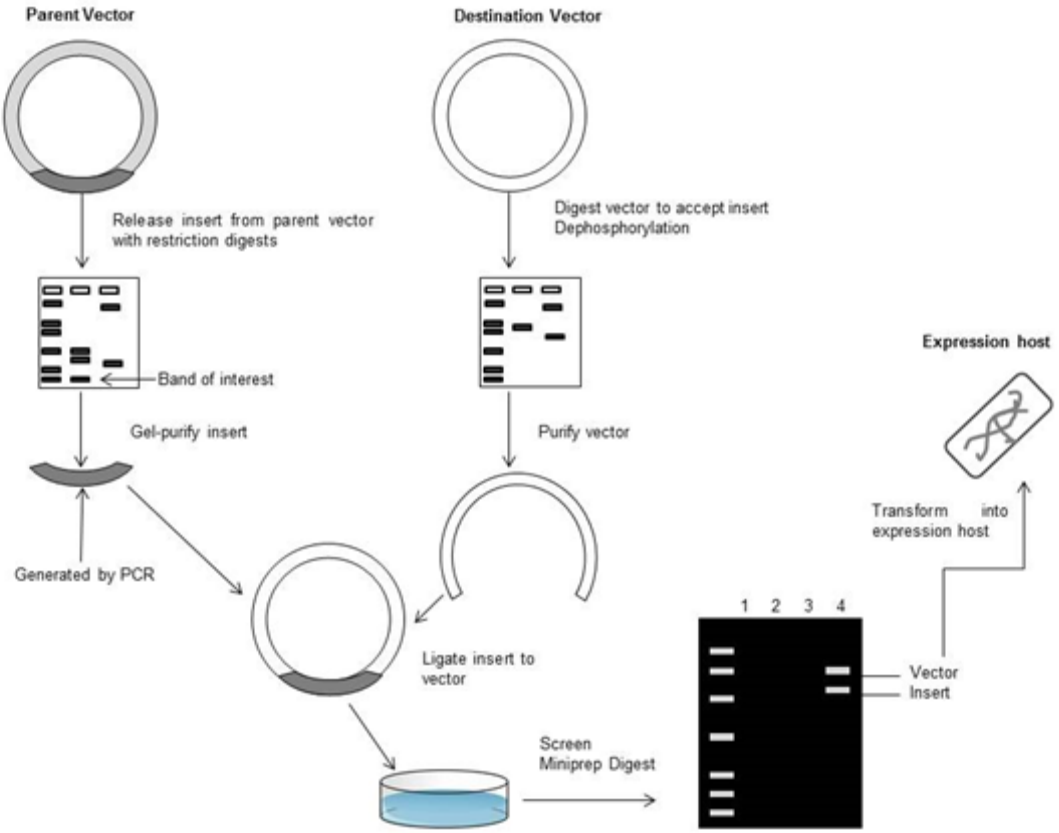

Figure 4.2. A brief summary of the methods followed for bacterial expression of *BFDV* CP (Adapted from Promega, 2013) [http://worldwide.promega.com/resources/product-guides-and-selectors/subcloning-notebook/)]. The parent vector in this instance would be either pGEM®T Easy or pSMART-HCKan; while the destination vector would be pET-28 b (+).

4.2.2 *In silico* antigenic predictions of synthetic *BFDV* coat protein (CP)

The synthetic *BFDV* coat protein gene was based on the complete genome sequence of *Beak and feather disease virus* isolate AFG3-ZA, Genbank Accession number: AY450443. The *BFDV* CP gene was translated using the 'Translate tool' at http://web.expasy.org/translate/ and the correct open reading frame was selected. The CP's antigenicity was predicted *in silico* using the Immune Epitope Database (http://tools.immuneepitope.org) employing the Kolaskar and Tongaonkar and BepiPred linear epitope prediction methods.

4.2.3 Primer design

The designed *BFDV* CP gene (Figure 4.1.) was synthesised by GenScript (USA) and optimised for heterologous expression in *Yarrowia lipolytica* (for use in another study). The initiation codon (CTG) and stop codon (TAA) were removed, and the restriction endonuclease recognition sites for *Sfi*I (5') and *Hind*III (3') were inserted, to facilitate cloning into the surface-display vector, pINA1317-YlCWP110.

Primers were designed to include restriction sites (highlighted in red) to amplify the CP gene out of the surface-display vector and to facilitate cloning into the bacterial expression vector pET-28b(+) (Novagen). Primer pairs were designed (Table 4.2) to contain approximately 40% - 60% G/C content and have similar Tm values. The forward primers BFDV-1F and BFDV-2F were designed to introduce an *Nco*I site or an *Nde*I site, respectively, for exclusion or inclusion of a 5' His-tag in pET-28b(+), respectively. Two additional nucleotides were incorporated after ATG in BFDV-1F to ensure a correct reading frame, translating to a supplementary alanine residue between the starting methionine residue and the first codon of the coat protein. The reverse primers BFDV-1R and BFDV-2R both introduce a 3' *Hind*III site, either with or without a stop codon, for the exclusion or inclusion, respectively, of a 3' His-tag in pET-28b(+).

Table 4.2. Table indicating the primers designed for amplification of the CP gene, restriction sites are indicated in red.

Primer Identification	Nucleotide sequence	Size (bp)	Tm (°C)	Introduced restriction site
BFDV-1F	5'-CCATGGCCTGGGGCACCTCTAACTG-3'	25	65.3	*Nco*I
BFDV-1R	5'-CAAGCTTGGTGGGGTTGGGGTTGTT-3'	25	64	*Hind*III
BFDV-2F	5'-CATATGTGGGGCACCTCTAACTGC-3'	24	59.6	*Nde*I
BFDV-2R	5'- CAAGCTTTTAGGTGGGGTTG-3'	21	54.1	*Hind*III

4.2.4 Amplification of *BFDV* CP gene by Polymerase Chain Reaction

The amplification of the synthesised *BFDV* CP gene was carried out using either BFDV-1F and BFDV-1R or BFDV-2F and BFDV-2R. Reagents were assembled as in Table 4.3 and amplification conditions were according to Table 4.4.

The optimal annealing temperatures were found by means of a thermal gradient, deviating 5 °C within the theoretical melting temperature determined [Range: 54-64 °C]. A range of magnesium chloride concentrations [1.5 mM-2.5 mM] were employed, in an attempt to enhance amplification.

Table 4.3. Reaction components used in PCR to amplify *BFDV* coat protein gene.

Reaction components	**Volume (µl)**
DNA template	3
200 µM dNTPs	1
Each 10 µM primer	1 each
10X ThermoPol Reaction Buffer	2.5
1U *Taq* DNA Polymerase (New England Biolabs)	0.26
Milli-Q water	10.24
TOTAL:	20

Table 4.4. Thermocycling (Vacutec G-storm) was carried out as per the following parameters.

Step	**Temperature**	**Time**	**Cycles**
Initial denaturation	95 °C	2 min	
Denaturation	94 °C	15s	x 30
Annealing	54-64 °C	30s	
Elongation	68 °C	2 min	
Terminal elongation	68 °C	7 min	
Hold	4 °C	5 min	

GeneRuler Express DNA Ladder (Fermentas, USA), comprising DNA standards ranging from 100 to 5000 bp, was used to determine amplicon size. The samples were loaded in a 6x loading dye solution (60mM Tris, 10mM EDTA, 0.02% bromophenol blue and 60% glycerol in H_2O). The gels were electrophoresed at 90 V until sufficient band migration had occurred. Gels were visualised using a DarkReader™ transilluminator (Fermentas) allowing excision of bands for further cloning.

4.2.5 Purification of DNA

Amplified fragments were purified using the Illustria™ GFX PCR DNA and Gel Band Purification Kit (GE Healthcare) according to the protocol for purification of DNA from agarose gel.

The amplified DNA was viewed and excised from the agarose gel with the use of a DarkReader™ transilluminator (Fermentas). The weight of the agarose gel band was determined and 10 µl of Capture buffer type 2 was added for every 10 mg of gel. The tubes were incubated at 60°C and mixed by inversion every 3 min until the agarose was completely dissolved. A volume of 600 µl of the Capture buffer type 2 sample mixture was transferred onto an assembled GFX MicroSpin column and Collection tube. The samples were incubated at RT for 1 min, followed by centrifugation at 16 000 x *g* for 30 s (Eppendorf Centrifuge 5417R). The flow through from the column was discarded and 500 µl of Wash buffer type 1 was added to the GFX MicroSpin column containing the bound DNA. The assembled column and collection tubes were centrifuged at 16 000 x *g* for 30 s. The GFX MicroSpin column was transferred to a sterile DNase-free 1.5 ml microcentrifuge tube, 30 µl of Elution buffer type 4 was added to the centre of the membrane and incubated at RT for 1 min. The assembled column and sample collection tube was centrifuged at 16 000 x *g* for 1 min to elute the purified DNA.

4.2.6 Subcloning of amplified *BFDV* CP gene into pGEM® T Easy bacterial vector

The high-copy number pGEM® T Easy vector map, with reference points, is shown below (Figure 4.3; Table 4.5).

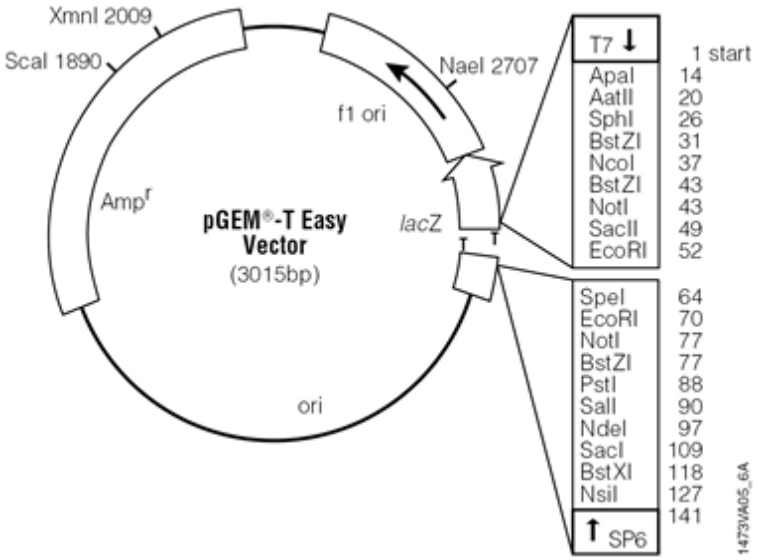

Figure 4.3. Vector map of pGEM®T Easy (Promega, USA), indicating position of SP6 and T7 sites flanking the multiple cloning region and Ampicillin resistance marker.

Table 4.5. Sequence reference points of pGEM®T Easy (Promega, USA).

pGEM®T Easy reference points	Position on vector
T7 RNA polymerase transcription initiation site multiple cloning region	1
Multiple cloning region	10-133
SP6 RNA polymerase promoter (-17 to +3)	124-143
SP6 RNA polymerase transcription initiation site	126
pUC/M13 Reverse sequencing primer binding site	161-177
lacZ start codon	165
lac operator	185-201
ß-lactamase coding region	1322-2182
Phage f1 region	2365-2820
Kanamycin resistance marker	200-1015
pUC/M13 forward sequencing primer binding site	2941-2957

4.2.6.1 Transformation of competent Top10 *Escherichia coli* cells

The Top10 *E. coli* cells were made competent by means of a modified version of the rubidium chloride ($RbCl_2$) method (Hanahan, 1983).

Briefly, 1% of an overnight LB media culture (5 µl of a Top10 *E. coli* glycerol stock inoculated in 5 ml LB media) was inoculated in 100 ml Psi-broth (2 g tryptone, 0.5 g yeast extract, 0.5 g $MgSO_4 \cdot 7H_2O$, with pH adjusted to 7.6 with KOH). It was incubated at 37 °C until an optical density (OD_{600}) of 0.4 was reached, approximately two hours after incubation. The suspension was incubated on ice for 15 min and then centrifuged for 5 min at 4000 x *g* at 4 °C. The supernatant was discarded and the pellet re-suspended in 40 ml ice cold TFB1 [100 mM Rubidium chloride ($RbCl_2$); 50 mM Manganese chloride ($MgCl_2 \cdot 4H_2O$); 30 mM Potassium acetate (KOAc); 10mM Calcium chloride ($CaCl_2 \cdot 2H_2O$); 15% w/v Glycerol].
It was incubated on ice for five min before centrifugation 5 min at 4000 x *g* at 4 °C. The supernatant was discarded and the pellet was gently resuspended in 4 ml cold TFB2 [10 mM 3-(N-morpholino) propanesulfonic acid (MOPS); 10 mM $RbCl_2$; 75 mM $CaCl_2 \cdot 2H_2O$; 15% w/v Glycerol] . The suspension was aliquoted (50 µl) in microcentrifuge tubes and incubated on ice for 15 min. The tubes were then snap-frozen with liquid nitrogen before storage at -80°C. The transformation efficiency of the cells was determined to be 1 x 10^8 cfu/µg DNA using equation 4.1.

$$\frac{colony\ forming\ units\ (cfu)}{ng\ DNA} = cfu/ng\ DNA$$

Equation 4.1. Equation for the calculation of transformation efficiency of competent cells.

The ligation reactions were made up according to Table 4.6. The negative control consisted of Milli-Q water being used in place of insert DNA. The reactions were mixed by gentle pipetting and subsequently incubated for 1 hour at 22 ˚C.

Table 4.6. Ligation reaction components for cloning *BFDV* CP into pGEM®T Easy vector (Promega, USA).

Reaction components	Volume (µl)
DNA template	7
Vector (50 ng/µl)	1
2x ligation buffer	2
5U/ µl T4 DNA ligase (Fermentas)	1
Bovine serum albumin	1
Milli-Q water	8
TOTAL:	20

The amount of DNA to be used was determined by the following formula:

$$ng\ of\ insert = \frac{\text{vector (ng)} x\ insert\ size\ (bp)}{\text{size vector (bp)}} \text{ x insert: vector molar ratio}$$

$$ng\ of\ insert = \frac{50\ \text{ng} x\ 717\ bp}{3015\ \text{bp}} \text{ x } \frac{3}{1}$$

$$ng\ of\ insert = 36\ \text{ng}$$

Equation 4.2. Equation for the calculation of DNA to be used in ligation reaction.

A 50 µl aliquot of competent cells was thawed on ice and 10 µl of ligation mixture was added to the cell suspension. The cells were incubated on ice for 30 min, heat shocked at 42 ˚C for 40 s and transferred immediately to an ice slurry for a further 2 min. Heat shocking facilitates the uptake of DNA as the cell membranes are permeable after treatment with rubidium chloride. Subsequently, 200 µl LB media (1% Tryptone; 1% NaCl; 0.5% Yeast Extract) supplemented with 50 µl of 1 M glucose and 10 µl of 2 M Mg^{2+} was added, and the mixture was incubated on a shaker at 37 ˚C for 1 hour before being spread-plated onto pre-warmed LB plates supplemented with 30 $mg.ml^{-1}$ ampicillin, 10 $mg.ml^{-1}$ IPTG and 40 $mg.ml^{-1}$ X-gal (5-bromo-4-chloro-3-indolyl-β-D-galactopyranoside) for selection purposes. Plates were incubated for 16 hours at 37 °C. White colonies were isolated using a sterile Gilson p10

white tip and inoculated into 5 ml LB media in 25 ml test tubes, supplemented with ampicillin (10 $mg.ml^{-1}$) to maintain selective pressure. This was incubated for 16 hours on a shaker at 37 °C.

4.2.6.2 Isolation of Plasmid DNA

Plasmid DNA was isolated from cultures showing visible growth, using the QIAprep® Spin Miniprep Kit. Microcentrifuge tubes (1.5 ml) were filled with *E. coli* culture and the cells pelleted by centrifugation (Eppendorf 5417R) at 14 000 x *g* at RT for 30 s. The supernatant was aspirated and the pellet was re-suspended in 250 µl Buffer P1 (re-suspension buffer). Buffer P2 – lysis buffer (250 µl) was added and the tube was mixed by inverting. Buffer N3- neutralisation buffer (350 µl) was added and the contents of the tube were mixed thoroughly by inverting until the solution turned from blue to colourless, indicating complete neutralisation. Centrifugation was carried out at 20 000 x *g* (13 000 rpm) for 10 min and the supernatant was applied to the QIAprep spin column. It was centrifuged for 1 min at 13 000 rpm and the QIAprep spin column was washed by addition of 750 µl Buffer PE- wash buffer and further centrifugation at 20 000 x *g* for 1 min. Residual wash buffer was removed after an additional centrifugation step at 20 000 x *g* for 1 min. The QIAprep column was placed in a clean 1.5 ml microcentrifuge tube and the DNA was eluted in 50 µl Buffer EB- elution buffer (10mM Tris-Cl, pH 8.5) after letting stand for 1 min. The eluted DNA was then placed back on the column and incubated for 1 min, in order to increase yield. The DNA was stored at -20 °C until required for downstream applications.

4.2.6.3 Restriction digest analysis of pGEM®T Easy recombinant plasmids

To confirm insertion of the *BFDV* CP in the recombinant plasmids, each clone was analysed by restriction enzyme digestion with *Eco*RI for excision of the *BFDV* CP gene, according to the reaction set-up in Table 4.7. The control plasmid was prepared similarly.

Table 4.7. Restriction enzyme analysis of pGEM®T Easy recombinant plasmids.

Reaction components	Volume (µl)
1X *Eco*RI buffer (50 mM Tris-HCl [pH 7.5 at 37 °C],10 mM $MgCl_2$, 100 mM NaCl, 0.02 % Triton X-100, 0.1 mg/ml BSA)	1.5
*Eco*RI (10 U/µl)	0.75
Plasmid DNA	5
Milli-Q	2.25
TOTAL:	10

Restriction enzyme treated clones were resolved on a 1% (w/v) agarose gel stained with 10 $mg.ml^{-1}$ ethidium bromide.

4.2.6.4 Subcloning of amplified *BFDV* CP gene into pSMART-HCKan vector system.

The pSMART-HCKan vector contains high-copy replication origins and kanamycin resistance, with SL1 and SR2 promoters flanking the multiple cloning region (Figure 4.4.). The sequence reference points are indicated in Table 4.8.

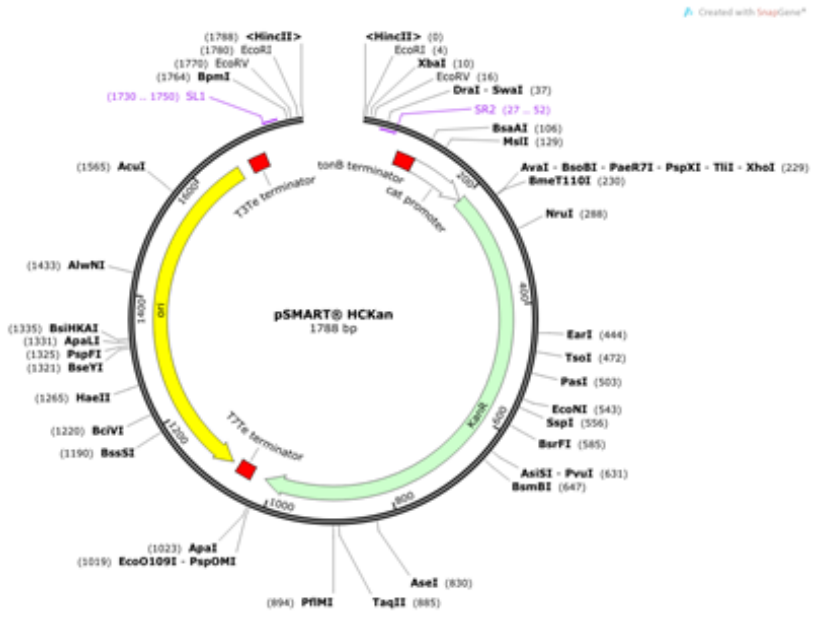

Figure 4.4. Vector map of the linearised pSMART-HC Kan vector system (Lucigen, 2013).

Table 4.8. Sequence reference points of pSMART-HCKan (Lucigen, USA).

pSMART-HCKan reference points	Position on vector
Transcription terminator SR2	27-52
ORF 1	200-1015
Kan2 marker	200-1015
pBR322 origin	1064-1679
Transcription terminator SL1	1730-1750

The restriction sites added in the design of the BFDV-1F and BFDV-1R primers allowed for blunt-ended ligation PCR product into the pSMART-HCKan system. Purified DNA was phosphorylated in order to be cloned into the linear dephosphorylated pSMART-HCKan vector. The amount of DNA to be used was determined to be 37.5 ng, according to equation 4.2, as follows:

$$\frac{30\ ng\ x\ 750}{1800}\ x\ \frac{3}{1} = 37.5\ ng$$

The reaction components were assembled as detailed in Table 4.9 and incubated for 10 minutes at 75 ˚C to phosphorylate insert DNA before ligation to the pSMART-HCKan vector.

Table 4.9. Reaction components needed to phosphorylate insert DNA, *BFDV* CP.

Reaction components	Volume (µl)
PCR product	2
10 mM ATPs	2
10 x Buffer A	2
T4 Polynucleotide Kinase (PNK) (10 U/µl)	1
Milli-Q water	13
TOTAL:	20

The ligation reaction components were assembled as listed in Table 4.10 and incubated for 2 hours at 22 ˚C. The transformation was carried out as described previously in Section 4.2.7.1. Incubation was carried out on a shaker at 37 ˚C for 1 hour and the mixture spread-plated onto pre-warmed LB plates (supplemented with 30 µg.ml^{-1} kanamycin for selection purposes). Plates were incubated for 16 hours at 37 °C. Colonies were isolated using a sterile Gilson p10 white tip and inoculated into 5 ml LB media in 25 ml test tubes, supplemented with kanamycin (30 µg.ml^{-1}) to maintain selective pressure. This was incubated for 16 hours on a shaker at 37 °C.

Plasmid DNA isolations (minipreps) were carried out using the lysis by boiling method adapted from Sambrook and co-workers (1989), as follows: 1 ml of *E. coli* overnight culture was harvested and centrifuged at 6000 x *g* to pellet the cells; the supernatant was discarded while the pellet was resuspended in 350 µl of STET buffer [8% w/v Sucrose, 5% v/v Triton X-100, 50 mM EDTA, 50 mM Tris (pH 8.0)]. For lysis, 25 µl of lysozyme (10 $mg.ml^{-1}$) was added and the suspension was boiled at 100 °C for 44 s. The reaction mix was centrifuged at 13 000 x *g* for 10 min; the resulting pellet was removed with a sterile toothpick and discarded. The supernatant was precipitated with 40 µl of 2.5 M sodium acetate (pH 5.2) and 420 µl isopropanol at -20 °C for 20 min. The mixture was centrifuged at 4 °C, 13 000 x *g*, for 20 min, the supernatant was aspirated and the pellet was washed in 70% ethanol. This mix was centrifuged for 10 min at 4 °C, 13 000 x *g*, followed by aspiration of the supernatant. The pellet was dried and resuspended in 40 µl of TE and RNAse (10 $\mu g.ml^{-1}$).

Table 4.10. Reaction components for cloning *BFDV* CP into pSMART-HCKan vector system (Lucigen, USA).

Reaction components	Volume (µl)
Phosphorylated insert DNA	1
pSMART-HCKan vector	1
10 mM ATPs	2
10X Primer Kinase Buffer	1
T4 DNA ligase (5 U/µl)	1
PEG6000	1
Milli-Q water	5
TOTAL:	10

4.2.6.5 Confirmation of inserts

Two confirmation PCRs were carried out in a 10 µl volume as detailed in Table 4.11; using the SL1/SR2 or BFDV-1F/BFDV-1R primers. The pSMART-HCKan vector has SL1 and SR2 promoters flanking the multiple cloning site; whilst the BFDV-1F/BFDV-1R primers will amplify the coat protein gene if present.

Table 4.11. Reaction components used in confirmation PCR with SL1 and SR2 primers and BFDV-1F and BFDV-1R primers

Reaction components	SL1/SR2	BFDV-1F/ BFDV-1R
	Volume (µl)	
DNA template	1	1
200 µM dNTPs	0.2	0.2
Each 10 µM primer	0.2	0.2
$MgCl_2$	0	0.4
10X ThermoPol Reaction Buffer	1	1
1.3 U *Taq* DNA Polymerase (New England Biolabs)	0.26	0.1
Milli-Q water	7.34	6.9
TOTAL:	10	10

Thermocycling (Vacutec G-storm) was carried out as per the conditions detailed in Table 4.12., and amplified fragments were viewed with the use of a DarkReader™ transilluminator (Fermentas).

Table 4.12. Thermocycling (Vacutec G-storm) conditions to amplify pSMART-HCKan multiple cloning site with SL1/SR2 primers and *BFDV* coat protein insert with BFDV-1F, BFDV-1R primers.

Step	SL1/SR2 primers			BFDV-1F/BFDV-1R primers		
	Temperature	Time	Cycles	Temperature	Time	Cycles
Initial denaturation	94 °C	5 min		94 °C	2 min	
Denaturation	94 °C	30s	x 20	94 °C	30s	x 20
Annealing	53 °C	30s		57 °C	30s	
Elongation	72 °C	40s		72 °C	90s	
Terminal elongation	72 °C	5 min		72 °C	2 min	
Hold	4 °C	5 min		4 °C	5 min	

Restriction digest analysis was carried out in order to screen for positive pSMART-HCKan recombinants with the restriction endonucleases *Nco*I and *Hind*III (Fermentas). Double digestion reactions were set up as shown in Table 4.13 and Table 4.14.

Table 4.13. Sequential restriction digest of pSMART-HCKan recombinant plasmids using *Nco*I.

Reaction components	Volume (µl)
1X Buffer Tango (33 mM Tris-acetate [pH 7.9 at 37 °C]; 10 mM Mg-acetate; 66 mM K-acetate; 0.1 mg/ml BSA)	2
*Nco*I (10 U/µl)	0.25
Plasmid DNA	5
Milli-Q	2.75
TOTAL:	10

Restriction digest with *Nco*I was carried out for one hour at 37 °C (Table 4.13), before addition of components for digest with *Hind*III, followed by further incubation for one hour at 37 °C (Table 4.14).

Table 4.14. Sequential restriction digest of pSMART-HCKan recombinant plasmids using *Hind*III after initial digest with *Nco*I.

Reaction components	Volume (µl)
1X Buffer Tango (33 mM Tris-acetate [pH 7.9 at 37 °C]; 10 mM Mg-acetate; 66 mM K-acetate; 0.1 mg/ml BSA)	2
*Hind*III (10 U/µl)	0.5
Milli-Q	2.5
TOTAL:	15

4.2.6.6 Sequence analysis of pSMART-HCKan recombinant plasmids

The recombinant pSMART-HCKan clones were sequenced using the SL1 and SR2 primer sites available on the vector. Sequencing reactions were prepared according to Table 4.15 and thermocycled as detailed in Table 4.16.

Table 4.15. Sequencing reactions prepared according to the recommendations of the Big®Dye Terminator Kit (Applied Biosystems, USA).

Reaction components	Volume (µl)
Premix	0.5
Sequencing primers: forward/reverse (3.2 picomolar/ primer)	1
Dilution buffer	2
DNA template (1788 bp- 20 ng)	6.5
TOTAL:	10

Table 4.16. Thermocycling (Vacutec G-storm) was carried out as per the following conditions.

Step	Temperature	Time	Cycles
Initial denaturation	96 °C	1 min	
Denaturation	96 °C	10 s	x 25
Annealing	50 °C	5 s	
Elongation	60 °C	4 min	
Hold	4 °C	5 min	

4.3 Results

4.3.1 *In silico* antigenic predictions of synthetic *BFDV* CP

In Figure 4.5. (A), the Kolaskar and Tongaonkar method predicts antigenic determinants between the following residues: 5-13, 76-84 and 166-178 with the most significant antigenic site situated in between the residues, 209-244, at the end of the sequence. The amino acids Cysteine (C), Leucine (L) and Valine (V), if present on the surface, form the basis of an antigenic determinant [Table 4.17 (A)] (Kolaskar & Tongaonkar, 1990; http://tools.immuneepitope.org).

The position of linear epitopes within the *BFDV* CP was also predicted using BepiPred linear epitope prediction (Larsen *et al*., 2006). It is highly probable that the peptides positioned between residues 85-107; 107-117; 140-156 and 199-211 (Refer to Figure 4.5. B & Table 4.17 B) are antigenic sites.

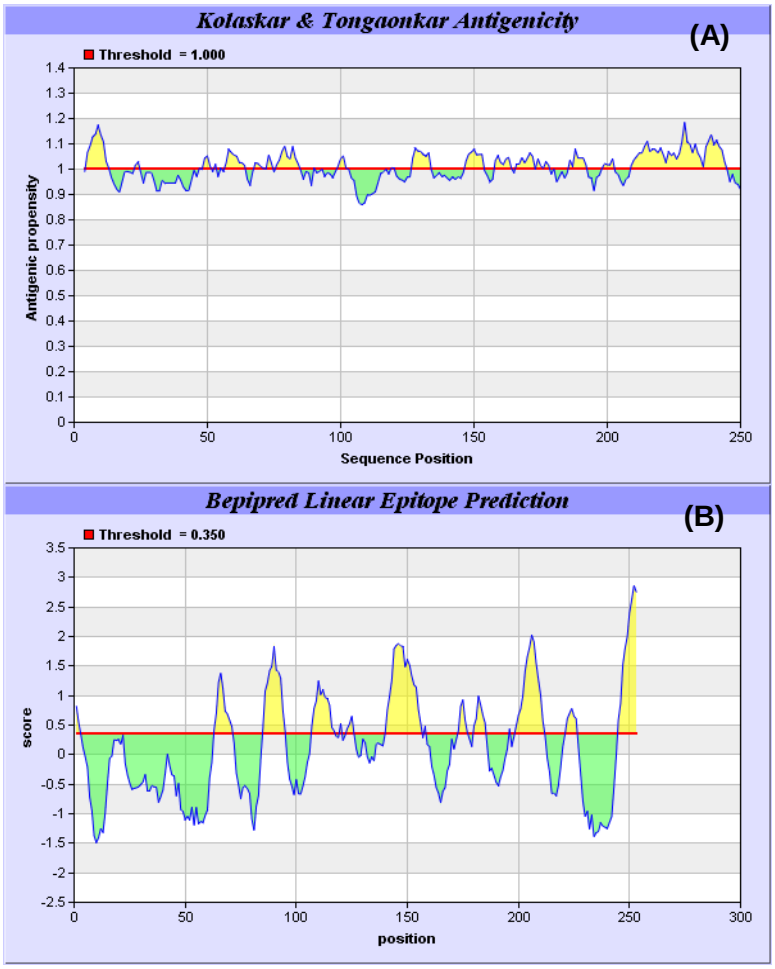

Figure 4.5. Antigenicity prediction profiles for the *BFDV* CP based on the (A) Kolaskar & Tongaonkar prediction; (B) Bepipre Epitope prediction. Peaks highlighted in yellow above the threshold, represent predicted antigenic regions.

Table 4.17. A) Antigenicity prediction for the *BFDV* CP based on the Kolaskar and Tongaonkar method and B) Linear epitope position in synthesised *BFDV* CP sequence using the BepiPred Linear Epitope prediction (http://tools.immuneepitope.org).

A. Kolaskar and Tongaonkar prediction					B. BepiPred Linear Epitope prediction			
No.	**Start Position**	**End Position**	**Peptide**	**Peptide Length**	**Start Position**	**End Position**	**Peptide**	**Peptide Length**
1	5	13	NCACAIFQI	9	1	2	WG	2
2	57	64	KFQILKQT	8	63	71	QTTQPGNVI	9
3	68	74	GNVIWKS	7	85	95	LNTPNPPTLNF	11
4	76	84	YITFALSDF	9	107	117	MetEMetRPTWGH	8
5	127	133	HTAVIQD	7	120	120	I	1
6	147	153	QDPVAPF	7	123	126	DGFG	4
7	158	164	KWYVSRG	7	140	156	KTTADQSQDPVAPFDGA	17
8	166	178	KRLLRPKPQITID	13	158	158	K	1
9	186	192	SAALWLN	7	173	177	PQITI	5
10	209	244	GAKVKHYGLAFSFPQPEVTITYVCMetITLYVQFRQ	36	180	185	LTTANQ	6
11					196	196	T	1
12					199	211	IPLQGGPNSAGAK	13
13					221	226	FPQPEV	6

4.3.2 Amplification of *BFDV* CP gene by Polymerase Chain Reaction

The *Beak and feather disease virus* isolate AFG3-ZA sequence, deposited in Genbank (Accession number: AY450443), was the template for the design of the synthesised *BFDV* CP gene. The complete open reading frame of the gene encoding the CP of *BFDV* was amplified by PCR using the primer sets BFDV-1F, BFDV-1R and BFDV-2F, BFDV-2R. These primers were specifically designed to introduce restriction sites at the flanks of the gene to facilitate cloning into the pET-28b(+) system. PCR amplification was expected to yield a product of 774 base pairs (bp). No amplicons were obtained at the theoretically determined annealing temperatures of the primer pairs (60 °C for primer pair BFDV-1F, BFDV-1R; and 53 °C for primer pair BFDV-2F, BFDV-2R). The highest level of optimisation was included varying magnesium chloride concentrations and setting up a thermal gradient (As seen in Figure 4.6).

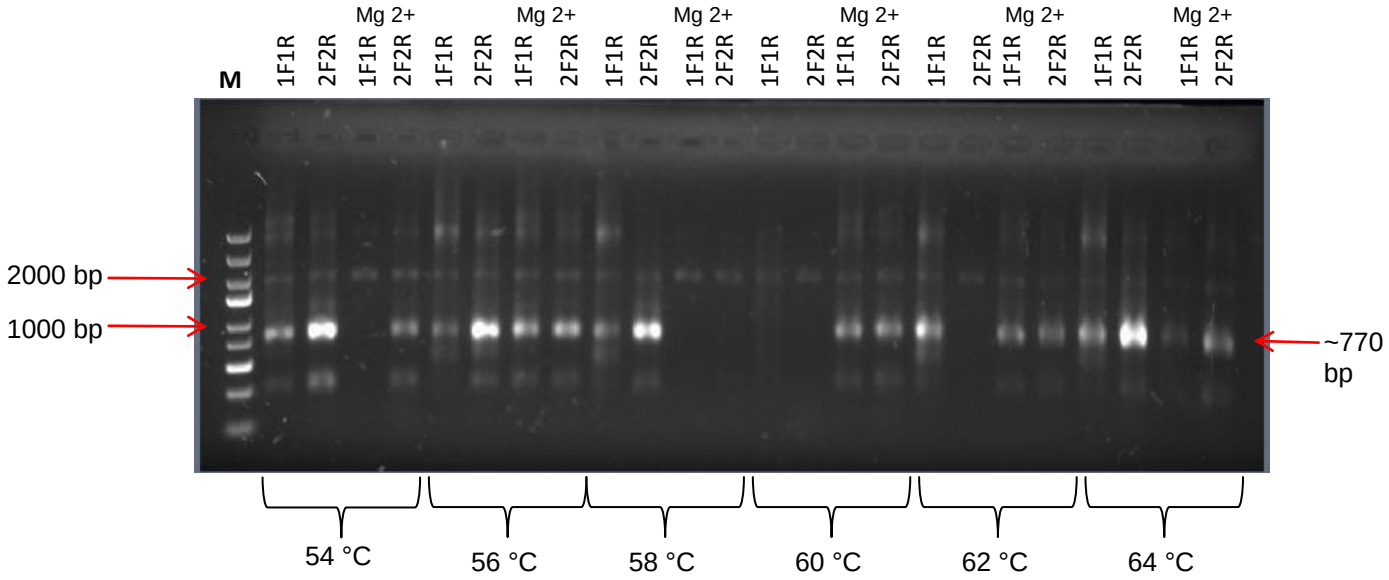

Magnesium concentration
Mg2+ at 54 °C → 2.5 mM
Mg2+ at 56 °C → 2.3 mM
Mg2+ at 58 °C → 2.1 mM
Mg2+ at 60 °C → 1.9 mM
Mg2+ at 62 °C → 1.7 mM
Mg2+ at 64 °C → 1.5 mM

Figure 4.6. Products obtained by thermal gradient, ranging between 54-64 °C and magnesium chloride concentrations between 1.5 mM - 3mM. The optimal T_A for both the primer pairs was found to be 54 °C, without addition of $MgCl_2$. Lane M represents the DNA marker, GeneRuler™ Express DNA Ladder.

4.3.3 Subcloning of amplified *BFDV* CP gene into the pGEM®T Easy vector system

The amplicons obtained using the two primer sets were ligated into the pGEM®T Easy vector using T4 DNA ligase. Figure 4.7. (A) shows undigested plasmid DNA obtained from a clone that contained a product that was amplified by primer pair BFDV-1F; BFDV-1R (Lane 1) as well as the primer pair BFDV-2F; BFDV-2R. (Lane 2). Undigested plasmid DNA showed band sizes of 2 kb with both PCR products, therefore different forms of the plasmid (supercoiled, nicked and linear) that were expected, were not observed.

Isolated recombinant plasmid DNA was digested with *Eco*RI and analysed using agarose gel electrophoresis to confirm the integration of the PCR products (~770 bp) into the vector (As seen in Figure 4.7 B). pGEM®T Easy plus the PCR product obtained from BFDV-1F; BFDV-1R (Lane 2); and BFDV-2F; BFDV-2R (Lane 3) were expected to release the insert of around 770 bp. However, a band of approximately 1500 bp is seen.

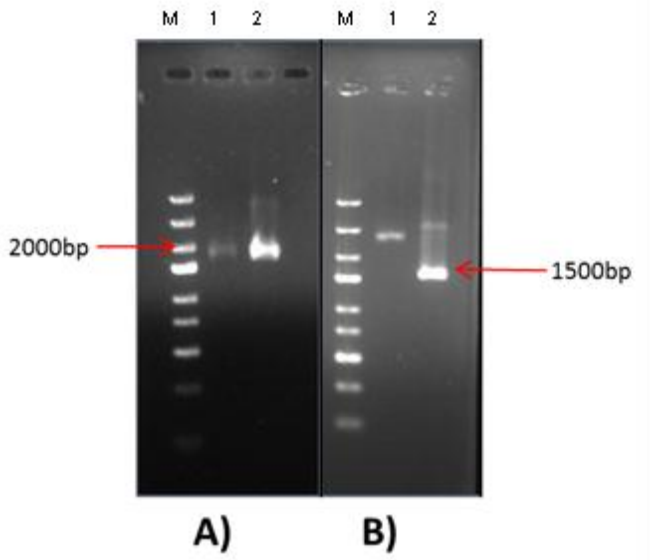

Figure 4.7. DNA isolated from pGEM®T Easy transformants after ligation of PCR products. A) Extracted undigested plasmid DNA. Lane M represents the DNA marker, GeneRuler™ Express DNA Ladder; Lane 1 shows plasmid DNA obtained from a clone that contained a product that was amplified by primer pair BFDV-1F; BFDV-1R, whilst Lane 2 shows plasmid DNA obtained from a clone that contained a product that was amplified by the primer pair BFDV-2F; BFDV-2R. B) *Eco*RI digests of recombinant pGEM®T Easy expected to contain CP PCR products. Lane M represents the DNA marker, GeneRuler Express DNA Ladder Lane 1 represents pGEM®T Easy plus the PCR product obtained from BFDV-1F; BFDV-1R; and Lane 2 represents pGEM®T Easy plus the PCR product obtained from BFDV-2F; BFDV-2R.

Cloning of the amplicon into the pGEM® T Easy vector using TA cloning was repeated on numerous occasions, with 10 clones (both white and blue colonies) being analysed each time, but consistently failed. Consequently, this approach was abandoned and the pSMART-HCKan vector was employed.

4.3.4 Subcloning of amplified *BFDV* CP gene into the pSMART-HCKan vector system.

The PCR product created by the primer set BFDV-1F; BFDV-1R had blunt ends and could be ligated into the blunt-ended vector (Figure 4.8).

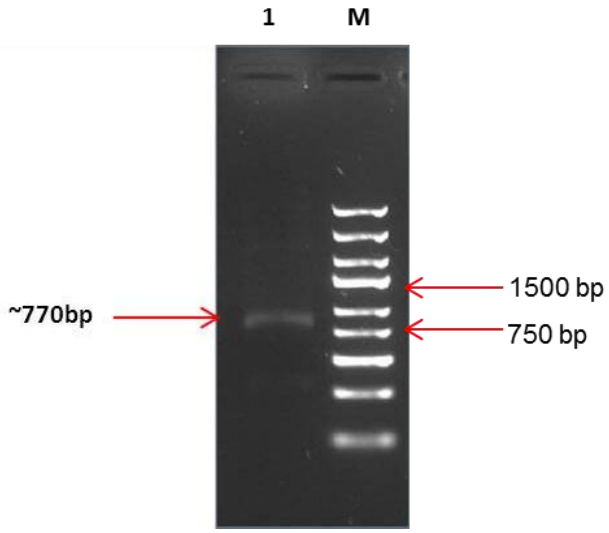

Figure 4.8. PCR amplicon used for cloning into the pSMART-HCKan vector. Lane 1 shows the ~770 bp insert obtained with the BFDV-1F; BFDV-1R primer set that was cloned in the pSMART-HCKan vector (Lucigen). Lane M represents the DNA marker, GeneRuler™ Express DNA Ladder.

The SL1 and SR2 primers flank the multiple cloning region and were expected to amplify the gene that had been inserted, giving a product of ~850 bp (Figure 4.9). However, a band around 200 bp was obtained, due to the primers amplifying a nonspecific product within the *BFDV* CP sequence.

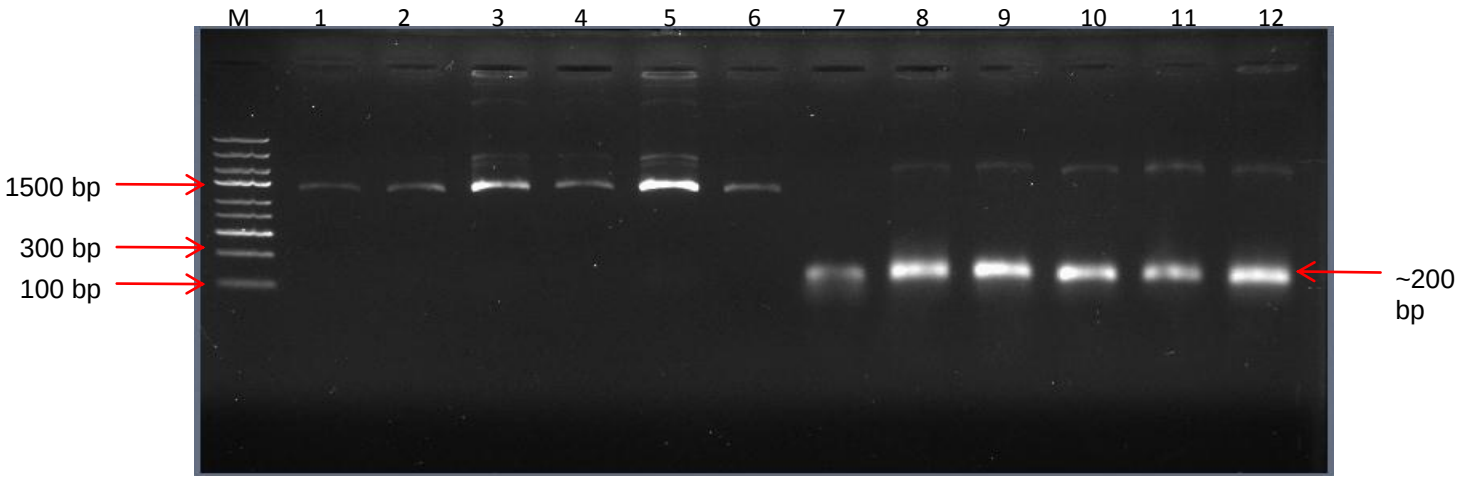

Figure 4.9. Plasmid DNA isolations from transformations of competent *E. coli* with PCR products from BFDV-1F and BFDV-1R ligated to pSMART-HCKan vector system (Lanes 1-6). PCR products (Lanes 7-12) obtained from the extracted plasmid DNA, using the pSMART-HCKan-specific primers SL1 and SR2. Lane M represents the DNA marker, GeneRuler™ Express DNA Ladder.

The extracted plasmid DNA was then used as a template for PCR using the CP-specific BFDV-1F; BFDV-1R primer pair (Figure 4.10). A band of 774 bp was expected, however a band size around 1.5 kb was seen which may have been plasmid DNA.

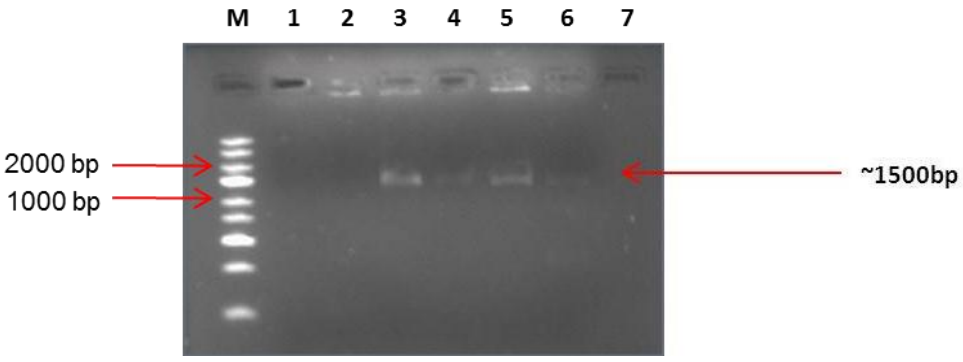

Figure 4.10. A 1% w/v agarose gel visualised under UV illumination indicating PCR amplification of the insert in the pSMART-HCKan vector using the primer set BFDV-1F; BFDV-1R. Lane 1 represents the DNA marker, GeneRuler™ Express DNA Ladder.

The extracted plasmid DNA was digested with *Nco*I and *Hind*III to remove inserts of ~774 bp from the 1788 bp pSMART-HCKan vector backbone, if the inserts had correctly ligated (Figure 4.11).

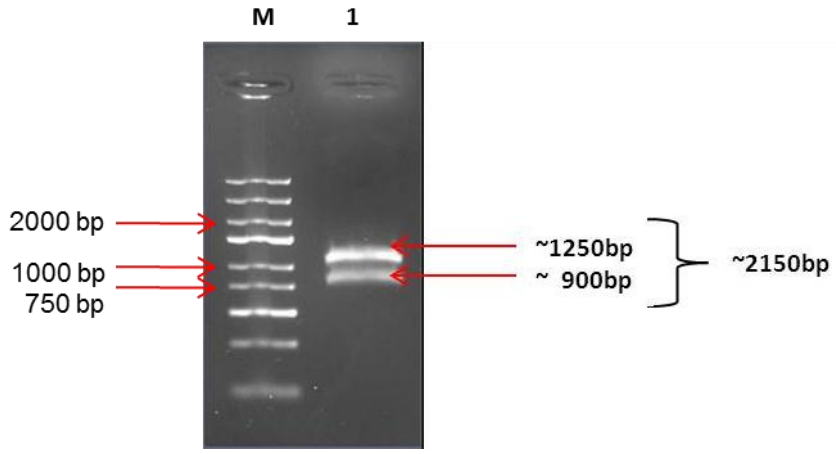

Figure 4.11. Plasmid isolates were cleaved with *Nco*I and *Hind*III to remove inserts of 774 bp from the 1788 bp pSMART-HCKan vector backbone (Lane 1). Lane M represents the DNA marker, GeneRuler™ Express DNA Ladder (Fermentas).

Two bands were obtained of approximately 1250 bp and approximately 900 bp in size, which did not correspond to the expected bands.

A plasmid map was generated which showed the position of the *Hind*III sites in the vector (Figure 4.12), and offers an explanation as to why the confirmation PCR with BFDV-1F; BFDV-1R gave an amplicon of ~1500 bp (Figure 4.10).

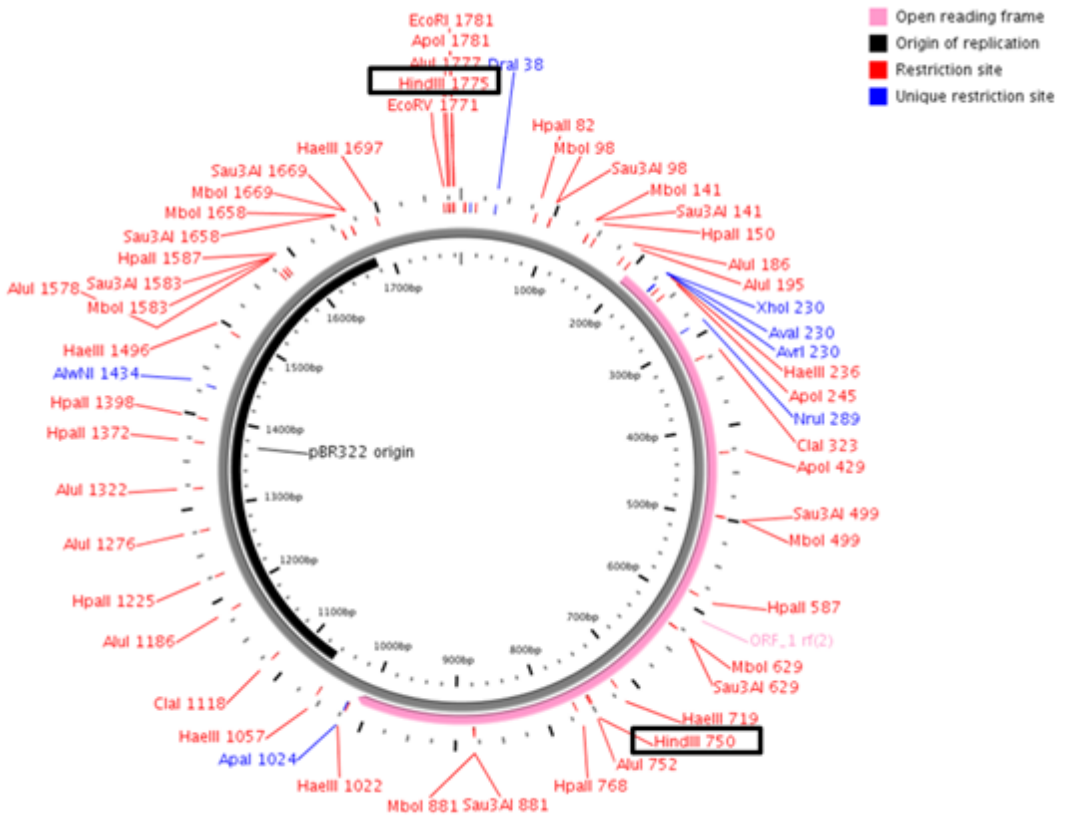

Figure 4.12. Plasmid map of the pSMART-HCKan sequence, indicating two *Hind*III sites. The *Hind*III site is not unique and is also found in the kanamycin resistance gene (750 bp). Created using plasmid mapper (Dong *et al*., 2004).

4.4 Discussion

Antigenic *BFDV* CP is needed in high quantities in order to establish reliable serological tests and vaccine options. This study set out with the aim of heterologously expressing *BFDV* CP in an *E. coli* expression system, for use in downstream serological test development.

The prediction of antigenic sites has implications in the design of serological tests and vaccine rationale. Therefore, antigenic predictions were conducted on the synthetic *BFDV* CP using two methods. The results using the Kolaskar and Tongaonkar method show that although there were around 10 predicted antigenic determinants; these peptides were not high above the threshold value of 1.000 (Figure 4.5 A; Table 4.17 A). This suggests that there the *BFDV* CP does not contain a high frequency of the hydrophobic residues, Cysteine, Leucine or Valine (Kolaskar & Tongaonkar, 1990).

BepiPred linear epitope prediction predicted the position of 13 B-cell epitopes in the *BFDV* CP (Figure 4.5 A; Table 4.17 B). B-cell epitopes are the sites of molecules that are

recognised by antibodies of the immune system therefore knowledge of B-cell epitopes may be advantageous in the design of vaccines and diagnostics tests (Larsen *et al*., 2006). This method makes use of a combination of a hidden Markov model and a propensity scale method by Parker and co-workers (1986) for each of the 20 amino acids. The scale consists of values assigned to each of the amino acid residues on the basis of their relative propensity to possess the property described by the scale. These properties hydrophilicity, flexibility, accessibility, turns, exposed surface, polarity and antigenic propensity of polypeptide chains (Larsen *et al*., 2006). The identified peptides found by the BepiPred linear epitope prediction have a high concentration of proline (P), glutamine (Q) and leucine (L) residues (Table 4.17 B). These residues have all been associated with linear epitopes (Sompuram *et al*., 2006). Previous research on this subject includes a study by Hattingh (2009), where *in silico* antigenic predictions, based on the determination of the location of ß-bends in multiple *BFDV* CP sequences, were used to show that genetic variance could possibly contribute to antigenic differences.

The synthesised *BFDV* CP gene was subsequently amplified by PCR, to introduce restriction sites in order to facilitate downstream cloning applications whilst removing the gene from the pINA1317-YlCWP110 vector.

The band of interest was obtained and subsequently purified; however, non-specific bands were also obtained (Figure 4.6.) due to the primers also binding to regions within the vector. The PCR was optimised with regards to annealing temperature and magnesium chloride concentration.

Although the primers were designed specifically for this sequence, various factors may have influenced the amplification. The annealing temperature that gave amplicons of the expected size was lower than the theoretically determined temperature. An annealing temperature that is too low may cause primers to bind nonspecifically to the template. Even though the ramp speed of the cycler was set at the maximum (3 °C/s), it may have still been too slow. Thus, allowing for spurious annealing to occur due to the lower temperature and sufficient time for nonspecific binding. The results also show that higher concentrations of magnesium increased nonspecific primer binding and intensity of unwanted products. Therefore, the PCR reaction was not supplemented with magnesium in subsequent amplifications.

Turning now to the experimental evidence on cloning into the pGEM®T Easy vector. The cloning was repeated on numerous occasions; the size of the undigested plasmid DNA obtained consistently gave bands of around ~2000 bp (Figure 4.7. A). This was unexpected, since the backbone of pGEM®T Easy is ~3015 bp in size and if the insert was included, the combined size of ~3800 bp should have been obtained. The integrity of the vector was

confirmed by ligating other genes into it, after which, the correct cloning products were obtained (data not shown).

Referring to Figure 4.7. (B) a band that corresponds to the expected size of the backbone of the vector can be seen (approximately 3 kb). In which case, the insert band is coincidentally double the size of the expected PCR product of (approximately 1.5 kb). It is theoretically possible, that high concentrations of insert relative to the vector could result in ligation of the insert to itself, and then the resultant product ligated to the vector.

Overall, cloning efficiency of PCR products is influenced by three factors: ligation efficiency, competent cells transformation efficiency and selection efficiency. Generally, selection of positive transformants is the limiting factor. Improving of this factor would therefore improve the entire cloning efficiency (Guo & Bi, 2002).

The type of antibiotic greatly impacts on selection efficiency. The vector pGEM®T Easy carries the gene for ampicillin resistance, serving as the basis for selection. Beta-lactamase expressed from the plasmid-borne *bla* gene hydrolyses and inactivates ampicillin. However, beta-lactamase is secreted by the bacteria causing a build-up of extracellular beta-lactamase. The selective pressure is consequently removed as the ampicillin is inactivated. In liquid cultures, possibly a large portion of the cells no longer have the plasmid, giving poorly yielding plasmid preparations. Alternatively, carbenicillin selection may be employed. It is also inactivated by beta-lactamase, albeit more slowly than ampicillin, therefore providing a far more effective means of selection (Corning, 2012).

In addition, blue-white screening may not be completely effective, as the vector may generate a dense background of blue colonies and many ambiguous light blue colonies. Blue-white selection works on the premise that positive recombinants interrupt the action of the *lacZ* gene. Consequently, β-galactosidase is no longer produced, giving rise to colonies that are white in colour. However, when the insert length is a multiple of 3 bp (including 3' A overhangs) and does not contain in-frame stop codons, positive transformants may be blue in colour. The initiation codon, CTG and stop codon, TAA were removed upon insertion of the restriction enzyme sites *Sfi*I (5') and *Hind*III (3'), for cloning in *Y. lipolytica*. The primer, BFDV-1R does not insert a stop codon. Consequently, a very high background of nonrecombinant clones were formed because all self-ligated vectors can be transformed and produce blue colonies. Blue colonies were selected and were found to not contain insert.

The subcloning strategy had to be rethought, as cloning in the pGEM®T Easy vector was unsuccessful. The pSMART-HCKan system (Lucigen) was chosen as it eliminates transcription both into and out of the insert DNA. It thus reduces cloning bias that is

commonly found with standard plasmids. In pGEM®T Easy, a strong promoter is used to transcribe the *lac*Z indicator gene. Plasmid instability caused by transcription of toxic coding sequences, strong secondary structure, or other deleterious features causes DNA cloned into these vectors to be lost. The pSMART vectors do not use a promoter or an indicator gene, so transcription across the insert is avoided. Conventional plasmids can also be lost due to accidental transcription from inserts containing *E. coli*-like promoters, which can cause instability by transcribing into essential regions of the vector. In pSMART vectors, strong transcription terminators flank the cloning site to block this transcription (Figure 4.4.), eliminating another cause of lost clones (Lucigen, 2013).

Figure 4.9. shows unexpected results, as neither of the two products obtained was anticipated. The band size of 2550 bp would correspond to the size of the plasmid DNA after ligation of the insert (~1,8 kb + 774 bp insert). A band of approximately 800 bp was expected after amplification with SL1 and SR2 primers. The results may also suggest that excess template was responsible for the anomalous results obtained.

The 100 bp band may have been due to the primers either amplifying a nonspecific product with the *BFDV* CP sequence, or the SL1 and SR2 sites on the vector.

Restriction enzyme sites are often incorporated into the amplification primers so that PCR products can have compatible restriction sites generated after restriction enzyme cleavage for cloning into compatible vectors. However, the possible secondary sites located within the amplified products often complicate the cloning and interpretation of results (Guo & Bi, 2002).

None of the screened Top10 *E. coli* colonies contained a recombinant plasmid that had a correctly inserted amplicon. In order for growth to occur in the presence of kanamycin, an insert must have been present in the pSMART-HCKan vector, which was subsequently transformed successfully into the cell. Kanamycin resistance of the Top10 *E. coli* is conferred only by the introduced vector. The linear pSMART-HCKan vector has deoxythymidine overhangs at the 3’ ends and therefore should theoretically not recircularise in the absence of insert. Yet, linear plasmids are unable to transform into bacteria. Therefore, the inability to detect positive recombinants was initially thought to be due to incorrectly inserted amplicon.

A plasmid map was generated which showed the position of the *Hind*III sites in the vector (Figure 4.12). This also then explained why the confirmation PCR, with BFDV-1F; BFDV-1R gave an amplicon of ~1548 bp. However, it was later discovered that the *Hind*III site is not unique in the pSMART-HCKan vector. There would, in fact, have been three sites present,

two situated within the vector (residues), one of which is present in the kanamycin resistance gene. During the restriction enzyme cleavage, the vector backbone was cleaved in the process. The other *Hind*III site was introduced using the primers. Sequencing results confirmed the absence of the insert.

Without being able to subclone the *BFDV* CP, the study was not able to proceed as planned and therefore experiments involving the expression of this protein in *E.coli* BL21(DE3), using the pET-28b(+) vector were not conducted. Despite reports of successful expression of *BFDV* CP, it is notoriously difficult to express this protein, especially in a bacterial system.

E. coli is one of the most widely used prokaryotic hosts for production of foreign proteins (Baneyx, 1999; Gustafsson *et al*., 2004; Jana & Deb, 2005). A high-level of protein expression can be achieved at minimal cost due to a large number of vectors and mutant host strains being readily available (Baneyx, 1999). However, the production of biologically active proteins in *E. coli* remains problematic due to the lack of post-translational modifications (Jana & Deb, 2005).

Alternatively, eukaryotic expression systems, including mammalian, yeast and insect cell systems could be used in place of a bacterial expression system as, protein modifications, processing and transporting occur in a manner similar to that of higher eukaryotes (Raidal *et al*., 2004).

Yeast cell-surface display is an attractive option for expression of heterologous proteins for various biotechnological and industrial applications (Bulani *et al*., 2012; Inaba *et al*., 2010). *Y. lipolytica* serves as an excellent host for expression of heterologous proteins, as it naturally secretes high amount of proteins and possesses a large range of genetic markers and molecular tools (Madzak *et al*., 2004). In addition, *Y. lipolytica* has GRAS (generally regarded as safe) status, and would not confer antibiotic resistance genes, as an expression cassette devoid of a bacterial moiety, was used to transform *Y. lipolytica* (Nicaud *et al*.,1998; Pignede *et al*., 2000). Furthermore, proteins heterologously expressed by means of cell-surface display are comparatively stable against environmental changes (Inaba *et al*., 2010).

The full length CP gene of *Beak and feather disease virus* was synthesised by GenScript (USA). This gene has been successfully cloned into the surface display plasmid (pINA1317-YlCWP110) of *Y. lipolytica* (Boucher, 2013, unpublished work). Both sources of protein have potential applications in serological diagnostics, and to serve as a novel strategy in the development of vaccines.

CHAPTER 5 DEVELOPMENT AND APPLICATION OF THE SLIDE AGGLUTINATION TEST AND COMPETITIVE ELISA FOR THE DETECTION OF ANTIBODIES AGAINST *BEAK AND FEATHER DISEASE VIRUS*

5.1 Introduction

The ability to detect antibodies against *Beak and feather disease virus* (*BFDV*) is essential to obtaining information on the serology of the virus as well as for diagnostic purposes. It lends importance to epidemiological studies; where the prevalence of infections and duration of the virus in a specific geographical location may be predicted. Consequently, the economic importance of the infection can be evaluated and possible control strategies may be identified.

Currently, *BFDV* infection may be diagnosed by a conventional PCR test, which detects and amplifies the ORF V1 (*rep*) in the *BFDV* genome (Ypelaar *et al*., 1999; Kondiah, 2004). However, PCR may be unreliable in diagnosing asymptomatic birds (Kondiah, 2004). Virus prevalence and sero-prevalence rates vary in literature, with the latter reported to be higher (Bert *et al*., 2005; Khalesi *et al*., 2005; Rahaus & Wolff, 2003).

The development of serological diagnostic tests has been hindered by the inability to cultivate *BFDV*. Despite these difficulties, various serological tests have been developed for the detection of antibodies against *BFDV*, including enzyme-linked immunosorbent assay (ELISA) and haemagglutination inhibition (HI) assays (Johne *et al*., 2004; Raidal *et al*., 1993b; Ritchie *et al*., 1991). Currently, HI is the only method available for the detection of anti-*BFDV* antibodies in psittacine sera. This assay detects both IgM and IgY antibodies from a wide range of species of psittacine birds, but it suffers from an appreciable amount of inter-test variation due to the variability in the agglutinating ability of *BFDV* isolated from different species, as well as amongst individuals of the same species (Sanada & Sanada, 2000).

The disease status or vaccine efficacy can be predicted by ELISA (Janeway *et al*., 2001). The most common types of the ELISA technique are:

(i) Direct ELISA

(ii) Indirect ELISA

(iii) Capture/Sandwich ELISA

(iv) Competitive ELISA.

With direct ELISA, antibodies are bound to the solid phase, detecting antigen in sera whereas indirect ELISA binds antigen to the solid phase so that antibody concentrations can be determined. In a capture or sandwich ELISA format, two antibodies with different specificities are required. The capture antibody is adsorbed to the plate, and the detection antibody is in solution (KPL, 2013).

The shortcoming of an existing indirect ELISA is that, it employs a secondary antibody directed against IgY from an African grey parrot (Johne *et al*., 2004). However, the cross-reactivity between IgY of different species is unknown (Shearer *et al*., 2009a). In essence, the validity of indirect ELISA results cannot be guaranteed especially when a sample from a rare species of psittacine bird is tested.

Consequently, a competitive ELISA is more likely to render reliable results. A competitive assay can be performed with either antigen or antibody adsorbed to the solid phase. However, in this case, an unknown amount of antibody from the sample and a secondary antibody would compete for binding to a limited number of antigens (KPL, 2013).

A competitive ELISA has been developed by Shearer and co-workers (2009a), using a baculovirus-expressed recombinant *BFDV* CP. The objective of this study was to design a competitive ELISA using recombinant *BFDV* coat protein (GenScript, USA) or using whole *Yarrowia lipolytica* cells expressing *BFDV* CP and a monoclonal antibody raised against this protein.

At present, a flock surveillance system for a rapid and simple diagnosis of *BFDV* infection does not exist. In the present study, a slide agglutination test was developed for rapid serological detection of birds exposed to *BFDV*.

5.2 Materials and Methods

A summary of the experimental procedure followed is shown in Figure 5.1.

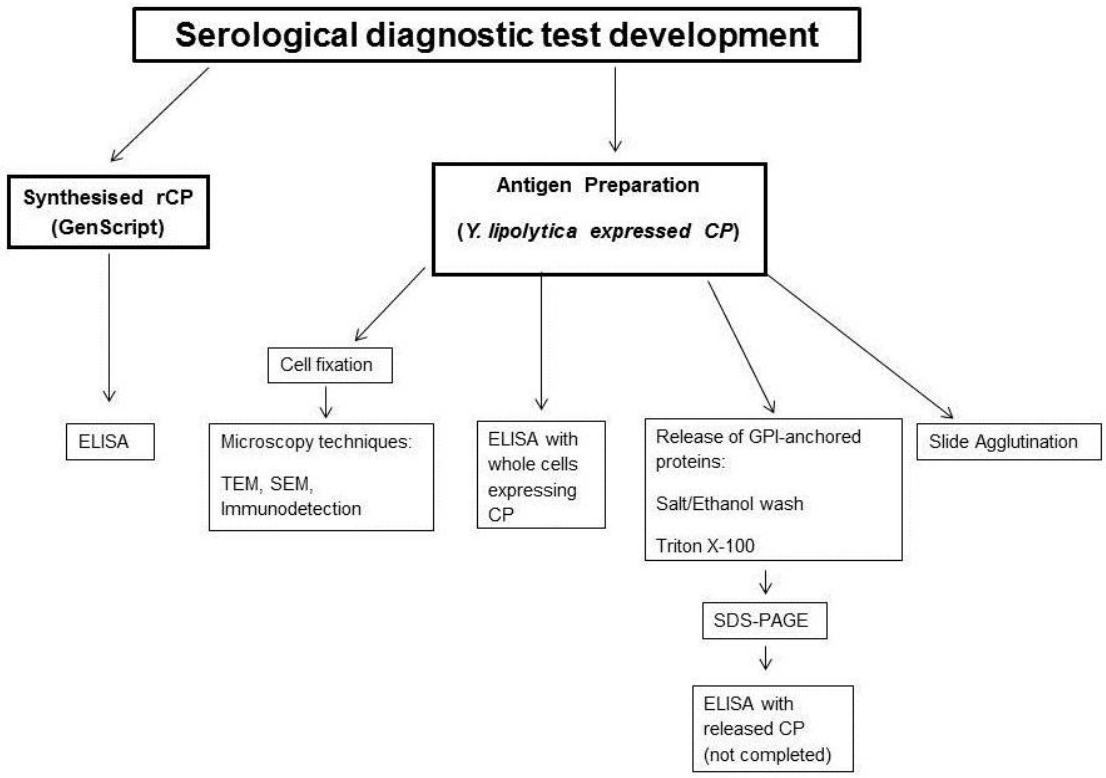

Figure 5.1. Summary of experimental procedure used in serological test development.

5.2.1 Antigen preparation

The putative coat protein has been shown to be a major antigenic determinant of *BFDV* (Stewart *et al*., 2007). A synthetic *BFDV* CP gene was designed, for heterologous expression based on published sequence data of a South African isolate [Genbank Accession number: AY450443]. Predicted antigenicity plots identified antigenic determinants on the CP using physico-chemical properties of amino acid residues and their frequencies of occurrence (Refer to Chapter 4, Figure 4.1).

Bacterial expression of *BFDV* CP was unsuccessful; however, *BFDV* CP was successfully cloned into the surface-display vector pINA1317-YlCWP110, containing the C-terminal end of the gene encoding the glycosylphosphatidylinositol cell wall protein (GPI-CWP1) from *Y. lipolytica*, strain Po1h (Boucher, 2013, unpublished work). The immobilised proteins on *Y. lipolytica*, strain Po1h served as the source of antigen in the slide agglutination test.

Yeast transformants, labelled Y16 and the untransformed *Y. lipolytica* strain Po1h, were inoculated into 5 ml YPD [1% (w/v) yeast extract, 2% (w/v) peptone, 2% (w/v) glucose] media and incubated overnight at 25 °C, as a pre-inoculum. YPD media (50 ml) was inoculated with 500 µl of pre-inoculum and incubated at 25 °C on a rotary shaker at a speed of 180 rpm, until the early stationary phase to determine a growth profile. The cultivation

broth occupied a volume equal to one tenth of the maximum volumetric capacity of the flask, to maximise oxygen transfer. Biomass was monitored by measuring optical density (OD_{600}) and samples (100 µl of culture supernatant) were taken at various time points (in hours). Yeast cells were collected and washed three times by centrifugation at 16 000 x *g* for 2 min, using phosphate-buffered saline PBS (pH 7.4). PBS (50 ml) was used as the antigen diluent.

5.2.2 *Y. lipolytica* Po1h cell fixation

Cells were fixed with the cross-linking fixative, formaldehyde, in order to preserve the protein in its spatial relationship to the cell (Thavarajah *et al*., 2012). The yeast cell pellet was collected by centrifugation (7000 x *g*; 10 min; at 4 °C), washed twice in sterile PBS (pH 7.4) and resuspended in 50 ml of PBS. Formaldehyde to a final concentration of 3% (v/v) was added and the suspension was left overnight at 4 °C. The formaldehyde was then removed by washing twice in PBS using centrifugation (7000 x *g*; 10 min; at 4 °C) (Eldar *et al*., 1997). The fixed cells were observed by microscopy techniques (Section 5.2.3; 5.2.4; 5.2.5) and the antigen stability was also tested by slide agglutination (Section 5.2.7).

5.2.3 Transmission electron microscopy (TEM) for detection of surface-displayed coat protein

Yeast transformant Y16 and untransformed *Y. lipolytica*, were prepared for TEM by re-suspending cell pellets in distilled water. A drop of sample solution was adsorbed to a copper 400 mesh Formvar carbon-coated grid and incubated for 1 min at RT. The cell suspension was then blotted off with Whatman filter paper. Samples were imaged at RT using a Philips CM100 (Eindhoven, The Netherlands) transmission electron microscope and operated at an acceleration voltage of 60 kV. Images were taken at a magnification of 10500 x.

5.2.4 Scanning electron microscopy (SEM) for detection of surface-displayed coat protein

Sample preparation for SEM involved washing of Y16 and untransformed *Y. lipolytica* cells in 0.1 M sodium phosphate buffer, pH 7.4. The cell pellets were re-suspended in the primary fixative, 3% (v/v) glutardialdehyde, for 7 days (van Wyk & Wingfield, 1991). The primary fixing can be done in a minimum of 3 hours to a maximum of 14 days. The cells were pelleted by low centrifugation and the pellet rinsed in 0.1 M sodium phosphate buffer to remove excess aldehyde fixative. Post-fixation was performed for 1 hour with 0.5 % (v/v) buffered osmium tetroxide. The suspension was washed twice with 0.1 M sodium phosphate buffer to remove excess osmium tetroxide. Dehydration by a graded ethanol sequence 50,

70, 95 and 100 % (x 2) for 30 min per step followed, while centrifugation took place between each dehydration step. The dehydrated cells, immersed in 100% ethanol, was placed in the pressure chamber and dried by critical point drying with carbon dioxide (CO_2). At the critical point equilibrium, no surface tensions exist between the liquid and the gas phases of CO_2. Samples were mounted on stubs, coated with gold in a SEM Coating System (Bio-Rad) and examined under a scanning electron microscope SEM (Shimadzu SSX-550 Superscan, Tokyo, Japan).

5.2.5 Immuno-detection of surface displayed coat protein

Cells were incubated on ice for 30 min with a monoclonal antibody (GenScript, USA) directed against the CP, as the primary antibody (1:50 diluted in PBS containing 2% bovine serum albumin). After washing with PBS, the secondary antibody, fluorescein isothiocyanate (FITC)-conjugated goat anti-mouse immunoglobulin G (IgG) [Sigma-Aldrich, USA], at a dilution of 1:200 in PBS with 2% BSA, was added and allowed to react with cells on ice for 30 min in the dark, in order to visualise the CP. Cells were washed with PBS to remove excess stain and fixed on microscope slides in DABCO (1,4-diazabicyclo[2.2.2]octane) (Sigma-Aldrich, USA). Indirect fluorescence of the immuno-stained yeast cells was observed by a confocal laser scanning microscope (CLSM, Japan) and photographed using a Nikon TE 2000.

5.2.6 Sample collection and serum extraction

Blood samples were obtained from birds housed at the Animal Facility, University of the Free State, Bloemfontein under Ethics approval number NR06/2013. Various species of psittacine birds, including: African Grey (*Psittacus erithacus*), Blue-fronted Amazon (*Amazona aestiva*), Brownheaded parrot (*Poicephalus cryptoxanthus*), Greyheaded parrot (*Psittacula finschii*), Golden-collared Macaw (*Primolius auricollis*) and Green-winged Macaw (*Ara chloropterus*), suspected to have naturally occurring anti-*BFDV* antibodies, were used to check the sensitivity of the antigen.

Blood was obtained for serum extraction, by pricking the brachial vein of the birds and collecting in a non-heparinised tube (Vacutainer®). The blood was allowed to clot at room temperature without disturbance, in a slanting position in order to obtain serum. Time, heat and vibration can haemolyse red blood cells, releasing mainly potassium and lactate dehydrogenase into the serum (Azoumanian, 2003).

The separated serum was collected in clean tubes to prevent deteriorating red blood cells from contaminating the serum. The serum was clarified by low speed centrifugation

(3000 rpm / 956 x *g* for 15 min), then stored at -20 °C until further use in slide agglutination and ELISA.

5.2.7 Slide agglutination test

Five day old culture of Y16 and the untransformed Po1h *Y. lipolytica* cell pellets were re-suspended in PBS, for use as the test antigen and mock antigen, respectively. All reagents were allowed to come to RT, so as to eliminate the possibility of aspecific reactions. The highest dilution of the antigen that gave clear agglutination with purified *BFDV* antibody raised in chickens (obtained from Livio Heath, University of Cape Town) was chosen for further use, as detailed below. A drop of the antigen (10 µl) was placed on a clean microscope slide, after which 10 µl of serum (Section 5.2.6) was added. The slide was rotated for 30 s and the presence or absence of agglutination was noted. A serum sample was considered positive when clear agglutination was observed, as easily visible clumps, whereas the absence of agglutination was interpreted as negative for *BFDV* antibodies. A scale (adapted from Kwapinski, 1972) was used to interpret agglutination results, and is portrayed in Table 5.1.

Table 5.1. Interpretation of the Slide Agglutination Test.

Amount of agglutination (%)	Degree of Agglutination
100	4+
75	3+
50	2+
25	1+
Trace	±
No agglutination	-

The agglutination reactions were photographed and to further illustrate the visual reaction, imaging was performed using a Nikon Eclipse 50i microscope with digital camera accessory (Nikon DS-Fi1-U2).

To evaluate both the repeatability and reproducibility, three parallel experiments were conducted for each serum sample. Specificity and sensitivity of *BFDV* CP antigen were evaluated with samples of serum from various parrot species; including African Grey parrot,

Blue-fronted Amazon parrot, Brownheaded parrot, Greyheaded parrot, Golden-collared Macaw and a Green-winged Macaw.

These birds were donated to the animal housing facility as they had been diagnosed as *BFDV* positive by PCR. To determine the specificity of the diagnostic antigen, chicken serum was also tested in the method above. The test was standardised using known anti-*BFDV* antibodies, as a positive control and untransformed *Y. lipolytica* Po1h as a negative control for *BFDV*.

5.2.8 Optimisation of the indirect Enzyme-Linked Immunosorbent Assay (ELISA) using purified recombinant coat protein (rCP) as coating antigen

Various dilutions of the recombinant coat protein (rCP) from GenScript [0.5, 0.75, 1.0, 1.25, and 1.5 $\mu g.ml^{-1}$] in 50 mM carbonate buffer (pH 9.6), were applied to wells of a 96-well Costar® polypropylene ELISA plate. The plate was allowed to coat at 4 °C overnight, following which, it was washed thrice, with wash buffer (PBS, 0.05% (v/v) Tween 20). Blocking buffer (PBS, 0.05% (v/v) Tween 20, 5% (w/v) skim milk powder) was added to all wells and the plate incubated for 90 min at RT. After washing the protein coated plates twice, the monoclonal antibody was prepared (10 $\mu g.ml^{-1}$) in blocking buffer and diluted by checkerboard titration. Referring to Figure 5.2, the monoclonal antibody was prepared (10 $\mu g.ml^{-1}$) in blocking buffer and added to well A1 and a two-fold serial dilution was performed across the plate (A1-A12); a two-fold serial dilution was then performed down the plate (A1-H1; A2-H2 D1-12 etc.).

The plates were incubated for 1 hour at 37 °C, with shaking. After washing thrice again, the Anti-Mouse: Horseradish Peroxidase (Sigma), raised in goat, was diluted in blocking buffer (1:10 000) and 50 µl of anti-mouse IgG was added to each well. The plate was incubated at 37 °C with shaking for 1 hour, washed three times with 100 µl of PBST and 50 µl of substrate 3,3′,5,5′-Tetramethylbenzidine (TMB) was added to each well. Colour development was allowed to occur for 10 min and the reaction was stopped by the addition of 50 µl of 2N H_2SO_4. Readings were taken at 450 nm using an ELISA plate reader (ELx800, BioTek).

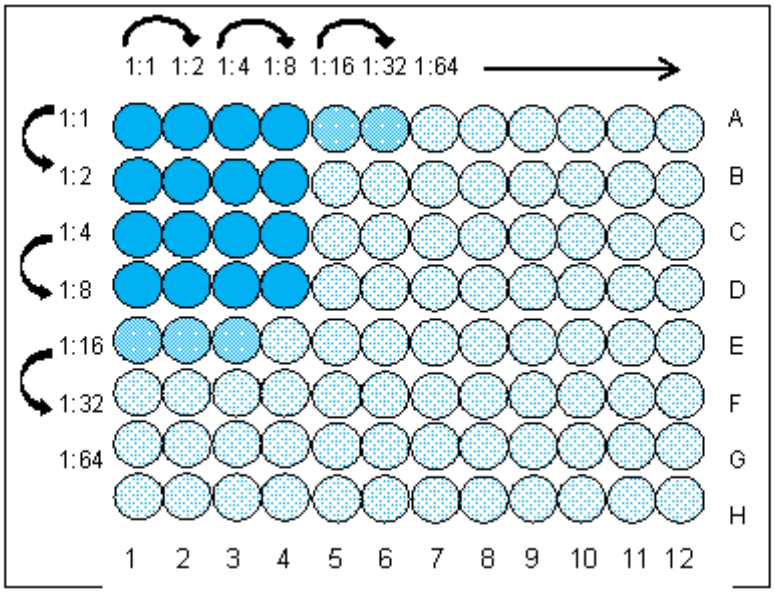

Figure 5.2. Diagram showing checkerboard titration of monoclonal antibody to determine the lowest concentration that would give the highest reactivity. The monoclonal antibody was prepared (10 µg.ml^{-1}) in blocking buffer and added to well A1 and a two-fold serial dilution was performed across the plate (A1-A12); a two-fold serial dilution was then performed down the plate (A1-H1; A2-H2 D1-12 etc.).

5.2.9 Indirect Competitive Enzyme-Linked Immunosorbent Assay (ELISA) using purified recombinant coat protein (rCP) as coating antigen

An optimal concentration of 1.5 µg.ml^{-1} rCP (GenScript) diluted in PBS (pH 7.4) was used in a competitive indirect ELISA to test serum samples collected as described in Section 5.2.1. The PolySorp® plate (Nunc, Denmark) was evaluated along with two different coating buffers, PBS (pH 7.4) and 50 mM carbonate/bicarbonate (pH 9.6). After blocking, 50 µl of serum, diluted 1:100 was added to each well. The plates were incubated; washed and 50 µl (1.0 µg.ml^{-1}) monoclonal antibody diluted in blocking buffer was applied to the wells. The plates were incubated; washed and anti-mouse IgG horseradish peroxidase (HRPO) (Sigma-Aldrich, USA) diluted 1:10 000 was added to each well. After incubation for one hour at RT and washing, positive reactors were visualised using the substrate (TMB). The plates were incubated at RT (23 °C) in the dark for 30 min and the absorbance values were read at 450 nm, using an ELISA plate reader (ELx800, BioTek). The absorbance was corrected for each test serum, as depicted in Section 5.3.7.

5.2.10 Optimisation of the indirect Enzyme-Linked Immunosorbent Assay (ELISA) using whole *Yarrowia lipolytica* Po1h cells

The yeast transformants, Y16 and the untransformed *Y. lipolytica* strain Po1h, were cultured as detailed in Section 5.2.1. The cells were pelleted by centrifugation (16 000 x *g* for 2 min) and the pellet washed twice with phosphate-buffered saline (PBS) (pH 7.4). PBS (50 ml) was used as the antigen diluent. A volume of 100 µl of cells in PBS was applied to the wells of a 96-well microtiter Polysorp plate (Nunc Immunoplate, Denmark). PBS was used as a background control and the untransformed *Y. lipolytica* strain Po1h cells were used as a negative control. The indirect ELISA was performed in the same manner as stated above, in Section 5.2.8. Blocking buffer (PBS, 0.05% (v/v) Tween 20, 5% (w/v) skim milk powder) was added to all wells and the plate incubated for 90 min at RT. The monoclonal antibody was prepared (1 µg.ml^{-1}) in blocking buffer and 50 µl was added to all the wells. The plate was incubated for 1 hour at 37 °C, with shaking. After washing thrice again with wash buffer, the (Goat) Anti-Mouse: Horseradish Peroxidase (Sigma) was diluted in blocking buffer (1:10 000) and 50 µl of anti-mouse IgG was added to each well. The plate was incubated at 37 °C with shaking for 1 hour, washed three times with 100 µl of PBST and 50 µl of substrate TMB was added to each well. Colour development was allowed to occur for 10 min and the reaction was stopped by the addition of 50 µl of 2N H_2SO_4. Readings were taken at 450 nm using an ELISA plate reader (ELx800, BioTek).

Further optimisation of this assay included, monoclonal antibody optimisation and anti-mouse IgG optimisation.

<u>Assay I: Monoclonal antibody optimisation</u>

The assay was repeated, however, the monoclonal antibody concentration was optimised by checkerboard titration (Figure 5.2). Briefly, the monoclonal antibody was prepared (10 µg.ml^{-1}) in blocking buffer and added added to well A1 and serially diluted down the plate (B1-H1); serial dilution then occurred across the plate (B1-12; C1-12; D1-12 etc.). Readings were taken at 450 nm using an ELISA plate reader (ELx800, BioTek).

<u>Assay II: Anti-mouse IgG optimisation</u>

The assay was repeated as detailed in Section 5.2.10, however, various anti-mouse IgG concentrations were tested (1 in 5000; 1 in 2500; 1 in 1750 and 1 in 1500). The monoclonal antibody concentration used in this assay, was the concentration determined by Assay I. Readings were taken at 450 nm using an ELISA plate reader (ELx800, BioTek).

Statistical analysis

Optical density values are absolute measurements that are influenced by variables such as temperature and evaporation. To account for variability, results can be expressed as a function of the reactivity of control samples included in each run. Therefore, absorbance or OD values were expressed as percentage positive (PP) relative to a high positive control serum. The following statistical calculations were used:

- Optical density (OD): Net OD = OD in wells with virus antigen minus OD in wells with control antigen
- Percent positivity (PP): PP = (Mean net OD of test sample / mean net OD of +control) x100

Statistical analysis, calculating the standard deviation and showing the minimum and maximum absorbance values, and the range between the two was also performed with IBM SPSS Statistics, version 21 (SPSS, IBM Corp; 2012).

5.2.11 GPI-anchored protein release for use as an ELISA antigen

Five day old transformants, Y16 and the untransformed *Y. lipolytica* strain Po1h, were cultured as detailed in Section 5.2.1. The Y16 cells were treated by salt/ethanol wash (Muller *et al*., 2012) as well as a detergent wash (Azzouz *et al*., 1990; Yano *et al*., 2003) so as to release the *BFDV* CP from the cell surface for use as an antigen in the development of ELISA.

For the salt/ethanol wash, 5 day old culture was centrifuged and re-suspended in the culture medium to a total volume of 90 µl. Then, 240 µl of salt/ethanol [10 mM Na_2HPO_4, 150 mM NaCl, 30% ethanol (v/v)] and Complete™ Protease Inhibitor Cocktail (Roche, Mannheim, Germany) was added, according to manufacturer's instructions. The mixture was incubated in an ice bath for 1 hour, where after, the suspension was centrifuged at 2000 rpm / 475 x *g* for 3 min and the supernatant was removed. A volume of 240 µl cold acetone was added to the supernatant for protein precipitation. The samples were kept on ice for 10 min and then centrifuged at 16 000 x *g* at 4 °C for 10 min. The pellets were washed twice with cold acetone, dried and subsequently re-suspended in 50 µl of H buffer (20 mM Tris-HCl (pH 7.4), 1 mM EDTA, 25 mM KCl, 50 mM sucrose).

For the isolation of proteins by means of a detergent, 5 day old cells were treated with 1.3% Triton X-100 in 50 mM Tris–HCl, pH 7.5 with Complete™ Protease Inhibitor Cocktail (Roche,

Mannheim, Germany). Triton X-100 is the preferred detergent for isolation of membrane proteins. It is a mild surfactant that breaks protein-lipid and lipid-lipid associations but not protein-protein interactions. Therefore, proteins are solubilised and isolated in their native and active form, retaining their structure. Extraction was carried out for 1 hour on ice. Cells were then carefully pelleted (500 x *g*) to avoid lysis. Proteins were subsequently precipitated with cold acetone dried and subsequently re-suspended in 50 ul of H buffer (composition supplied above).

5.2.12 Detection of *BFDV* CP by SDS-polyacrylamide gel electrophoresis

Sodium dodecyl sulphate polyacrylamide gel electrophoresis (SDS-PAGE) of the samples was performed as described by Laemmli (1970). The 10 % (w/v) resolving gel was prepared using: 2.33 ml 30% acrylamide solution/ 0.8% bisacrylamide stock solution (Bio-Rad), 1.75 ml 1.5 M Tris-HCl pH 8.8 containing 0.4% SDS, 60 µl 10% ammonium persulfate (APS), 13 µl TEMED and distilled H_2O up to a final volume of 10 ml.

As polymerisation occurs as soon as TEMED is added, the mixture was quickly swirled and pipetted into the casting frame and allowed to set. A layer of distilled water was applied to the top of the resolving gel before polymerisation occurred which took approximately 15 minutes. The overlay prevents oxygen from diffusing into the gel and inhibiting polymerisation. After the resolving gel solidified, the layer of water was discarded (Sambrook & Russel, 2006).

The concentration of APS used was higher than that recommended by other researchers, eliminating a degassing step to rid the acrylamide solution of dissolved oxygen (Sambrook & Russel, 2006).

A 4.2% (w/v) stacking gel was prepared with 280 µl 30% acrylamide solution/0.8% bisacrylamide stock solution, 500 µl 1M Tris-HCl (pH 6.8) stock solution containing 0.4% SDS, 10 µl 10% ammonium persulphate, 8 µl TEMED and distilled H_20 up to a final volume of 2 ml. The stacking gel was applied to the top of the resolving gel and the comb inserted before polymerisation occurred for approximately 10 min. The stacking gel sweeps up proteins in a sample between two moving boundaries, thereby compressing by the time it reaches the resolving gel.

The protein samples were prepared as follows: 10 µl protein sample, 10 µl of 2x protein loading buffer (62.5 mM Tris-HCl, pH 6.8, 2% SDS, 0.01% Bromophenol blue, 25% glycerol) and 5% β-Mercaptoethanol, as the reducing agent. The samples were heated for 5 min at

95 °C. Prestained protein marker (Precision Plus Protein Standards, Bio-Rad) comprising proteins ranging in size from 10 to 250 kD proteins was used to determine the size of the expressed protein. Protein samples were loaded onto the gel and subjected to electrophoresis at 100 V for 120 min, in 1× Tris-Glycine-SDS electrophoresis buffer (25 mM Tris, 192 mM glycine, 0.1% SDS, pH 8.3) (Bio-Rad). The SDS-PAGE gel was subsequently stained overnight with Bio-Safe Coomassie [45% methanol, 10% glacial acetic acid, 0.2% Coomassie Brilliant Blue] (Bio-Rad) with gentle shaking. The gel was then de-stained with distilled water for at least 4 hours at RT with gentle agitation; whereafter, it was viewed under white light with the Biorad Gel Doc™ EZ Imager system.

For increased sensitivity, silver staining was employed to detect bands present in low concentrations.

The solutions in Table 5.2 were used in the silver staining protocol.

Table 5.2. Reagents used in silver staining gel protocol (University of Rochester Proteomics Centre, 2009).

Silver staining solutions	
Fixing solution	40% ethanol/10% acetic acid
Sensitising solution	30% ethanol/0.2% sodium thiosulphate/6.8% sodium acetate
Silver nitrate solution	0.25% silver nitrate in water
Developing solution	2.5% sodium carbonate/0.15% formaldehyde (formaldehyde added immediately before use)
Stop solution	5% acetic acid
Destain solution	
Farmer's reducer	30 mM potassium ferricyanide (9.876 mg/ml); 100 mM sodium thiosulphate combined in a 1:1 ratio.

The gel was placed in fixing solution and shaken for 1 hour, after which it was drained. The gel was covered with sensitising solution and shaken for 30 min. Upon removal of the sensitising solution, the gel was washed thrice with distilled water (5 min each time). The silver nitrate solution was added and the gel shaken for 20 min. The wash step was repeated twice with distilled water (1 min each time). Developing solution was added to the gel and shaken until a brown precipitate appeared. The developing solution was poured off and fresh developer added, continuing as needed until the intensity of bands increased. After draining the developing solution, stop solution was added with shaking for 10 min. Following the removal of the stop solution, the gel was washed thrice with distilled water (5 min each time).

The image was acquired using the silver staining protocol with the Biorad Gel Doc™ EZ Imager system.

5.3 Results

5.3.1 Antigen preparation

Y. lipolytica Po1h (Y16) and untransformed *Y. lipolytica* Po1h were grown for 20 hours under aerobic conditions until the early stationary phase (Figure 5.3). The plasmid carried by the Po1h strain employs the growth-phase dependent promoter, hp4d, which heterologously expresses proteins as the cells enter the stationery phase (Nicaud *et al*., 2002; Madzak *et al*., 2004). Therefore, it is necessary to determine the time the cells would enter the stationary phase. Furthermore, it is important to note the phase in which the cells are, as the production of secondary metabolites places the cells under environmental stress. The effect of the environmental stress on the expressed protein is unknown.

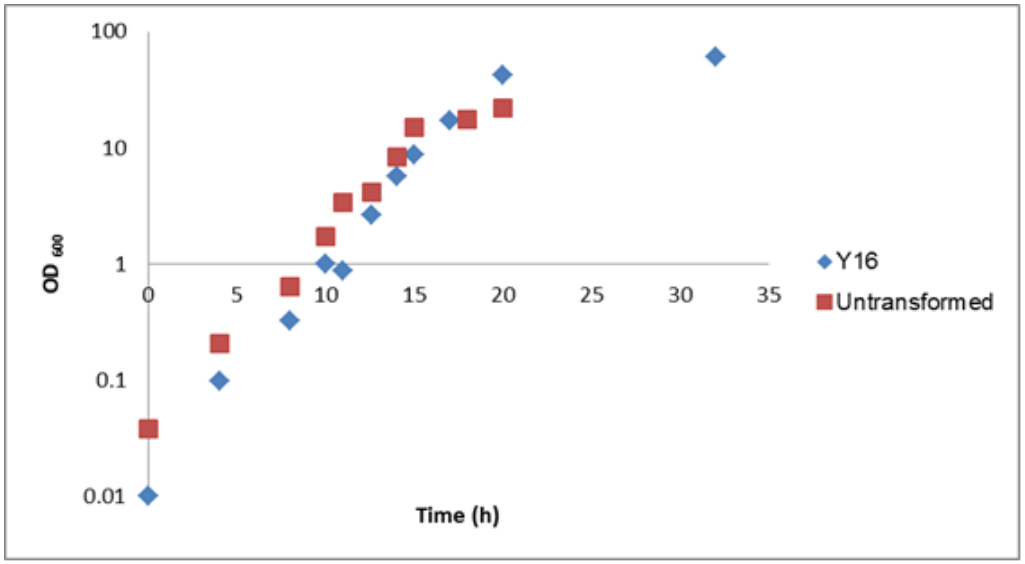

Figure 5.3. Time course depicting cell growth of transformed *Yarrowia lipolytica* Po1h, Y16 and untransformed *Yarrowia lipolytica* Po1h until the early stationary phase.

5.3.2 Transmission electron microscopy for detection of surface-displayed coat protein

Transmission electron microscopy showed transformed *Y. lipolytica* Po1h cells with protrusions on the cell surface (Figure 5.4. A), whilst untransformed *Y. lipolytica* Po1h cells had a smooth cell wall surface (Figure 5.4. B). These differences may be attributed to the presence of the *BFDV* CP being displayed on the cell wall.

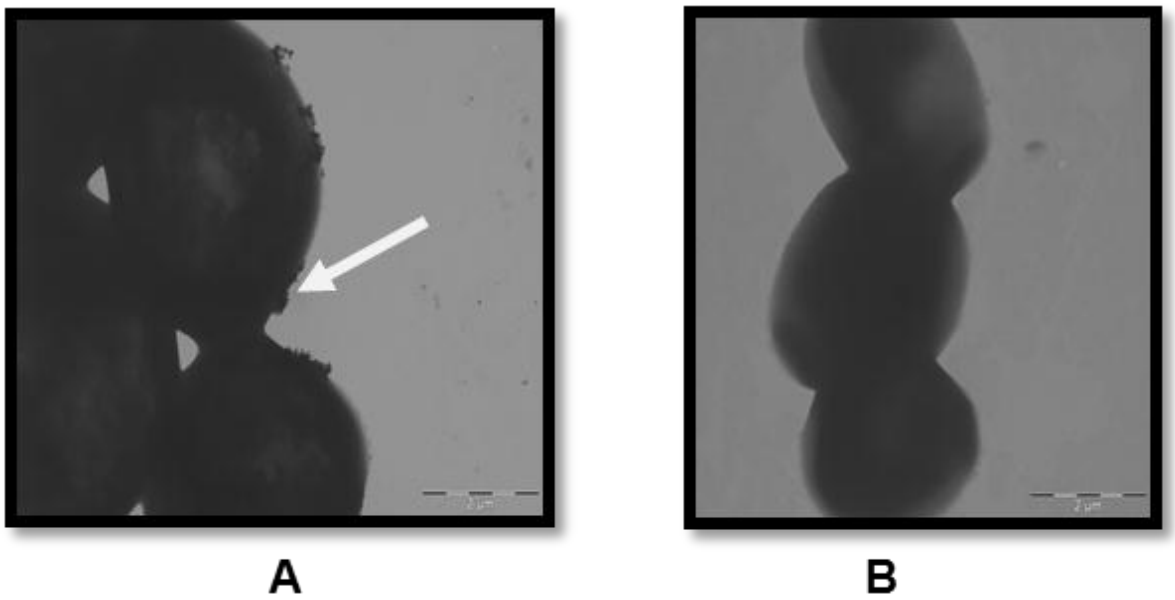

Figure 5.4. Transmission electron micrograph of (A) transformed *Y. lipolytica* Po1h; showing protrusions on the cell surface, as indicated by the arrow and (B) untransformed *Y. lipolytica* Po1h, with a smooth cell wall surface. Scale: 2 µm.

5.3.3 Scanning electron microscopy for detection of surface-displayed coat protein

Scanning electron microscopy showed transformed *Y. lipolytica* Po1h cells with a mesh-like substance between cells (Figure 5.5. A), whilst untransformed *Y. lipolytica* Po1h cells did not display this phenomenon (Figure 5.5. B). The synthetic *BFDV* CP contains a total of 112 hydrophobic residues, with a high distribution of phenylalanine (17), isoleucine (16) and leucine (15) residues as analysed with CLC Main Workbench, 6.6.1. These amino acids tend to cluster together in order to exclude water molecules, this may explain the presence of the mesh-like substance observed with the transformed *Y. lipolytica* cells as illustrated in Figure 5.5. A.

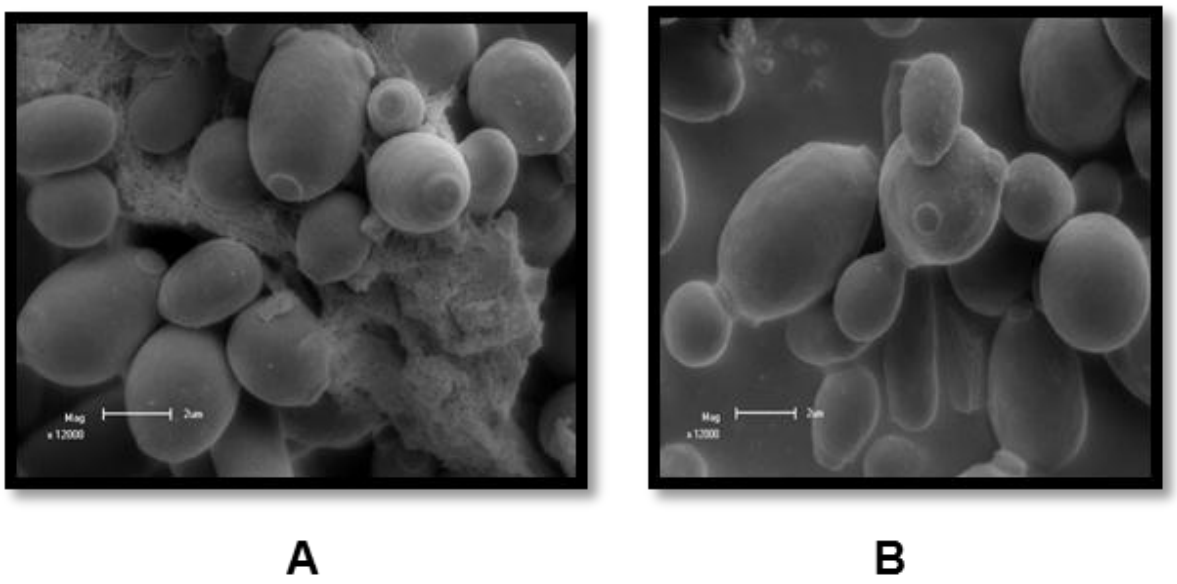

Figure 5.5. Scanning electron micrographs of (A) transformed *Y. lipolytica* Po1h, showing a mesh-like substance and (B) untransformed *Y. lipolytica* Po1h, with a smooth cell wall surface. Scale: 2 µm.

5.3.4 Immuno-detection of surface displayed coat protein in *Yarrowia lipolytica*

Immunofluorescent labelling of yeast cells was performed using a mouse-raised monoclonal antibody (GenScript, USA) directed against the CP and fluorescein isothiocyanate (FITC)-conjugated goat anti-mouse immunoglobulin G (IgG). As FITC has excitation and emission spectrum peak wavelengths of approximately 495 nm and 519 nm (Janeway *et al*., 2001), images were observed by fluorescence microscopy using a blue or green filter.

Transformed *Y. lipolytica* Po1h (Y16) cells expressing *BFDV* CP exhibited fluorescence (Figure 5.6. A-D). However, the untransformed *Y. lipolytica* Po1h cells did not show any immunofluorescence (Figure 5.6. E-H). The fluorescence seemed to be intracellular rather than surface-based, showing that the protein had not yet been directed to the cell surface in the 3 day old cells used. Therefore, 5 day old cells were used in succeeding diagnostic tests to ensure maximum cell-surface display of *BFDV* CP.

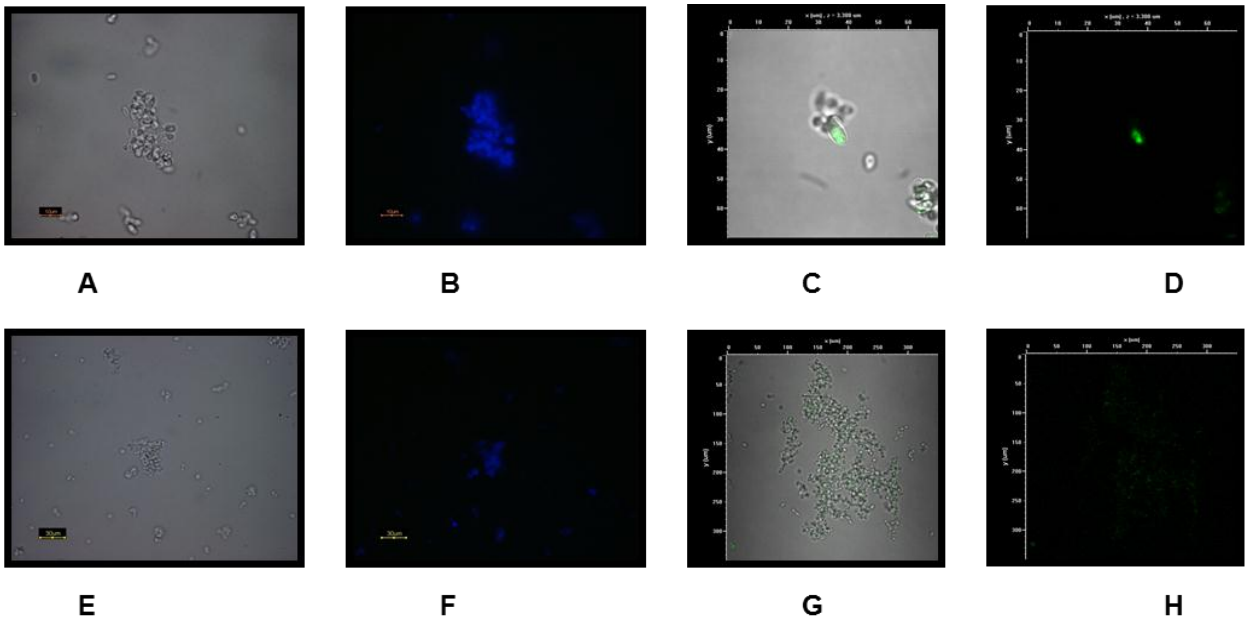

Figure 5.6. (A-D) Immuno-detection of surface-displayed *BFDV* CP on transformed *Y. lipolytica* strain Po1h shows fluorescence. **(E-H)** Immuno-detection performed on untransformed *Y. lipolytica* strain Po1h, shows limited fluorescence, in relation to transformed *Y. lipolytica* strain Po1h.

5.3.5 Slide Agglutination test

The controls formed part of every test. Untransformed *Y. lipolytica* Po1h and test serum was used as the negative control. No agglutination was seen with untransformed *Y. lipolytica* Po1h and each serum tested (Figure 5.7. A). The positive control was transformed *Y. lipolytica* Po1h, denoted Y16, and known positive *BFDV* antibodies (Figure 5.7. B). Agglutination was visible to the naked eye and can be seen as a dark mass under the microscope.

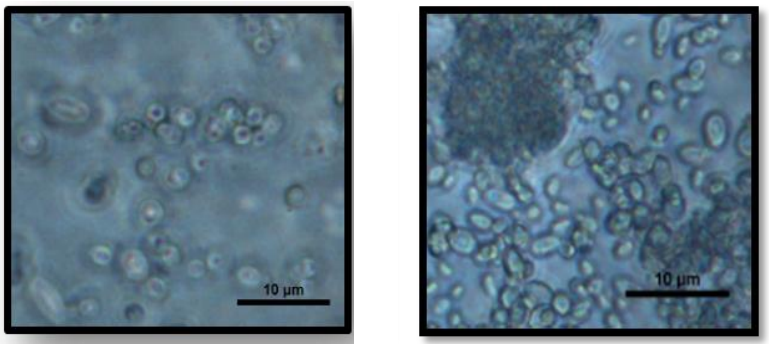

Figure 5.7. Agglutination reactions observed with a Nikon Eclipse 50i microscope (Nikon Cooperation, Tokyo) and digital camera accessory (Nikon DS-Fi1-U2). A) Negative control: Untransformed *Y. lipolytica* Po1h and test serum and B) Positive control: Transformed *Y. lipolytica* Po1h, denoted Y16, and known positive *BFDV* antibodies. Scale: 10 µm.

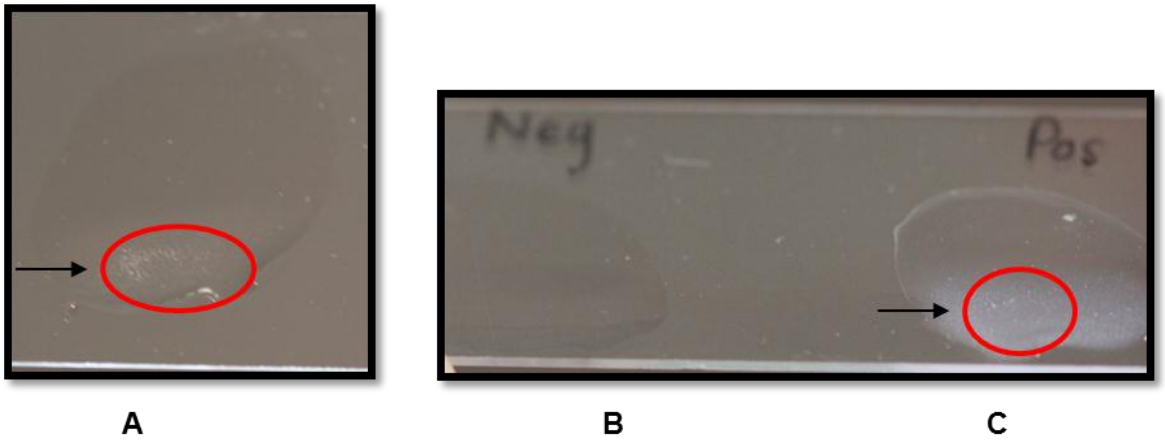

Figure 5.8. Visual reactions of the slide agglutination test observed with. A) Transformed *Y. lipolytica strain* Po1h and test serum of a golden-collared Macaw, showing positive slide agglutination test result B) Negative control: Untransformed *Y. lipolytica strain* Po1h cells and test serum C) Positive control: Transformed *Y. lipolytica strain* Po1h and known positive *BFDV* antibodies.

Visual reactions of the slide agglutination test are shown. A positive slide agglutination test was observed with transformed *Y. lipolytica* strain Po1h and test serum of a golden-collared Macaw (Figure 5.8. A). Untransformed *Y. lipolytica* strain Po1h cells and test serum formed the negative control (in Figure 5.8.B). Transformed *Y. lipolytica* strain Po1h and known positive *BFDV* antibodies formed the negative control in Figure 5.8.C.

Six species of parrots were part of this study and all except the Golden-collared Macaw and Green-winged Macaw were housed at the animal housing facility, UFS, Bloemfontein (Table 5.3). The birds that were housed at the UFS had a history of *BFDV* infection, as they tested positive by PCR before being donated by bird breeders. All of the birds tested positive by slide agglutination, therefore showing that the test detected antibodies against *BFDV* in all parrots.

Table 5.3. Various parrot species used in this study. The clinical symptoms were noted and the results of the slide agglutination test and PCR test are shown. The observation of clinical symptoms correlated with PCR results. All birds tested in this study showed the presence of anti-*BFDV* antibodies.

Species	**Clinical symptoms**	**Results**		
		Degree of Agglutination	Sero-status	PCR Diagnosis
African Grey parrot (*Psittacus erithacus*)	Absent	4+	+	-
Blue-fronted Amazon parrot (*Amazona aestiva*)	Claw deformities	3+	+	+
Brownheaded parrot (*Poicephalus cryptoxanthus*)	Absent	2+	+	-
Greyheaded parrot (*Psittacula finschii*)	Absent	3+	+	-
Golden-collared Macaw (*Primolius auricollis*)	Absent	3+	+	-
Green-winged Macaw (*Ara chloropterus*)	Absent	3+	+	-

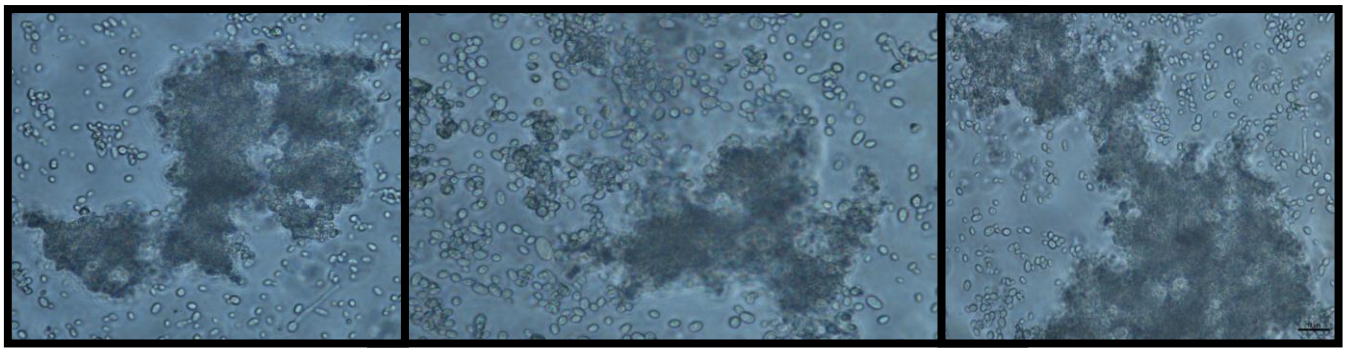

A **B** **C**

Figure 5.9. Agglutination reactions observed with a Nikon Eclipse 50i microscope (Nikon Cooperation, Tokyo) and digital camera accessory (Nikon DS-Fi1-U2). Test serum obtained from A) Greyheaded parrot B) Brownheaded parrot C) Blue-fronted Amazon parrot, respectively. Scale: 10 µm.

The African Grey parrot showed the highest degree of agglutination of all the birds tested. This bird did not show any clinical symptoms, which may be attributed to an elevated amount of protective antibodies (Table 5.3). It is important to note the higher degree of agglutination seen with the Blue-fronted Amazon parrot (Figure 5.9. A & B), as compared to the

Brownheaded and Greyheaded parrots, respectively. The birds at the UFS were re-tested by PCR at the time of slide agglutination testing and only the Blue-fronted Amazon parrot (*Amazona aestiva*) tested positive by PCR. Viral DNA may have been absent in the blood of the birds that tested negative. It is interesting to note that the Blue-fronted Amazon parrot was the only bird housed at the UFS, to display clinical symptoms in the form of claw deformities (Table 5.3.). It can be speculated that this bird may have been actively fighting off infection at the time of testing.

Chicken serum was tested, in order to determine the specificity of the test antigen. Initially, a positive agglutination test was observed with chicken serum, suggesting that the antigen was aspecific, as seen in Figure 5.10. (A). The serum was obtained from chickens that were housed next to the birds used in this study. As the virus is extremely environmentally stable, the chickens were accidentally exposed to *BFDV* and had produced anti-*BFDV* antibodies, even though *BFDV* does not infect chickens. This further reiterates how resistant the virus is to disinfectants, and the role proper bio-security plays in restricting the spread of the virus.

Serum from chickens (from a farm in Glen, Bloemfontein), that had not been exposed to *BFDV* was then used to test the specificity of the test antigen and a negative agglutination test was obtained, as seen in Figure 5.10 (B). Thus, the expressed antigen is *BFDV* CP and is specific for anti-*BFDV* antibodies.

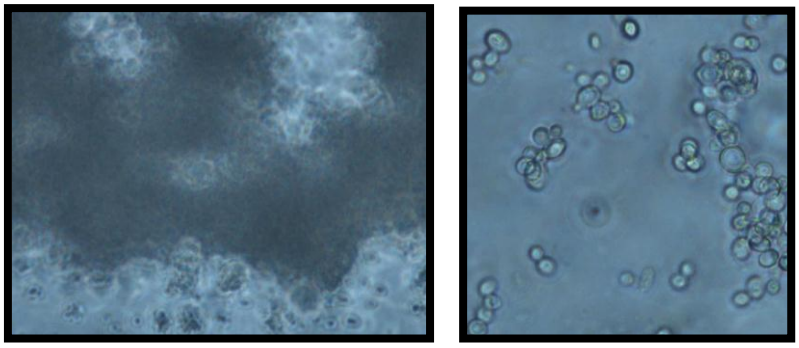

A **B**

Figure 5.10. Agglutination reactions of A) Chicken serum displaying positive slide agglutination test result, presence of anti-*BFDV* antibodies in chicken serum and B) Naïve chicken serum where the absence of agglutination is noted. Scale: 10 µm.

Agglutination ability of *Y. lipolytica* Po1h, Y16 cells decreases with an increase in age. A high degree of agglutination was seen when fresh yeast cells were used (Figure 5.11. A) and the reaction could be visualised with the naked eye. However, a loss in slide agglutination

activity was observed when Y16 cell pellets are stored at 4 °C for extended periods of time, as can be seen in Figure 5.11. (B).

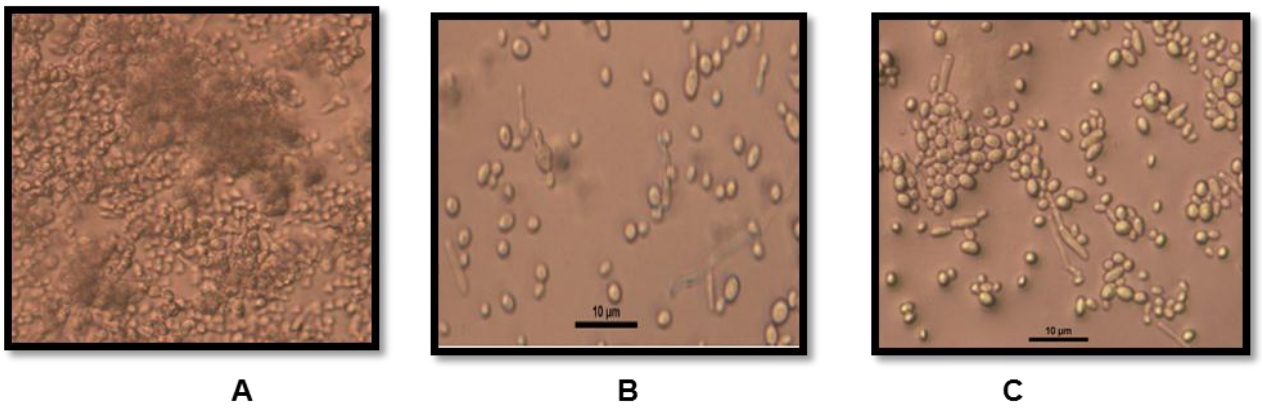

Figure 5.11. A) Fresh *Y. lipolytica* Po1h, Y16 cells and positive serum with agglutination ability intact. B) Unfixed *Y. lipolytica* Po1h, Y16 cells, showing hyphal structures and a loss in agglutination ability. C) Formaldehyde-fixed *Y. lipolytica* Po1h, Y16 cells, also showing hyphal structures and a very low degree of agglutination. Scale: 10 µm.

When Y16 cells were fixed with formaldehyde and stored at 4 °C for the same amount of time, trace amounts of agglutination were observed, which could only be visualised under the microscope, as seen in Figure 5.11. C. Fixation with formaldehyde did not completely prevent a loss in agglutinating ability, suggesting that the cells had been placed under environmental stress. The fixation did not prevent a transition to the hyphal stage which may potentially damage the protein or even prevent it from being displayed on the cell surface (Figure 5.11.).

5.3.6 Optimisation of the indirect Enzyme-Linked Immunosorbent Assay (ELISA) using purified recombinant coat protein (rCP) as coating antigen

In order to optimise antigen and antibody concentrations, an indirect ELISA was performed. The recombinant protein, that was experimentally produced by GenScript, USA (rCP) was diluted to various concentrations and applied to wells of the ELISA plate, along with various dilutions of monoclonal antibody. The optimal amount of protein used in the indirect ELISA was determined to be 1.5 $\mu g.\mu l^{-1}$ and the optimal concentration of monoclonal antibody was 1 $\mu g.\mu l^{-1}$ as seen in Table 5.4. The indirect ELISA performed well at many other combinations, but the above protein concentration and monoclonal antibody dilution were selected as they had a good absorbance value and a useful dynamic range.

Table 5.4. Absorbance values obtained at 450 nm with various concentrations of monoclonal antibody (horizontal) and experimentally produced *BFDV* CP (rCP) [vertical].

Absorbance values at 450 nm										
rCP concentration (µg/ml)	**Monoclonal antibody concentration (µg/ml)**									
	10	9	8	7	6	5	4	3	2	1
0,5	0.079	0.108	0.091	0.102	0.091	0.085	0.088	0.093	0.096	0.098
0,75	0.084	0.104	0.098	0.101	0.094	0.093	0.098	0.101	0.1	0.051
1,0	0.075	0.089	0.093	0.092	0.088	0.099	0.093	0.1	0.105	0.098
1,5	0.089	0.096	0.1	0.101	0.095	0.101	0.104	0.097	0.105	0.106

5.3.7 Indirect Competitive Enzyme-Linked Immunosorbent Assay (ELISA)

In a competitive ELISA, three serum samples (Macaw 1; Macaw 2; Greenwing) were tested with two different coating buffers (PBS, pH 7.4; 50 mM carbonate/bicarbonate, pH 9.6). As seen in Figure 5.12 and Table 5.5., the choice in coating buffer may affect assay response. The net optical density for each of the serum samples was plotted against the time points of 10, 15, 20 and 25 minutes.

This competitive ELISA was not quantitative, as a standard curve had not been set up. The recombinant antigen used in this study was produced by GenScript (USA) in order to produce the monoclonal antibody directed against it. Therefore, limited quantities are available and these efforts were abandoned.

Table 5.5. Data obtained in a competitive ELISA, using experimentally expressed *BFDV* CP from GenScript (USA), as antigen. Absorbance was taken at 450 nm, read at 25 minutes, comparing PBS (pH 7.4) and 50 mM carbonate/bicarbonate (pH 9.6) for use in ELISA.

Serum tested	Coating Buffer									
	50 mM Carbonate/bicarbonate (pH 9.6)					PBS (pH 7.4)				
	OD_{450nm}	OD_{net}	PP* (%)	- control	+ control	OD_{450nm}	OD_{net}	PP* (%)	- control	+ control
Macaw 1	0.408	0.258	113.16	0.15	0.228	0.532	0.394	240.24	0.138	0.164
Macaw 2	0.479	0.329	144.30			0.479	0.341	207.93		
Green-wing	0.365	0.215	94.30			0.442	0.304	185.37		

*PP - Percent Positivity

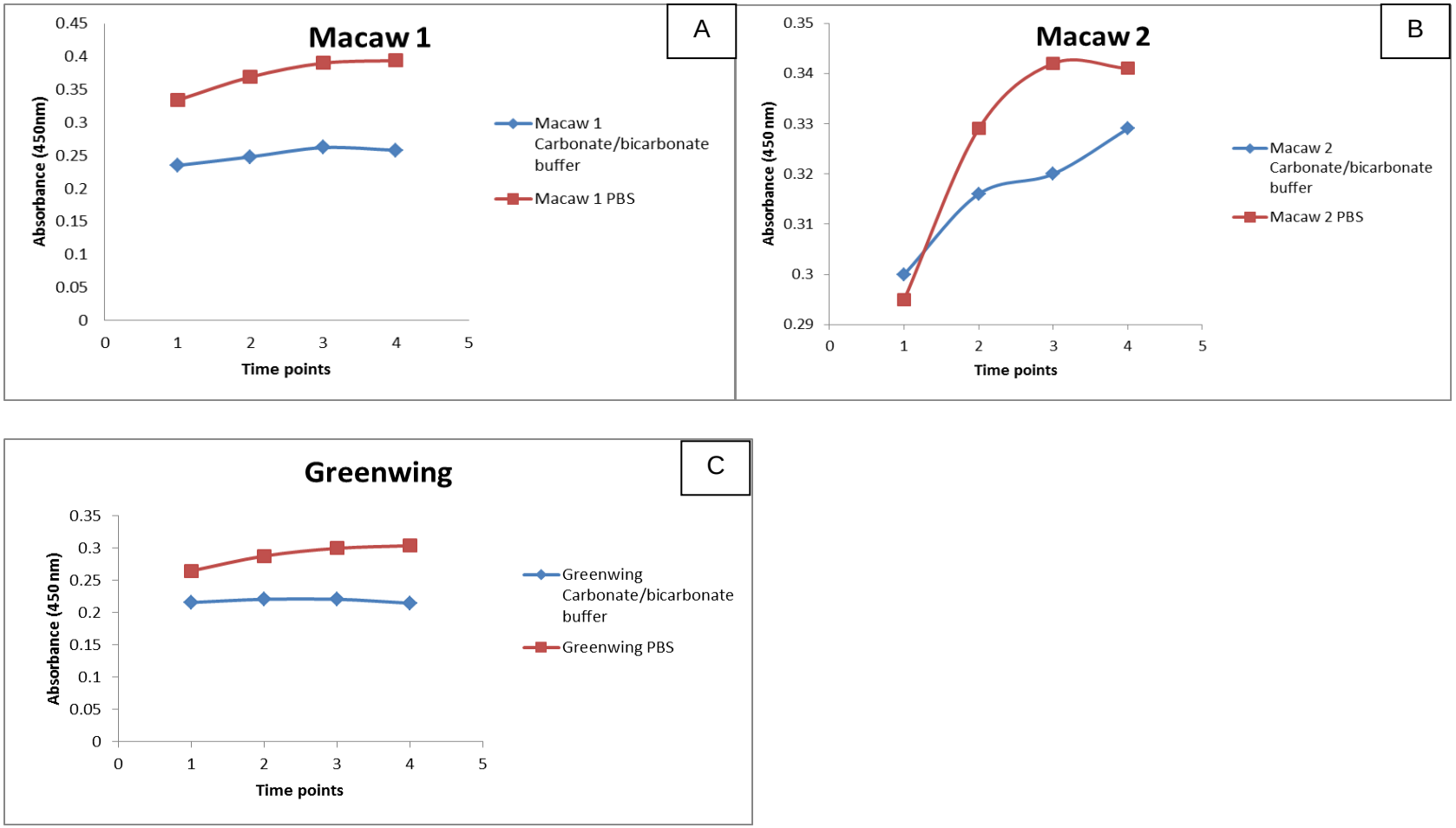

Figure 5.12. Graphs showing that the use of different coating buffers affects assay response. The net optical density is plotted against the time points of 10, 15, 20 and 25 minutes for the serum tested from Macaw 1 (A); Macaw 2 (B); Greenwing (C).

5.3.8 Optimisation of the indirect Enzyme-Linked Immunosorbent Assay (ELISA) using whole *Y. lipolytica* Po1h cells

The protein could not be extracted with a detergent or a salt/ethanol wash, the next steps involved the use of whole *Y. lipolytica* cells and the optimisation of the reagents for use in the indirect ELISA.

Table 5.6. Descriptive statistics of indirect ELISA without modifications to protocol, as analysed by SPSS (SPSS, IBM Corp.; 2012). The table gives the range, minimum and maximum absorbance values, mean and standard deviation.

Descriptive Statistics

Coating of wells	N[a]	Range[b]	Minimum[c]	Maximum[d]	Mean[e]	Std. Deviation[f]
PBS	12	.097	.050	.147	.08892	.031742
WT	12	.119	.045	.164	.06008	.033033
Y16	12	.133	.041	.174	.07625	.057291

[a] N represents the number of repetitions of each variable (PBS, WT, and Y16).

[b]Range gives the difference between the highest and lowest absorbance values obtained.

[c,d]Minimum and Maximum gives the lowest and highest absorbance values obtained, respectively.

[e]Mean gives the sum of the absorbance values divided by N (12).

[f]Standard deviation gives the amount by which the absorbance values differ from each other.

The absorbance values obtained with this indirect ELISA were extremely low; showing that optimisation of reagents was needed. The standard deviation of wells coated with Y16 cells was around 0.057 (represented by the red box, Table 5.6.), which is higher than the controls (0.032 and 0.033). This may be resultant of variance in expression levels between Y16 cells.

Table 5.7. The minimum and maximum absorbance values obtained during monoclonal antibody optimisation, as analysed by SPSS (SPSS, IBM Corp.; 2012).

Descriptive Statistics								
Absorbance	A	B	C	D	E	F	G	H
Minimum	.767	.787	.648	.835	1.099	.695	.721	.766
Maximum	1.349	1.492	1.855	1.578	1.761	1.793	1.545	1.662

Monoclonal antibody concentration was optimised and Table 5.7 shows the minimum and maximum absorbance values obtained. The optimal monoclonal concentration was found by checkerboard titration, in row C, column 12 in a 96-well plate (Refer to Figure 5.2). The absorbance at 450 nm equalled 1.855 (represented by the red box, Table 5.7.).

The initial concentration of 10 $\mu g.ml^{-1}$ (A1) and a two-fold serial dilution was performed across the plate, such that a 1:2048 dilution was found in A12 (4.88×10^{-3} $\mu g.ml^{-1}$). Then a two-fold serial dilution was performed down the column so that concentration at C12 was a 1:8192 dilution; which is a concentration of 1.22×10^{-3} $\mu g.ml^{-1}$, when used with 100 µl of whole *Y. lipolytica* Y16 cells.

Table 5.8. The minimum and maximum absorbance values obtained during anti-mouse IgG optimisation, as analysed by SPSS (SPSS, IBM Corp.; 2012).

Descriptive Statistics		
Anti-mouse IgG dilution	Minimum	Maximum
Y16_1in5000	.09	.16
Y16_1in2500	.10	.37
PBS_1in5000	.08	.12
PBS_1in2500	.09	.11
WT_1in5000	.17	.21
WT_1in2500	.16	.20
Y16_1 in 1750	.07	.14
Y16_1 in 1500	.07	.17

The monoclonal antibody concentration used in this assay equalled 1.22×10^{-3} $\mu g.ml^{-1.}$ When optimising anti-mouse IgG concentrations, low absorbance values were obtained (as seen in Table 5.8). The highest absorbance value was 0.37 when using a 1:2500 dilution of anti-mouse IgG. The difference in absorbance between cells expressing *BFDV* CP (Y16) and untransformed *Y. lipolytica* cells (WT) is not substantial. Higher values were obtained when a 1:10 000 concentration (no modification to manufacturer's recommended dilution) was used, as seen in Table 5.7. Therefore, only the monoclonal antibody and not the anti-mouse IgG concentration needed further optimisation.

5.3.9 GPI-anchored protein release for use as an ELISA antigen

5.3.9.1 Detection of *BFDV* CP by SDS-polyacrylamide gel electrophoresis

SDS PAGE analysis, as seen in Figure 5.13, revealed that GPI-anchored protein extraction was unsuccessful by both membrane solubilisation and salt/ethanol washing. The band of interest was expected around 20 kD. However, untransformed *Y. lipolytica* cells showed bands with the membrane solubilisation method. Transformed *Y. lipolytica* (Y16) cells that had been treated to a salt/ethanol wash showed the presence of faint bands.

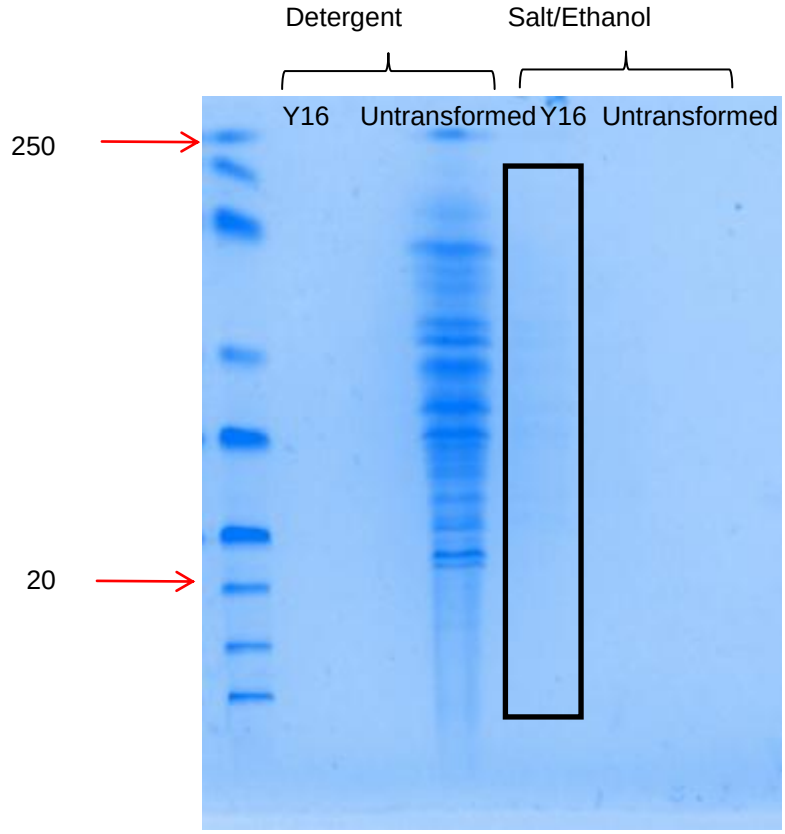

Figure 5.13. SDS PAGE analysis, stained with Coomassie blue, of proteins expressed using cell surface display. GPI-anchored protein extraction was attempted by a wash with a detergent (Triton-X100) and salt/ethanol washing. The band of interest was expected around 20 kD, but was not observed.

Silver staining of an SDS PAGE gel, as seen in Figure 5.14 revealed the presence of faint bands in the transformed *Y. lipolytica* (Y16) cells that had been treated to a salt/ethanol wash, however the *BFDV* CP (~20 kD) could not be released.

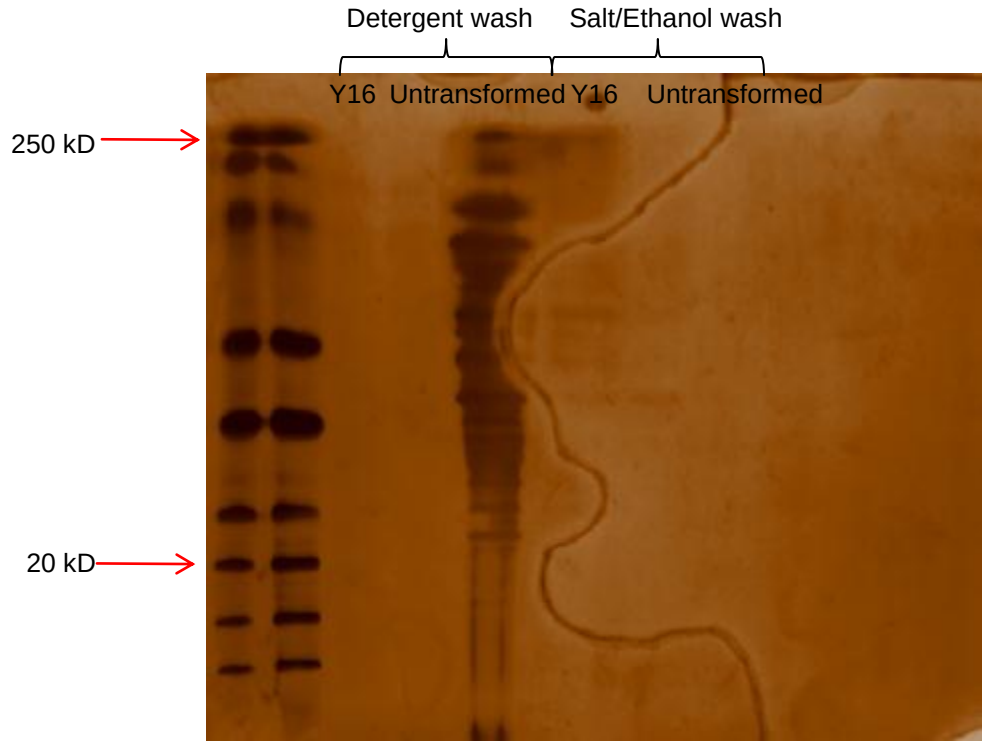

Figure 5.14. SDS PAGE analysis, silver stained, of proteins expressed using cell surface display. GPI-anchored protein extraction was attempted by membrane solubilisation and salt/ethanol washing. *BFDV* CP could not be extracted by either method, however, untransformed *Y. lipolytica* cells showed bands with the membrane solubilisation method. Transformed *Y. lipolytica* (Y16) cells that had been treated to a salt/ethanol wash showed the presence of faint bands; however the *BFDV* CP (~20 kD) could not be extracted.

5.4 Discussion

BFDV has a wide global distribution; accordingly, the monitoring and control of the spread of the virus requires the development of safe, standardised reagents and assays for diagnosis. As mentioned previously, antibody detection currently suffers from inter-test variation. Novel diagnostic tests are crucial for both the detection of viral antigen and anti-*BFDV* antibodies.

This study set out with the aim of using recombinantly expressed *BFDV* CP to develop a rapid agglutination test to accurately detect exposure to *BFDV*. It also asked whether a competitive ELISA could be developed to diagnose *BFDV* infection, using recombinantly expressed CP.

Initially, microscopy analysis was used to detect the presence of *BFDV* CP on the transformed *Y. lipolytica* cells. Comparison of images revealed that, in TEM analysis, protrusions are observed on the surface of the transformed *Y. lipolytica* cells (Figure 5.4); whilst, SEM analysis showed a mesh substance between the cells (Figure 5.5), which is not

seen in the untransformed *Y. lipolytica* cells. These two microscopic techniques vary in magnification, resolution as well as the dimensional view offered. TEM gives a two dimensional view of the cell; whereas SEM analysis gives a three-dimensional view. Another factor that should be taken into consideration is the preparation of the samples for these two techniques. SEM preparation of the samples involved osmication and dehydration; therefore, the mesh substance may be disrupted cell matter. The surface-displayed *BFDV* CP may not have withstood the preparation process and may have become dislodged.

Immunodetection employed a fluorescently-labelled secondary antibody and a primary antibody reactive to *BFDV* CP to stain the transformed *Y. lipolytica* cells. This enabled visualisation of the location of the protein (Figure 5.6). DABCO, a free radical scavenger, was used as an antifading agent in fluorescence microscopy (Aitken *et al*., 2008). A limited effect on dye stability was observed in the presence of this additive. A question of DABCO's efficacy was raised; as fluorescence decreased with an increase in exposure to light. The fluorescence that is seen with the untransformed *Y. lipolytica* Po1h cells (Figure 5.6. F) may be non-specific in nature and is not relative to the fluorescence seen with the transformed *Y. lipolytica* Po1h cells. A higher degree of fluorescence was observed with the transformed *Y. lipolytica* Po1h cells (Figure 5.6. B).

The results obtained from the slide agglutination and PCR analyses are presented in Table 5.3. The birds tested negative by PCR but had a history of *BFDV* infection. All of the birds tested positive by slide agglutination, therefore showing that the test detected antibodies against *BFDV* in all the parrots.

The reaction contributing to the agglutination of the Y16 cells by *BFDV* antibodies (as seen in Figures 5.7.-5.11.) consists of two stages; first, a specific, and rapid combination of antibody with antigen. The second is a slower stage involving the aggregation of the primary compound particles and requires the presence of an electrolyte, such as that present in the antigen diluent (PBS). The action of the electrolytes reduces the surface potential of *Y. lipolytica* cells, causing the cells to react as hydrophobic colloids allowing for clumping to take place (Kwapinski, 1972). Agglutination is a reversible reaction, occurring essentially under equilibrium conditions, as represented by the following equation (Equation 5.1):

$$\underset{\text{large aggregates}}{\text{Ag} + \text{Ab} \leftrightarrows (\text{AgAb})} + \underset{\text{excess soluble}}{\text{Ag} \leftrightarrows \text{Ag2Ab}}$$

Equation 5.1 Equation showing the reversible nature of agglutination (Kwapinski, 1972).

Due to the soluble nature of the antigen-antibody complexes, if a large excess of antigen was present, the size of the complexes decreased with increasing antigen concentration

(Kwapinski, 1972). Therefore, the dilution of test antigen was standardised, so as to ensure reproducible results.

In Figure 5.9., maximal agglutination has taken place, allowing formation of a large lattice-like complex. The agglutination occurs due to there being a dilution of antibody that allows each molecule to interact with the antigen. Note that the concentrations of antibody and antigen in this zone are not the same, but rather it is the relative concentration of these molecules that allows lattice formation.

Initially, no agglutination was observed during the testing of the serum sample obtained from the African Grey parrot (Table 5.3.). Only when the serum sample was diluted could agglutination be detected. The failure of sera to agglutinate antigen at lower dilutions, although clumping is observed at higher dilutions, is referred to as the pro-zone phenomenon (Kwapinski, 1972). This is as a result of an excessive amount of antibody being present, relative to the constant antigen concentration. The abundance of antibodies causes each antigen molecule to bind to a single antibody. Consequently, cross-linking of antigen does not occur and aggregation is not observed (Stanley, 2002). The converse, referred to as the post-zone phenomenon, occurs when there are insufficient antibodies for crosslinking to occur, thus, showing little or no agglutination. Both phenomena are illustrated in Figure 5.15. Slide agglutination results therefore need to be interpreted with caution as there is the potential for misdiagnosis.

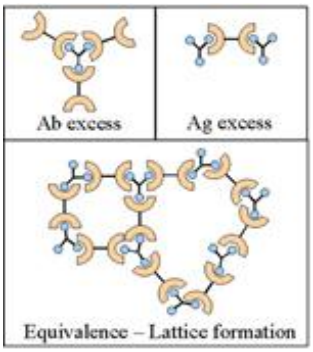

Figure 5.15. Diagram showing the effect excess antibody or antigen on agglutination (Mayer, 2013).

The birds that were housed at the UFS had a history of *BFDV* infection, having tested positive by PCR, upon arrival. The African Grey parrot showed the highest degree of agglutination of all the birds tested. This bird did not show any clinical symptoms, which may be attributed to an elevated amount of protective antibodies (Table 5.3.). It is important to note the higher degree of agglutination seen with the Blue-fronted Amazon parrot (Figure 5.9 C), as compared to the Brownheaded and Greyheaded parrots, respectively. The birds at the UFS were re-tested by PCR at the time of slide agglutination testing and only the Blue-

fronted Amazon parrot tested positive by PCR. This is of note as this was the only bird housed at the UFS, to display clinical symptoms in the form of claw deformities (Table 5.3.). Interestingly, this bird joined the study in 2011, having been diagnosed with *BFDV*, however, throughout the duration of its stay at the animal housing facility, it tested negative by PCR consistently. This bird is identified as A2A and A2B as reported in Chapter 3 (Refer to Ch 3, Figure 3.2. B). In 2013, the bird tested positive by PCR and also showed a greater degree of agglutination as compared to all the other birds.

It can be speculated that this bird may have been actively fighting off infection at the time of testing. A lower antibody titre is seen amongst infected birds showing clinical signs. This is substantiated by previous reports by Ritchie and co-workers (1992); in which it was suggested that some birds may be able to mount an immune response strong enough to reduce the severity of the disease. Therefore, the birds have been exposed to the virus but remain clinically normal.

The Macaws, tested as part of a diagnostic service offered by the Veterinary Biotechnology diagnostic laboratory, UFS, were PCR negative and also showed an absence of clinical symptoms (Table 5.3.). However, these birds tested positive by the slide agglutination test. These birds were housed in the same hand-rearing room as their chicks. The chicks showed signs of delayed development and abnormal feathering, weight loss, vomiting, cropstasis and suffered convulsions (personal communication, Anonymous; 2013). Chicks are more susceptible to infection than older birds (Jones, 2006); due to host conditions rather than antigenic or genotypic traits of *BFDV* (Ritchie *et al*., 2003).

In an analysis of *BFDV* transmission, Rahaus and co-workers (2008), found that *BFDV* was transmitted vertically, due to the presence of viral DNA in both embryonated and non-embryonated eggs. Therefore, it is not uncommon to see asymptomatic parents producing offspring that display clinical signs of *BFDV*. However, Ritchie *et al*.,1992 highlighted in epidemiological studies, that horizontal transmission of the virus occurs more commonly than vertical transmission. Thus, asymptomatic parent birds may not be actively infected, however, they still shed virus via feather dust and excrete virus via the gastrointestinal tract. Regardless of the mode of transmission, asymptomatic birds are carriers of the virus and serve as a source of virus in the aviary and may therefore spread the virus to their chicks and should be segregated from the rest of the aviary.

Referring to Table 5.3., only the Blue-fronted Amazon parrot tested positive by PCR. A strong relationship between the presence of clinical and PCR-positive status has been reported in previous studies (Kondiah, 2004) and is corroborated in this study. PCR negative results may be due to an absence of viral DNA, as the immune system mounts a response

great enough to clear the virus from the body. It has been previously reported that the absence of virus in the bloodstream may be as a result of the virus being tied up in inclusion bodies in the organs of the birds, as a means of escaping immune detection (Kondiah, 2004).

However, all the birds tested in this study showed prior exposure to *BFDV*, as antibodies were detected. A time study would be able to show whether the antibodies are being actively produced or whether whether the birds have already eliminated the virus, and antibodies are still being detected. These birds could potentially be carriers, serving as a source of virus in the aviary. PCR results may be unreliable when diagnosing birds, especially when clinical symptoms are absent, as was mentioned in Chapter 3, Section 3.3.1. This further emphasises the need for serological diagnosis to be conducted in conjunction with molecular diagnosis.

Fixation of transformed *Y. lipolytica* Po1h cells did not prevent a loss in slide agglutination activity with cells kept at 4 °C. *Y. lipolytica* exhibits fungal dimorphism with the display of both hyphae and pseudohyphae (Hurtado & Rachubinski, 2002). Fungal dimorphism involves extensive adaption of the cellular machinery in response to environmental signals. An increased polarisation of the cytoskeleton results in a drastic change in the pattern of cell wall biosynthesis, thus triggering the switch to hyphal form. As *BFDV* CP is displayed on the cell surface; the effect of hyphal formation on the displayed protein is indeterminate. Formaldehyde is a 2-phase fixative, with an initial cross linking phase that is completed 24-48 h after penetration, whilst the latter phase of crosslinking may take about 30 days to generate stable covalent cross linkages. Although the penetration time is relatively fast, a longer time is needed for fixation. The factors that could influence fixation include time, pH, temperature and viscosity (Thavarajah *et al*., 2012). It is proposed that these variables be tested to find the optimum conditions for preservation of structure and antigenicity of *Y. lipolytica* cells expressing *BFDV* CP. Alternatively, other methods of fixation should be investigated.

One unanticipated finding from the slide agglutination assay was that, serum obtained from chickens displayed an antibody response to *BFDV* antigen (as can be seen in Figure 5.10. A). It could be suggested that the antigen shows a certain degree of aspecificity and the slide agglutination assay detected an antibody response to a similar immunogen. Another member of the *Circoviridae* family, *Chicken anaemia virus* (*CAV*) like *BFDV* causes immunosuppression and is fatal (Lukert *et al*., 1995; Studdert, 1993). However, no significant similarity is seen between *BFDV* and *CAV* in nucleotide or amino acid sequences (Bassami *et al*., 1998).

Another possible explanation for this is that the chicken had been exposed to virus. This chicken was housed in a pen in direct contact with that of the parrots. When chicken serum obtained from a farm in Glen, Bloemfontein that had not had any contact with parrots, no agglutination was observed (depicted in Figure 5.10 B). In a vaccination study by Shearer and co-workers (2009a), viral DNA was detected consistently in the blood of all control birds that had not been vaccinated against *BFDV*. It was proposed that the environment was contaminated with feather dander from *BFDV*-infected birds. Therefore, there has been horizontal transmission of virus to chickens (Ritchie *et al*., 1989b; Rahaus *et al.*, 2008). The antigen is thus specific for *BFDV*; however, the main concern emerging from this finding is that there is a lack of effective bio-security measures. *BFDV* has been described as being impervious to many of the methods used to inactivate viruses, such as high temperature, low pH, organic solvents and commercial disinfectants. As evidence, of this, the coat protein retains its ability to agglutinate red blood cells at extreme temperatures (Raidal & Cross, 1994a; Todd, 2000). The CP is the main antigenic determinant, contributing to *BFDV*'s environmental stability. Thus, it may persist in the aviary for a prolonged period of time, having implications for virus epidemiology and disease control (Todd, 2000).

Various types of agglutination tests have been successfully applied to the following avian viruses: *Newcastle disease virus* (*NDV*) [Raggi, 1960; Joshi & Joshi, 2009], *Infectious bursal disease virus* (*IBDV*) [Nakamura *et al*., 1993], *Egg-drop syndrome virus* (*EDSV*) [Sree *et al*., 1998], and *Avian influenza virus* (*AIV*) [Chen *et al*., 2007; Wang *et al*., 2010]. The tests described, were mostly based on antigen detection. The tests described use native virus as antigen (Raggi *et al*., 1960) or make use of latex agglutination for detection of antigen and were not quantifiable.

Presented here is the first report of a novel slide agglutination test for the detection of *Beak and feather disease virus* antibodies, using the *Y. lipolytica* cell surface-displayed coat protein as the test antigen. This method uses the relatively large *Y. lipolytica* cell to enable visualisation of the linking of antigen to antibody in serum.

Importantly, the expressed CP retained the integrity of whole virus coat protein as it was able to be recognised by naturally occurring anti-*BFDV* sera. The agglutination test is sensitive for detecting small amounts of antibody, since relatively few antibody molecules can effectively link together large numbers of particulate antigens to produce easily visible clumps (Kwapinski, 1972).

The newly developed slide agglutination test can accurately detect exposure to *BFDV* and no evidence of a species-specific barrier exists thus far. However, testing of more species and multiple samples is necessary.

Birds held in quarantine can be rapidly tested to determine exposure to *BFDV*. Therefore, it should prove to be a useful assay in serological surveillance, allowing breeders to ensure that the virus is not introduced into the aviary. Sero-profiling would minimise the chances of obtaining a bird that does not display clinical signs of the disease, but has had prior exposure to *BFDV* and tests negative by PCR. These carrier birds should also be quarantined before breeding occurs, with proper disinfection of aviaries to help curb the spread of the virus.

The slide agglutination test is advantageous to bird breeders, as the cost of this test is significantly lower than that of the competitive ELISA, PCR or real-time PCR tests. Moreover, the test can be completed in 1 minute. It is an efficient test that does not require expensive equipment or skilled personnel. As interpretation of the test is visual, there is no difficulty in discerning between positive and negative samples. This assay is not quantitative; however, it can be modified to be a semi-quantitative assay, in order to determine antibody titre. Serum samples were used undiluted in this assay; in order to quantify antibodies; one can make dilutions of the serum sample and would have to know the amount of protein expressed on the cell surface of *Y. lipolytica* Po1h. The monoclonal antibody directed against the *BFDV* CP can be used in place of chicken-raised antibodies as a positive control as a more reliable, quantifiable positive control.

So far this chapter has focussed on a discussion of results obtained from the development of a slide agglutination assay. The following section will discuss the results obtained from the development of an ELISA, using both the synthetic rCP (GenScript, USA) and whole *Y. lipolytica* cells expressing *BFDV* CP and a monoclonal antibody raised against this protein.

Low absorbance values were obtained initially, using Costar® plates and bicarbonate buffer as the coating buffer. The two most common coating buffers are bicarbonate buffer at pH 9.6 or PBS (pH 7.4) and stabilise the antigen used to coat the ELISA plate. In a competitive ELISA, these two buffers were compared and assay response was shown to be affected. PBS showed up to a 30% increase in absorbance, as it maximised adsorption to the plate and optimised interactions with the antibody. The plate type was changed from Costar® to PolySorp® (Section 5.2.9) as higher absorbances were obtained with this plate. Drying of antigen during the initial coating phase did not show any noticeable difference in absorbance values as compared to when the antigen was allowed to coat without drying at 4 °C. This is due to the fact that PolySorp® plates are surface treated, to allow a high affinity to molecules of a hydrophobic nature.

A reliable and consistent source of antigen is needed. Even though work with the experimentally produced *BFDV* CP (GenScript, USA) seemed promising, it was decided that this would not be sustainable in the long-term.

It was supposed that the yeast cell-surface display system would be advantageous as a whole-cell immunoadsorbent, due to the rigidity of the cells and since a larger amount of molecules can be displayed per cell. A variety of steps were taken to optimise the indirect ELISA using whole *Y. lipolytica* Po1h cells expressing *BFDV* CP as antigen. The assay made use of a monoclonal antibody directed against the major structural protein (CP) of *BFDV*.

The absorbance values obtained with this indirect ELISA were low; showing that optimisation of reagents was needed. Although this is a sustainable source of protein, the indirect ELISA could not be reproduced consistently, due to variance seen in absorbance readings. Integration of the expression cassette in the yeast genome is random in nature (Madzak *et al*., 2004). Therefore, expression levels may be influenced by the integration location, causing variance in the number of proteins expressed on each cell surface. A whole cell ELISA, using *S. cerevisiae* cells with cell-surface display of the IgG-binding domain showed postive results (Nakamura *et al*., 2001). However, success was not seen in this study. Even though ELISA plates are designed to stably bind antigen; the hydrophilic nature of *Y. lipolytica* cells may cause it to wash off during the ELISA process.

Cut off values are calculated to separate positive results from negative results and need to be determined using a panel of negative control sera. A cut-off value could not be assigned in this assay as there is difficulty in accessing negative control sera.

Attempts were made to release GPI-anchored proteins from *Y. lipolytica* cells expressing *BFDV* CP for use as an ELISA antigen, after attempts at whole cell ELISA had failed. Two methods were attempted: a salt/ethanol wash and a detergent wash. Even though this method was repeated several times, the protein of interest was not obtained. Release of GPI anchored proteins can be accomplished by treatment with Phospholipase C, which is specific for the phosphatidylinositol group found in the GPI anchor (PLC-PI). However, this method is not cost effective for large-scale purification of protein.

Fixation methods did not improve Y16 cell antigenic stability with slide agglutination (Figure 5.11), as *Y. lipolytica* cells are dimorphic in nature (Hurtado & Rachubinski, 2002). Therefore, alternative fixation methods would be advisable. However, a more viable solution would be to know the exact amount of protein as a competitive ELISA is a quantitative test and relies on the drawing up of a standard curve.

The competitive ELISA would have a greater analytical sensitivity than the slide agglutination test, which is used as an initial screening test. Moreover, competitive ELISAs have a distinct advantage over indirect ELISAs, in that secondary antibodies specific to the IgG of the species tested are not required. For current large-scale screening and sero-surveillance, competitive ELISAs have largely replaced indirect ELISAs (Gorham, 2004). In a study on *CAV*, competitive ELISA was described as advantageous in terms of speed and cost when compared with the indirect ELISA format (Todd *et al*., 1999). Moreover, the disease status or vaccine efficacy can be predicted (Janeway *et al*., 2001).

In this study, recombinant *Y. lipolytica* Po1h cells or bacterially expressed *BFDV* CP was used as antigen. *BFDV* coat protein is the main immunogen; hence, the heterologously expressed CP and the monoclonal antibody developed against it form the basis of the serological diagnostic assays described. The monoclonal antibody directed against the major structural protein (CP) of *BFDV*, was used as the primary antibody in the indirect ELISA. In further studies, it would be used as the competing antibody in the competitive ELISA to detect anti-*BFDV* antibodies. The use of MAb's against recombinant protein is useful in the diagnosis of BFD, since an indirect ELISA cannot be performed as there are no commercially available anti-parrot antibodies. Also, the cross-reactivity between different species is unknown. The applicability of this test has the potential to be limited as individual isolates of *BFDV* differ within the CP gene.

Previous research findings into the existence of novel serotypes and antigenic homology in *BFDV* have been inconclusive (Khalesi *et al*., 2005; Shearer *et al*., 2009a). The only cross-reactivity study conducted thus far, by Khalesi *et al*., (2005) did not demonstrate the existence of serotypes using polyclonal antisera. However, some of the individual epitopes of the capsid protein which correlate to particular psittacine species may vary. Even though Shearer and co-workers (2008), found a strain that infects cockatiels, the monoclonal antibody used in the study recognised *BFDV* from a sulphur-crested cockatoo and a rainbow lorikeet in addition to that found in a cockatiel (Shearer *et al*., 2008). This indicates that there is some antigenic homology between isolates. In a PhD study by Kondiah (2008), negative antigen-antibody reactions were seen in an ELISA, using chicken-raised antibodies, and detected with anti-chicken HRP. Two different *BFDV* isolates were involved in the antigen and antibody preparations, respectively. This negative antigen-antibody reaction was attributed to the presence of different epitopes on the *BFDV* CP used as coating antigen, thereby suggesting the possibility of antigenic variants of *BFDV* (Kondiah, 2008). As the coat protein of *BFDV* is a major constituent of infectious virus particles, it is a likely target for immune surveillance. This may represent an attempt by the virus to evade the immune system, or may be the result of host-virus interactions specific to individual species.

Shearer and co-workers (2009a) proposed that the epitope detected by a monoclonal antibody used in their study, may not be present in some *BFDV* isolates. However, enough major epitopes should be conserved between isolates to allow anti-*BFDV* sera to react with the recombinant protein (Shearer *et al*., 2009a). Importantly, sero-diagnosis was conducted across a range of species suggesting either that the birds were infected with a similar strain, or supporting the notion that there is a high degree of antigenic homology.

The premise of a competitive ELISA is that, bound sera will block the monoclonal antibody from binding, even if the test serum does not react with the exact epitope detected by the monoclonal antibody. Thus, the competitive ELISA should be reliable for use with sera from many species, unless experimental evidence comes forth that novel *BFDV* serotypes exist or that the epitope detected by the monoclonal antibody is not immunodominant (Shearer *et al*., 2009a).

Whilst this study did not fulfil the aim of establishing a standardised competitive ELISA for the detection of antibodies against *BFDV* in parrot sera, it did substantiate information that would lead to a quantifiable and standardised competitive ELISA. Overall, there is an indication that the *Y. lipolytica* Po1h, expressing *BFDV* CP did show slightly higher absorbance readings, indicating that this method shows promise. However, substantial work is needed to optimise the ELISA in order to develop a competitive ELISA as the amount of surface-displayed *BFDV* CP could not be standardised.

Current breeding farms in South Africa vary in scale, from large-scale farms to smaller collections of birds housed in close contact. In the latter situation, losses are not as severe when birds are infected with *BFDV* and there is no significant incentive to the breeders to carry out good bio-security measures. Prevention and control of *BFDV* in South Africa is a daunting task and infections can only be controlled by wide-scale vaccination and testing.

CHAPTER 6 GENERAL DISCUSSION AND CONCLUSIONS

6.1 General Discussion

Given the significant negative economic impact that beak and feather disease (BFD) has on the parrot breeding industry, it is becoming increasingly important to have rapid and standardised testing programmes to curb the spread of the virus. Novel diagnostic tests are crucial for both the detection of viral antigen and anti-*BFDV* antibodies. The study was set out to evaluate and improve the current diagnostic strategy for *Beak and feather disease virus* (*BFDV*) and has identified the need for standardised and sensitive diagnostics and the motivation for rapid serological diagnostic tests. Existing molecular techniques were compared with newly developed assays and novel serological tests were developed, using the following objectives:

1. Compare polymerase chain reaction (PCR) and quantitative real-time polymerase chain reaction (qPCR) as diagnostic tools for *BFDV*.
2. Recombinantly express *BFDV* coat protein in a bacterial host.
3. Develop serological diagnostic tests for *BFDV.*

The conventional PCR test to detect *BFDV* (Ypelaar *et al*., 1999; Kondiah, 2004) was conducted on a large number of samples and was most effective in birds displaying clinical signs. However, positive PCR results were also obtained from birds without clinical symptoms. This shows that the virus may also be detected in the absence of clinical signs (Hess *et al*., 2004; Rahaus & Wolff, 2003).

It is likely that symptoms are resultant of an immune response to the infection. Therefore, the absence of clinical signs does not preclude the possibility of viral replication while the presence of clinical symptoms does not assure that replication has continued after the initial stimulation of the immune system. PCR provides little quantitative assessment of the infection level and does not indicate whether the virus is replicating or actively causing disease. Thus, a positive PCR result does not indicate that the bird is currently infected by the virus, but it says that viral DNA was detected in the sample which may be remnants of viral particles that have been phagocytosed.

PCR as a diagnostic technique is hampered by whether it is always capable of detecting all strains of the virus. This is due to the test being designed on the assumption that only one virus strain exists (Khalesi, 2007; Ypelaar *et al*.,1999).

Recently, there has been a shift from conventional PCR to real-time PCR in clinical diagnostic settings for human microbial infections (Espy *et al*., 2006). Similarly, real-time PCR may change how *BFDV* is currently identified and quantified; thereby playing an important role in identifying subclinical illness. In this study, an evaluation of PCR and real-time PCR revealed that real-time PCR was more sensitive and detected *BFDV* in samples that did not test strongly positive in conventional PCR.

In this study, viral load was quantified in relation to a known DNA standard, concluding that the virus is not presented in low quantities, as was initially hypothesised. Molecular quantification of a microorganism may be influenced by variation in template amount between samples, poor or variable template quality, variation in performance of DNA dependent DNA polymerase as well as variation in amplification between sample and standard DNA (Mackay *et al*., 2007).

As high viral loads were obtained in this study, faint bands obtained by conventional PCR may likely be due to primer mismatches. Primers may preferentially amplify certain strains (Mackay *et al*., 2007), as seen currently in this study with conventional PCR. The findings of the current study are consistent with those of various authors and shows that PCR may not detect all isolates, even when conserved primers are used (Bassami *et al*., 2001; Ritchie *et al*., 2003; Heath *et al*., 2004; Johne *et al*., 2004).

This problem may also eventually translate to problems with real-time PCR. Even though the primers designed for real-time PCR were designed on a highly conserved region in *rep*, slight sequence variation is seen by melt-curve analysis. This further proves how *BFDV* responds to immune pressure, even in a highly conserved sequence. Even though some degree of primer mismatch may be tolerated, it is undesirable for quantitative purposes and may also result in reduced amplification efficiency (Mackay *et al*., 2007). Therefore, real-time PCR cannot be used in isolation; it must be accompanied with ongoing sequencing and phylogenetic analyses. Therefore it may be more beneficial to design probes that allow rapid detection of SNPs in the *BFDV* sequence in real-time or infection with multiple strains.

Real-time assays described by Katoh and co-workers (2008) as well as Shearer and co-workers (2009b) also focused on *rep*, describing it as the more conserved gene when compared to CP as the target in molecular diagnostics. These assays were quantitative and did not display evidence of genetic variance. Analysis of the CP by real-time PCR showed the possible existence of genotypes (Raue *et al*., 2004). This assay was not quantitative, but it can be modified to include quantification by the methods outlined in this study.

When taking into account the rapid rate at which *BFDV* evolves, and the mixing of birds from diverse species due to the pet trade, there is a great risk of increasing the potential for highly virulent genotypes to arise. These genetic variants may differ based on host specificity and/or geographical location (Bassami *et al*., 2001).

Genetic diversity presents a challenge in designing molecular assays for accurate diagnosis, while still maintaining sensitivity and specificity. It may be that only the predominant variants of *BFDV* can be detected. Thus it is necessary to ensure that diagnostic tests detect all variants of *BFDV*, which requires that sequence information be made available more rapidly.

A limitation of this study was that the samples were not representative of *BFDV* infection rates in South Africa. Due to the stigma of *BFDV*, sample information was not always supplied by the breeders. Furthermore, breeders were responsible for sample collection and even though instructions were supplied with the testing kit, breeders had not been trained on correct sampling methods. Variable sample collection, incorrect marking of samples and exposure to feather dust may be a cause of significant error in diagnostics.

As previously discussed, serological diagnostics requires consistent, high-quality viral antigen. As an antigen source, CP is the most suitable as it has been shown to be the main immunogen (Stewart *et al*., 2007). However, attempts to propagate *BFDV* in cell or tissue culture have failed thus far (Todd, 2000; Heath *et al*., 2006). Therefore, a variety of expression systems have been employed to express *BFDV* CP (Duvenage *et al*., 2013; Heath *et al*., 2006; Johne *et al*., 2004; Kondiah, 2008; Patterson *et al*., 2012; Stewart *et al*., 2007).

Previous expression studies in a Masters study by Alta Hattingh showed that the use of *E. coli* as an expression host is not recommended (Hattingh, 2009). However, a PhD study by Kulsum Kondiah showed that bacterial expression of CP was successful, albeit at low levels (Kondiah, 2008).

Even though *E. coli* is one of the most widely used expression vectors, expression of the *BFDV* CP is highly problematic. Without being able to subclone the *BFDV* CP, the study was not able to proceed as planned and therefore experiments involving the pET-28b(+) vector and *E.coli* BL21(DE3) were not conducted. The current investigation was limited by the fact that expression of *BFDV* coat protein is problematic and a lack of practical technical expertise on bacterial expression also hindered the study.

However, the full length coat protein of *Beak and feather disease virus* was successfully cloned into the surface display plasmid (pINA1317-YlCWP110) of *Y. lipolytica*

(Boucher, 2013, unpublished work). This viral antigen had applications in serological diagnostics, as well as a novel vaccine strategy.

No serotypes have been identified as yet (Khalesi *et al*., 2005); however there would be eventual differentiation into strains / serotypes, as seen in the related *Porcine circovirus* (Yang *et al*., 2012). Nevertheless, antigenic changes have been predicted *in silico*, which may all contribute to the pathogen evading the host immune system. These predicted antigenic changes must be kept in mind in the design of serological tests and vaccines.

Serological results augment diagnostic molecular data and further information can be provided on the progress of the infection and the immune status of the bird (Khalesi *et al*., 2005). In the absence of clinical symptoms and negative PCR results, exposure to the virus can be detected through the detection of antibodies. As there are currently no vaccines available, any detected antibodies must result from the natural exposure to field virus.

Rapid agglutination assays have shortened the diagnosis time of various avian viruses (Raggi *et al*., 1960; Joshi & Joshi, 2009; Nakamura *et al*., 1993; Sree *et al*., 1998; Chen *et al*., 2007). However, no agglutination assays have been described for *BFDV*, until now. The antigen used in the slide agglutination test is a recombinantly-expressed protein, based on the *BFDV* CP gene. This protein is expressed on the cell surface of *Y. lipolytica* Po1h. The test relies on the agglutination of antibodies against *BFDV* and the test coat protein antigen and can be completed in 1 minute. Interpretation of the test is visual, and there is no difficulty in discerning between positive and negative samples. The other assays described in other avian viruses are based on latex agglutination, in which latex particles are coated with antibody or involve the use native antigen that is not coupled to any carrier particle.

Clinically normal birds may have been exposed to the virus; however they are able to mount an immune response strong enough to reduce the severity of the disease (Ritchie *et al*., 1992). Detection of antibodies in newly purchased birds would minimise the spread of disease from birds that have carrier status and test negative by PCR being introduced to the rest of the collection. A two-step testing approach is recommended, whereby birds are tested for the presence of both viral antigen using PCR, and antibodies to the virus, with the slide agglutination method.

However, despite the fact that this method is fast and simple, sensitivity is lacking compared to what would be expected from a competitive ELISA. It is proposed that the slide agglutination test should be used as an initial screening assay in a two stage testing regime.

An indirect ELISA was set up to optimise reagents for use in a competitive ELISA. A competitive ELISA is more likely to render reliable results as it uses a monoclonal antibody as the competing antibody and does not rely on the use of an antibody directed against IgG obtained from a specific bird species. Even though results attained with the experimentally produced *BFDV* CP seemed promising, it was decided that it would not be sustainable in the long-term. Therefore, the competitive ELISA was not developed with the use of the experimentally produced coat protein.

A sustainable source of antigen, *Y. lipolytica* expressed *BFDV* CP, was used in an indirect ELISA, however reproducible results were not obtained. Due to the random nature of integration of the expression cassette in the yeast genome, variance in the number of proteins expressed on each cell surface was observed.

Attempts to cleave the protein were not successful and treatment with Phospholipase C, specific for the phosphatidylinositol group found in the GPI anchor would not be cost effective in terms of large-scale purification of protein, as would be necessary in a diagnostic setting.

It is necessary to have a sustainable source of antigen that can be quantified. Results are promising for the development of a competitive ELISA, if one can standardise the amount of antigen expressed. In order to make any assumptions on quantitative detection of antibodies, it is vital that the amount of coating antigen is known. In future investigations it might be possible to use a single-copy integration strain, to be able to accurately quantify expressed protein. The copy numbers of the expression cassettes can then be estimated using the data obtained by real-time PCR analysis (Zhang *et al*., 2013), as in Chapter 3.

The most important limitation identified in this study was that a wide range of serum samples were not able to be obtained, as breeders are not able to draw sufficient blood in order to obtain serum. Breeders were advised to consult a veterinary surgeon, which is an added cost. Therefore, breeders were not willing to send in serum samples for the slide agglutination test, due to the cost of veterinary fees rather than the cost of the slide agglutination test.

6.2 Recommendation for future research

Serological test development will be further researched, with development of a competitive ELISA. Antigenic variance has been suggested for *BFDV*; however, no serotypes have been identified to date. Future research would involve the identification of novel serotypes and the adaptation of serological assays to accommodate these serotypes.

The successful control of BFD in both pet and wild birds depends on the development of vaccines that incite a strong, specific immune response and that can be efficiently produced in large quantities. In order to examine the potential of vaccination for the prevention and control of *BFDV*, the nucleotide sequence encoding the full-length capsid protein of *BFDV* was heterologously expressed by means of a novel yeast expression system (Boucher, 2013, unpublished work). Future work on this project will focus on increasing the production volume of the recombinant protein.

Cytokine mRNA quantification by real-time PCR will allow for investigation into cytokine profiles. Knowledge of the local cytokine pattern is essential to elucidate immune and pathological pathways and will be useful in vaccination studies.

Real-time PCR has great potential to elucidate viral replication and track infection in various tissues, such as the liver (Kondiah, 2004) and detect where the virus resides when it is absent from the bloodstream. There may also be a need to develop assays that would co-detect the presence of multiple *BFDV* strains in a sample.

6.3 Conclusion

The overall objectives of improving the current diagnostic strategy for *BFDV* were met, even if not in the original plan that was put forth. An implication of these findings is that both molecular and serological diagnosis should be used in the testing of *BFDV* samples, to obtain an overview of the bird's clinical history. New techniques described should be used in conjunction with existing tests and should not completely replace conventional techniques.

Beak and feather disease has a significant impact on psittacines in South Africa. The slide agglutination test described would be of great benefit for both diagnosis and prevention of infection. The rapid screening test would be cheap and efficient for breeders to identify potential threats and exercise appropriate biosecurity measures. The slide agglutination test would therefore have great application for screening a bird for prior exposure to the virus. Several courses of action are suggested for breeders to have a good concept of hygiene. These include: i) training on sample collection ii) accurate interpretation of PCR results; iii) limitations of PCR technology; and iv) basic epidemiology.

The legal trade in parrots needs to be regulated, with strict testing regimes and suitable quarantine measures. This will prevent the spread of *BFDV* into new areas as well as the introduction of new strains that could recombine with existing strains.

SUMMARY

Beak and feather disease (BFD), caused by *Beak and feather disease virus* (*BFDV*) is a dermatological condition afflicting parrot species. It is becoming increasingly difficult to ignore not only the significant negative economic impact that the virus has on the parrot breeding industry but also the detrimental effect it has on the survival of the endemic Cape parrot (*Poicephalus robustus*). The virus, a member of the *Circoviridae*, is known to possess a non-enveloped, circular, single-stranded DNA genome. Two major open reading frames (ORFs) encode the replication associated protein (Rep) and the coat protein (CP). The study was set out to evaluate and improve the current diagnostic strategy for *BFDV*, with both molecular and serological techniques.

The following objectives were attempted:

1. To evaluate polymerase chain reaction (PCR) and quantitative real-time polymerase chain reaction (qPCR) as diagnostic tools for *BFDV*.

Detection of *BFDV* with conventional PCR is not always sensitive, especially in birds without clinical symptoms. Furthermore, genetic variance was suggested to have a detrimental effect on primer hybridisation. A real-time assay was designed to address these problems. It amplified a 115 bp fragment of ORF V1 and was able to quantify viral load.

2. To recombinantly express *BFDV* coat protein.

A sustainable source of the main immunogen, coat protein, was needed for use in serological test development. Bacterial expression of *BFDV* CP was unsuccessful; however, *BFDV* CP from an alternative expression study was used as a serological diagnostic antigen.

3. To develop serological diagnostic tests for *BFDV.*

A novel slide agglutination test was developed and will serve as an initial screening tool in serological diagnosis. Steps were made in the development of a competitive Enzyme Linked Immunosorbent Assay (ELISA) for a quantitative indication of immune response to *BFDV*.

A significant proportion of asymptomatic *BFDV* infections exist. Using a combination approach of both molecular and serological tests increases the capacity to detect infections or exposure to virus. New techniques described should be used in conjunction with existing tests and should not completely replace conventional techniques for diagnosis of *BFDV* infection or detection of exposure to the virus.

Keywords: *Beak and feather disease virus*; diagnostics; PCR; real-time PCR; genetic variance; slide agglutination; ELISA

OPSOMMING

Beak and feather disease (BFD), wat veroorsaak word deur *Beak and feather disease virus* (*BFDV*) is 'n dermatologiese toestand wat papegaai spesies versmag. Dit word toenemend moeilik om nie net die beduidende negatiewe ekonomiese impak wat die virus het op die papegaai teling bedryf nie, maar ook die nadelige uitwerking wat dit op die voortbestaan van die endemiese Kaapse papegaai (*Poicephalus robustus*) te ignoreer. Die virus, 'n lid van die *Circoviridae*, is bekend as 'n nie-omvou, sirkulêre, enkelstring DNA genoom in besit te neem. Twee groot oop lees rame (OLRe) enkodeer die replikasie verwante proteïene (Rep) en die kapsied proteïen (KP). Die studie was uiteengesit om die huidige diagnostiese strategie vir *BFDV* te evalueer en te verbeter, met beide molekulêre en serologiese tegnieke.

Die volgende doelwitte is gepoog:

1. Om polimerase kettingreaksie (PKR) en kwantitatiewe werklike tyd polimerase kettingreaksie (qPCR) as diagnostiese instrumente vir *BFDV* te vergelyk.

Opsporing van *BFDV* met konvensionele PCR is nie altyd sensitief nie, veral in voëls sonder kliniese simptome. Verder is genetiese afwyking voorgestel om 'n nadelige uitwerking op primer verbastering te hê. 'n qPCR toets is ontwerp om hierdie probleme aan te spreek. Dit versterk 'n 115 bp fragment van OLR V1 en was in staat om virale lading te kwantifiseer.

2. Om die *BFDV* kapsied proteïen in 'n bakteriële gasheer uit te druk.

'n Volhoubare bron van die hoof immunogeen, kapsied proteïen, is wat nodig is vir die gebruik in serologiese toets ontwikkeling. Bakteriële uitdrukking van *BFDV* KP was onsuksesvol, maar *BFDV* KP van 'n alternatiewe uitdrukking studie is gebruik as 'n serologiese diagnose antigeen.

3. Om serologiese diagnostiese toetse vir *BFDV* te ontwikkel.

'n Plaat agglutinasie toets is ontwikkel en sal as 'n aanvanklike keuring instrument in serologiese diagnose dien. Stappe is gedoen in die ontwikkeling van 'n mededingende Ensiem-Gekoppelde Immunosorbent toets (ELISA) vir 'n kwantitatiewe aanduiding van immuun reaksie op *BFDV*.

'n Beduidende hoeveelheid van asimptomatiese *BFDV* infeksies kom voor. 'n Kombinasie van beide molekulêre en serologiese toetse verhoog die kapasiteit om infeksies of die

blootstelling aan die virus op te spoor. Nuwe tegnieke wat beskryf is moet in samewerking met bestaande toetse gebruik moet word en nie konvensionele tegnieke heeltemal vervang.

Sleutelwoorde: *BFDV*; diagnose; PKR; real-time PCR; genetiese afwyking; plaat agglutinasie; ELISA

LIST OF REFERENCES

Abe, A., Inoue, K., Tanaka, T., Kato, J., Kajiyama, N., Kawaguchi, R., Tanaka, S., Yoshiba, M. & Kohara, M. (1999). Quantitation of hepatitis B virus genomic DNA by real-time detection PCR. *J Clin Microbiol* **37**, 2899-2903.

Aitken, C. E., Marshall, R. A. & Puglisi, J. D. (2008). An oxygen scavenging system for improvement of dye stability in single-molecule fluorescence experiments. *Biophys J* **94**, 1826-1835.

Albertyn, J., Tajbhai, K. M. & Bragg, R. R. (2004). Psittacine beak and feather disease virus in budgerigars and ring-neck parakeets in South Africa. *Onderstepoort J Vet Res* **71**, 29-34.

Altschul, S. F., Madden, T. L., Schaffer, A. A., Zhang, J., Zhang, Z., Miller, W. & Lipman, D. J. (1997). Gapped BLAST and PSI-BLAST: a new generation of protein database search programs. *Nucleic Acids Res* **25,** 3389-3402.

Animal Health/World Bank. 2010. Good practices for biosecurity in the pig sector – Issues and options in developing and transition countries. FAO Animal Production and Health Paper No. 169. Rome, FAO.

Aslanzadeh, J. (2004). Preventing PCR amplification carryover contamination in a clinical laboratory. *Ann Clin Lab Sci* **34**, 389-396.

Azoumanian, L. (2003). Tech Talk. *Vacutainer technical notes* **2**. Retrieved from http://www.bd.com/vacutainer/pdfs/techtalk/TechTalk_Jan2004_VS7167.pdf

Azzouz, N., Ranck, J. L. & Capdeville, Y. (1990). Purification of the temperature-specific surface antigen of *Paramecium primaurelia* with its glycosylphosphatidylinositol membrane anchor. *Protein Exp Purif* **1**, 13-18.

Baneyx, F. (1999). Recombinant protein expression in E*scherichia coli. Curr Opin Biotechnol* **10**, 411-421.

Bassami, M. R., Berryman, D., Wilcox, G. E. & Raidal, S. R. (1998). Psittacine *beak and feather disease virus* nucleotide sequence analysis and its relationship to porcine circovirus, plant circoviruses, and chicken anemia virus. *Virology* **249**, 453-459.

Bassami, M. R., Ypelaar, I., Berryman, D., Wilcox, G. E. & Raidal, S. R. (2001). Genetic diversity of *beak and feather disease virus* detected in psittacine species in Australia. *Virology* **279**, 392-400.

Bert, E., Tomassone, L., Peccati, C., Navarrete, M. G. & Sola, S. C. (2005). Detection of *beak and feather disease virus* (*BFDV*) and avian polyomavirus (APV) DNA in psittacine birds in Italy. *J Vet Med B Infect Dis Vet Public Health* **52**, 64-68.

Biagini, P., Gallian, P., Attoui, H., Touinssi, M., Cantaloube, J., de Micco, P. & Lamballerie, D. (2001). Genetic analysis of full-length genomes and subgenomic sequences of TT virus-like mini virus human isolates. *J Gen Virol* **82**, 379-383.

Biagini, P., Bendinelli, M., Hino, S., Kakkola, L., Mankertz, A., Niel, C., Okamoto, H., Raidal, S., Teo, C. G. & Todd, D. (2012). Family - Circoviridae. In *Virus Taxonomy: Ninth Report of the International Committee on Taxonomy of Viruses,* pp. 343-349. Edited by A. M. Q. King, E. Lefkowitz, M. J. Adams and E. B. Carstens. San Diego: Elsevier.

Bonne, N., Clark, P., Shearer, P. & Raidal, S. (2008). Elimination of false-positive polymerase chain reaction results resulting from hole punch carryover contamination. *J Vet Diagn Invest* **20**, 60-63.

Bonne, N. J. (2009). Psittacine beak and feather disease: vaccination, haematological response and PCR methodology. Ph.D. Thesis, Murdoch University, Perth.

Bonne, N., Shearer, P., Sharp, M., Clark, P. & Raidal, S. (2009). Assessment of recombinant *beak and feather disease virus* capsid protein as a vaccine for psittacine beak and feather disease. *J Gen Virol* **90**, 640-647.

Borst, A., Box, A. T. & Fluit, A. C. (2004). False-positive results and contamination in nucleic acid amplification assays: suggestions for a prevent and destroy strategy. *Eur J Clin Microbiol Infect Dis* **23**, 289-299.

Boyes, S. (2013). *Rescuing South Africa's Endangered Cape Parrot.* Retrieved from http://newswatch.nationalgeographic.com/2013/03/23/rescuing-the-endangered-cape-parrot/.

Bulani, S. I., Moleleki, L., Albertyn, J. & Moleleki, N. (2012). Development of a novel rDNA based plasmid for enhanced cell surface display on *Yarrowia lipolytica*. *AMB Express* **2**, 1-8.

Bustin, S. A., Benes, V., Nolan, T. & Pfaffl, M. W. (2005). Quantitative real-time RT-PCR-a perspective. *J Mol Endocrinol* **34**, 597-601.

Chen, J., Jin, M., Yu, Z., Dan, H., Zhang, A., Song, Y. & Chen, H. (2007). A latex agglutination test for the rapid detection of *Avian influenza virus* subtype H5N1 and its clinical application. *J Vet Diagn Invest* **19**, 155-160.

Claas, E. C. J., Melchers, W. J. G. & van den Brule, A. J. C. (2007). The role of real-time PCR in routine microbial diagnostics. In *Real-time PCR in Microbiology. From diagnosis to characterization*, pp.231-267. Edited by I. M. Mackay. Norfolk, UK: Caister Academic Press.

Corning (2012). Ampicillin vs. Carbenicillin. Technical note. Retrived from http://cellgro.com/media/upload/file/productinfosheets/new/Ampicillin%20vs_%20Carbenicillin.pdf

Crowther, J. R. (1995). *ELISA: Theory and Practice*. Totowa, NJ: Springer.

Crowther, R. A., Berriman, J. A., Curran, W. L., Allan, G. M. & Todd, D. (2003). Comparison of the structures of three Circoviruses: *Chicken Anemia Virus, Porcine Circovirus Type 2,* and *Beak and Feather Disease Virus*. *J Virol* **77***,* 13036-13041.

de Kloet, E. & de Kloet, S. R. (2004). Analysis of the beak and feather disease viral genome indicates the existence of several genotypes which have a complex psittacine host specificity. *Arch Virol* **149**, 2393-2412.

Department of Environment and Heritage, Australian Government (2006). Hygiene Protocols for the Prevention and Control of Diseases (Particularly Beak and Feather Disease) in Australian Birds. Commonwealth of Australia 2013.

Doneley, R. J. T. (2003). Acute Beak and Feather Disease in juvenile African Grey parrots – an uncommon presentation of a common disease. *Aust Vet J* **81**, 206-207.

Dong, X., Stothard, P., Forsythe, I. J. & Wishart, D. S. (2004). PlasMapper: a web server for drawing and auto-annotating plasmid maps. *Nucleic Acids Res* **32**, W660-W664.

Duvenage, L., Hitzeroth, I. I., Meyers, A. E. & Rybicki, E. P. (2013). Expression in tobacco and purification of *beak and feather disease virus* capsid protein fused to elastin-like polypeptides. *J Virol Methods* **191**, 55-62.

Eldar, A., Horovitcz, A. & Bercovier, H. (1997). Development and efficacy of a vaccine against *Streptococcus iniae* infection in farmed rainbow trout. *Vet Immunol Immunopathol* **56**, 175-183.

Espy, M. J., Uhl, J. R., Sloan, L.M., Buckwalter, S. P., Jones, M. F., Yao, J. D. C., Wengenack, J. E., Rosenblatt, F. R., Cockerill, III, F. R. & Smith, T. F. (2006). Real-Time PCR in clinical microbiology: applications for routine laboratory testing. *Clin Microbiol Rev* **19,** 165-256**.**

Gibbs, M. J. & Weiller, G. F. (1999). Evidence that a plant virus switched hosts to infect a vertebrate and then recombined with a vertebrate-infecting virus. *Proc Natl Acad Sci USA* **96**, 8022-8027.

Gorham, J., Knowles, D., Li, H. & Pastoret, P. (2004). Biotechnology in the diagnosis of infectious diseases and vaccine development. In *Manual of standards for diagnostic tests and vaccines for terrestrial animals*, pp. 69-90*.* 5th edn. Paris: Office International des Epizooties.

Greenacre, C. B., Latimer, K. S., Niagro, F. D., Campagnoli, R. P., Pesti, D. & Ritchie, B. W. (1992). Psittacine Beak and Feather Disease in a Scarlet Macaw (*Ara macao*). *J Assoc Avian Vet* **6**, 95-98.

Guo, B. & Bi, Y. (2002). Cloning PCR Products: An Overview. In *Methods in Molecular Biology **192**: PCR Cloning Protocols*, pp 111-119. Edited by B-Y Chen and H.W. Janes. Totowa, NJ: Humana Press Inc.

Gustafsson, C., Govindarajan, S. & Minshull, J. (2004). Codon bias and heterologous protein expression. *Trends Biotechnol* **22**, 346-353.

Hanahan, D. (1983). Studies on transformation of *Escherichia coli* with plasmids. *J Mol Biol* **166**, 557-580.

Hattingh, A. R. (2009). Antigenic investigation of genetically different strains of *Beak and feather disease virus*. M.Sc. Dissertation. University of the Free State, Bloemfontein.

Heath, L., Martin, D. P., Warburton, L., Perrin, M., Horsfield, W., Kingsley, C., Rybicki,

E. P. & Williamson, A. (2004). Evidence of unique genotypes of *beak and feather disease virus* in Southern Africa. *J Virol* **78**, 9277-9284.

Heath, L., Williamson, A. & Rybicki, E. P. (2006). The capsid protein of *beak and feather disease virus* binds to the viral DNA and is responsible for transporting the replication-associated protein into the nucleus. *J Virol* **80**, 7219-7225.

Hess, M., Scope, A. & Heincz, U. (2004). Comparitive sensitivity of polymerase chain reaction diagnosis of psittacine beak and feather disease on feather samples, cloacal swabs and blood from budgerigars (*Melopsittacus undulates*, Shaw 18005). *Avian Pathol* **33**, 477-481.

Hopp, T. P. & Woods, K. R. (1981). Prediction of protein antigenic determinants from amino acid sequences. *Proc Natl Acad Sci USA* **78**, 3824-3828.

Hurtado, C. A. R. & Rachubinski, R. A. (2002). Isolation and characterization of *YlBEM1*, a gene required for cell polarization and differentiation in the dimorphic yeast *Yarrowia lipolytica*. *Eukaryot Cell* **1**, 526-537.

Ilyina, T. V. & Koonin, E. V. (1992). Conserved sequence motifs in the initiator protein for rolling circle replication encoded by diverse replicons from eubacteria, eukaryotes and archeabacteria. *Nucleic Acids Res* **20**, 3279-3285.

Inaba, C. Higuchi, S., Moriska, H., Kuroda, K. & Ueda, M. (2010). Synthesis of functional dipeptide carnosine from nonprotected amino acids using carnosinase-displaying. *Appl Microbiol Biotechnol* **86,** 2895-1902.

Jacobson, E.R., Clubb, S., Simpson, C., Walsh, M., Lothrop, C. D., Gaskin, J., Bauer, J., Hines, S., Kollias, G.V., Poulos. P., et al. (1986). Feather and beak dystrophy and necrosis in cockatoos: clinicopathologic evaluations. *J Am Vet Med Assoc* **189**, 999-1005.

Jana, S. & Deb, J. K. (2005). Strategies for efficient production of heterologous proteins in *Escherichia coli. Appl Microbiol Biotechnol* **67**, 289-298.

Claas, E. C. J., Melchers, W. J. G. & van den Brule, A. J. C. (2007). The role of real-time PCR in routine microbial diagnostics. In *Real-time PCR in Microbiology. From diagnosis to characterization*, pp.231-267. Edited by Mackay, I. M. Norfolk, UK: Caister Academic Press.

Janeway, C. A. Jr., Travers, P., Walport, M., & Shlomchik, M. (2001). The Immune System in Health and Disease. In *Immunobiology*. Edited by Murphy, M. K. & Travers, P. New York, USA: Garland Science.

Jergens, A. E., Brown, T. P. & England, T. L. (1988). Psittacine beak and feather disease syndrome in a cockatoo. *J Am Vet Med Assoc* **193**, 1292-1294.

Johne, R., Raue, R., Grund, C., Kaleta, E. F. & Müller, H. (2004). Recombinant expression of a truncated capsid protein of *Beak and feather disease virus* and its application in serological tests. *Avian Pathol* **33**, 328-336.

Jones, A. K. (2006). Psittacine beak & feather Disease. Retrieved from http://www.theparrotsocietyuk.org/veterinary-advice/psittacine-beak-and-feather-disease.

Joshi, N. & Joshi, R. K. (2009). Detection of *Newcastle disease virus* (NDV) antigen by co-agglutination test using antibody coated *Staphylococcus aureus*. *Indian J Comp Microbiol Immunol Infect Dis* **30**, 67-69.

Kane, J. F. (1995). Effects of rare codon clusters on high-level expression of heterologous proteins in *Escherichia coli*. *Curr Opin Biotechnol* **6**, 494-500.

Katoh, H., Ohya, K. & Fukushi, H. (2008). Development of novel real-time PCR assays for detecting DNA virus infections in psittaciform birds. *J Virol Methods* **154**, 92-98.

Khalesi, B., Bonne, N., Stewart, M., Sharp, M. & Raidal, S. (2005). A comparison of haemagglutination, haemagglutination inhibition and PCR for the detection of psittacine beak and feather disease virus infection and a comparison of isolates obtained from loriids. *J Gen Virol* **86**, 3039-3046.

Khalesi, B. (2007). Studies of *beak and feather disease virus* infection. Ph.D. Thesis. Murdoch University, Perth.

Kolaskar, A. S. & Tongaonkar, P. C. (1990). A semi-empirical method for prediction of antigenic determinants on protein antigens. *FEBS Lett* **276**, 172-174.

Kondiah, K. (2004). Establishment of serological and molecular techniques to investigate diversity of Psittacine beak and feather disease virus in different psittacine birds in South Africa. M.Sc. Thesis. University of the Free State, Bloemfontein.

Kondiah, K., Albertyn, J. & Bragg, R. R. (2006). Genetic diversity of the Rep gene of *beak and feather disease virus* in South Africa. *Arch Virol* **151**, 2539-2545.

Kondiah, K. (2008). Development of a DNA vaccine for the prevention of Psittacine beak and feather disease. Ph.D. Thesis. University of the Free State, Bloemfontein.

KPL, Inc. (2013). Technical guide for ELISA. Retrieved from http://kpl.com/docs/techdocs/KPL%20ELISA%20Technical%20Guide.pdf.

Kundu, S., Faulkes, C. G., Greenwood, A. G., Jones, C. G., Kaiser, P., Lyne, O. D., Black, S. A., Chowrimootoo, A. & Groombridge, J. J. (2012). Tracking viral evolution during disease outbreak: the rapid and complete selective sweep of a circovirus in the endangered echo parakeet. *J Virol* **86**, 5221-5229.

Kurland, C. & Gallant, J. (1996). Errors of heterologous protein expression. *Curr Opin Biotechnol.* **7**, 489-493.

Kwapinski, J. B. G. (1972). The agglutination test. In *Methodology of immunochemical and immunological research*, pp. 296-316. Edited by Wiley-Interscience. New York.

Laemmli, U. K. (1970). Cleavage of structural proteins during the assembly of the head of bacteriophage T4. *Nature* **227**, 680-685.

Larsen J. E., Lund, O. & Nielsen, M. (2006). Improved method for predicting linear B-cell epitopes. *Immunome Res* **2**, 2.

Latimer, K. S., Rakich, P. M., Kircher, I. M., Ritchie, B. W., Niagro, F.D., Steffens, W. L. III. & Lukert, P. D. (1990). Extracutaneous viral inclusions in psittacine beak and feather disease. *J Vet Diagn Invest* **88**, 204-207.

Latimer, K. S., Rakich, P. M., Steffens, W. L. III., Kircher, I. M., Ritchie, B. W., Niagro, F. D. & Lukert, P. D. (1991a). A novel DNA virus associated with feather inclusions in Psittacine beak and feather disease. *Vet Pathol* **28**, 300-304.

Latimer, K. S., Rakich, P. M., Niagro, F. D., Ritchie, B. W., Steffens, W. L. III., Kircher, I. M., Campagnoli, R. P., Pesti, D. A. & Lukert, P. D. (1991b). An updated review of psittacine beak and feather disease. *J Assoc Avian Vet* **5**, 211-220.

Latimer, K. S., Niagro, F. D., Campagnoli, R. P., Ritchie, B. W., Pesti, D. A. & Steffens W. L. III. (1993). Diagnosis of concurrent avian polyomavirus and psittacine beak and feather disease virus infections using DNA probes. *J Assoc Avian Vet* **7**, 141-146.

Lefeuvre, P., Lett, J. M., Varsani, A. & Martin, D. P. (2009). Widely conserved recombination patterns among single-stranded DNA viruses. *J Virol* **83**, 2697-2707.

Locatelli, G., Santoro, F., Veglia, F., Gobbi, A., Lusso, P. & Malnati, M. S. (2000). Real-time quantitative PCR for human herpesvirus 6 DNA. *J Clin Microbiol* **38**, 4042-2028.

Lucigen. (2013). Simplifying genomics manual: CloneSmart® Cloning kits (pSMART vectors) Retrieved from: http://lucigen.com/store/docs/manuals/MA004-CloneSmart-HCLC-Blunt-Cloning.pdf

Lukert, P., de Boer, G. F., Dale, J. L., Keese, P., McNulty, M. S., Randles, J. W. & Tischer, I. (1995). Circoviridae. In *Virus Taxonomy: Sixth Report of the International Committee on Taxonomy of Viruses*, pp. 166-168. Edited by F. A. Murphy, C. M. Fauquet, D. H. L. Bishop, S. A. Ghabrial, A. W. Jarvis, G. P. Martelli, M. A. May & M. D. Summers. NY: Springer–Verlag.

Mackay, I. M., Mackay, J. F., Nissen, M. D. & Sloots, T. P. (2007). Real-time PCR; History and Fluorgenic Chemistries. In *Real-Time PCR in Microbiology From diagnosis to characterization*, pp. 1-40. Edited by I. M. Mackay. UK: Calister Academic Press.

Madzak, C., Otterbein, L., Chamkha, M., Moukha, S., Asther, M., Gaillardin, C., Beckerich, J. (2004). Heterologous production of laccase from basidiomyces *Pycnoporus cinnabarinus* in the dimorphic yeast *Yarrowia lipolytica*. *FEMS Yeast Res* **5**, 635-646.

Maloy, S., Stewart, V. & Taylor, R. (1996). *Genetic analysis of pathogenic bacteria*. Cold Spring Harbor, NY: Cold Spring Harbor Laboratory Press.

Mankertz, A., Persson, F., Mankertz, J., Blaess, G. & Buhk, H. J. (1997). Mapping and characterization of the origin of DNA replication of porcine circovirus. *J Virol* **71**, 2562-2566.

Mankertz, A., Caliskan, R., Hattermann, K., Hillenbrand, B., Kurzendoerfer, P., Mueller, B., Schmitt, C. Steinfeldt, T. & Finsterbusch, T. (2004). Molecular biology of porcine circovirus: analyses of gene expression and viral replication. *Vet Microbiol* **98**, 81-88.

Maramorosch, K., Murphy, F. A. & Shatkin, A. J. (2001). *Advances in Virus Research*, 1st edn. San Diego: Academic Press.

Mayer, G. (2010). Immunoglobulins – antigen-antibody reactions and selected tests. Retrieved from pathmicro,med.sc.edu/mayer/ab-ag-rx.htm

McOrist, S., Black, D. G., Pass, D. A., Scott, P. C. & Marshall, J. (1984). Beak and feather dystrophy in wild sulphur-crested cockatoos (*Cacatua galerita*). *J Wildl Dis* **20**, 120-124.

Müller, A., Klöppel, C., Smith-Valentine, M., Van Houten, J. & Simon, M. (2012).

Selective and programmed cleavage of GPI-anchored proteins from the surface membrane by phospholipase C. *BBA Biomembranes* **1818**, 117-124.

Nakamura, T., Kato, A., Lin, Z., Hiraga, M., Nunoya, T., Otaki, Y., Ueda, S. (1993). A rapid quantitative method for detecting infectious bursal disease virus using polystyrene latex microspheres. *J Virol Methods* **43**, 123-129.

Nakamura, Y., Shibasaki, S., Ueda, M., Tanaka, A., Fukunda, H. & Kondo, A. (2001). Development of novel whole-cell immunoadsorbents by yeast surface display of the IgG-binding domain. *Appl Microbiol Biotechnol* **57**, 500-505.

Niagro, F. D., Forsthoefel, A. N., Lawther, R. P., Kamalanathan, L., Ritchie, B. W., Latimer, K. S. & Lukert, P. D. (1998). *Beak and feather disease virus* and *Porcine circovirus* genomes: intermediates between the geminiviruses and plant circoviruses. *Arch Virol* **143**, 1723-1744.

Nicaud, J. M., Gaillardin, C., Seman, M. & Pigenede, G. (1998). Process of non-homologous transformation of *Yarrowia lipolytica*. French Patent Application PCT/FR99/0209.

Nicaud, J., Madzak, C., van den Broek, P., Gysler, C., Duboc, P., Niederberger, P. & Gaillardin, C. (2002). Protein expression and secretion in the yeast *Yarrowia lipolytica*. *FEMS Yeast Res* **2**, 371-379.

Nitsche, A. (2007). Oligonucleotide design for in-house real-time PCR applications in microbiology. In R*eal-Time PCR in Microbiology: From Diagnosis to Characterisation*, pp. 41-69. Edited by I. M. Mackay. Norwich: Horizon Scientific Press.

Novy, R., Drott, D., Yaeger, K. & Mierendorf, R. (2001). Overcoming the codon bias of *E. coli* for enhanced protein expression. *Innovations Newsletter of Novagen Inc* **12**.

Parker, J., Guo, D., Hodges, R. (1986). New hydrophilicity scale derived from High-Performance Liquid Chromatography peptide retention data: correlation of predicted surface residues with antigenicity and X-ray-derived accessible sites. *Biochemistry* **25**, 5425-5432.

Pass, D. A. & Perry, R. A. (1984). The pathology of Psittacine beak and feather disease. *Aust Vet J* **61**, 69-74.

Patterson, E. I., Forwood, J. K. & Raidal, S. R. (2012). Homology modelling and structural comparisons of capsid-associated proteins reveal important virus-specific antigens. *CSTA* **1**, 9-16.

Paweska, J.T., Sewlall, N.H., Ksiazek, T.G., Blumberg, L.H., Hale, M.J., Lipkin, W.I., Weyer, J., Nichol, S.T., Rollin, P.E., McMullan, L.K. *et al*. (2009). Nosocomial outbreak of novel arenavirus infection, southern Africa. *Emerg Infect Dis* **15**, 1598-1602.

Pignede, G., Wang, H., Fudalej, F., Gaillardin, C. Seman, M., Nicaud, J. M. (2000). Characterization of an extracellular lipase encoded by *LIP2* in *Yarrowia lipolytica*. *J Bacteriol* **182**, 2802-2810.

Posada, D. & Crandall, K. A. (2001). Evaluation of methods for detecting recombination from DNA sequences: computer simulations. *Proc Natl Acad Sci* **98**, 13757-13762.

Pyne, M. (2005). Psittacine beak and feather disease. National Wildlife Rehabilitation Conference. Retrieved from http://www.awrc.org.au/uploads/5/8/6/6/5866843/awrc_michael_pyne.pdf.

Queipo-Ortuno, M. I., Colmenero, J. D., Reguera, J. M., Garcia-Ordonez, M. A.,Pachom, M. E., Gonzalez, M. & Morata, P. (2005). Rapid diagnosis of human brucellosis by SYBR Green I-based real-time PCR assay and melting curve analysis in serum samples. *Clin Microbiol Infect* **11**, 713-718.

Raggi, L. G. (1960). Research note – A rapid macroscopic plate agglutination test for Newcastle disease – a preliminary report. *Avian Dis* **4**, 320-323.

Rahaus, M. & Wolff, M. H. (2003). Psittacine beak and feather disease: a first survey of the distribution of *beak and feather disease virus* inside the population of captive psittacine birds in Germany. *J Vet Med B Infect Dis Vet Public Health* **50**, 368-371.

Rahaus, M., Desloges, N., Probst, S., Loebbert, B., Lantermann, W. & Wolff, M. H. (2008). Detection of *beak and feather disease virus* DNA in embryonated eggs of psittacine birds. *Vet Med* **53**, 53-58.

Raidal, S. R., Firth, G. A. & Cross, G. M (1993a). Vaccination and challenge studies with Psittacine beak and feather disease virus. *Aust Vet J* **70**, 437-441.

Raidal, S. R., McElnea, C. L. & Cross, G. M. (1993b). Seroprevalence of Psittacine beak and feather disease virus in wild psittacine birds in New South Wales. *Aust Vet J* **70**, 137-

139.

Raidal, S. R. (1994). Studies on psittacine beak and feather disease. Ph.D. Thesis. University of Sydney, Sydney.

Raidal, S. R. & Cross, G. M. (1994a). The haemagglutination spectrum of psittacine beak and feather disease virus. *Avian pathol* **23**, 621-630.

Raidal, S. R. & Cross, G. M. (1994b). Control by vaccination of psittacine beak and feather disease in a mixed flock of *Agapornis spp*. *Aust Vet Practit* **24**, 178-180.

Raidal, S. R., Bonne, J. N. & Stewart, M. (2004). Development of recombinant proteins as a candidate vaccine for Psittacine Beak and Feather Disease. Murdoch University, Perth. Report for the Australian Government Department of the Environment and Heritage.

Raue, R., Johne, R., Crosta, L., Bürkle, M., Gerlach, H. & Müller, H. (2004). Nucleotide sequence analysis of a C1 gene fragment of psittacine beak and feather disease virus amplified by real-time polymerase chain reaction indicates a possible existence of genotypes. *Avian pathol* **33**, 41-50.

Riddoch, P. A., Raidal, S. R. & Cross, G. M. (1996). Psittacine circovirus antibody detection and an update on the methods for diagnosis of psittacine Beak and feather disease. *Aust Vet Practit* **26**, 134-139.

Ritchie, B. W., Niagro, F. D., Lukert, P. D., Latimer, K. S., Steffens, W. L. III. & Pritchard, N. (1989a). A review of psittacine beak and feather disease characteristics of the PBFD virus. *J Assoc Avian Vet* **3**, 143-149.

Ritchie, B. W., Niagro, F. D., Lukert, P.D., Steffens, W. L. III. & Latimer, K. S. (1989b). Characterization of a New Virus from Cockatoos with Psittacine beak and feather disease. *Virology* **171**, 83-88.

Ritchie, B. W., Niagro, F. D., Latimer, K. S., Lukert, P. D., Steffens, W. L. III., Rakich, P. M. & Pritchard, N. (1990). Ultrastructural, protein composition and antigenic comparison of Psittacine beak and feather disease virus purified from four genera of psittacine birds. *J Wildl Dis* **26**, 196-203.

Ritchie, B. W., Niagro, F. D., Latimer, K. S., Steffens, W. L. III., Pesti, D. & Lukert, P. D. (1991). Hemagglutination by psittacine beak and feather disease virus and use of hemagglutination inhibition for detection of antibodies against the virus. *Am J Vet Res* **52**,

1810-1815.

Ritchie, B. W., Niagro, F. D., Latimer, K. S., Steffens, W. L. III., Pesti, D., Campagnoli, R. & Lukert, P.D. (1992). Antibody response to and maternal immunity from an experimental Psittacine beak and feather disease vaccine. *Am J Vet Res* **53**, 1512-1518.

Ritchie, B. W. & Carter, K. (1995). *Avian Viruses Function and Control*. 1st edn. Lake Worth, Florida: Wingers Publishing Inc.

Ritchie, P. A., Anderson, I. L. & Lambert, D. M. (2003). Evidence for specificity of Psittacine beak and feather disease virus among avian hosts. *Virology* **306**, 109-115.

Rocha, P.C. (2004). Codon usage bias from tRNA's point of view: redundancy, specialization, and efficient decoding for translation optimization. *Genome Res* **14**, 2279-2286.

Roche Applied Science, (2010). LightCycler® 2.0 Instrument Operator's Manual, Software version 4.05, Manual B: for general laboratory use, 102, 149.

Royer, R. L., Nawagitgul, P., Halbur, P. G. & Paul, P. S. (2001). Susceptibility of porcine circovirus type 2 to commercial and laboratory disinfectants. *J Swine Health Prod* **9**, 281-284

Rybicki, E. P., Williamson, A. & Heath, L. (2005). *Beak and feather disease virus* sequences, composition and vaccines and the use thereof in therapy, diagnosis and assay. Retrieved from http://www.wipo.int/pctdb/fr/wo.jsp?WO=2005082929&IA=IB2005000405&DISPLAY=STATUS

Saitou, N. & Nei, M. (1987). The neighbor-joining method: A new method for reconstructing phylogenetic trees. *Mol Biol Evol* **4**, 406-425.

Sambrook, J., Fritsch, E. F. & Maniatis, T. (1989). Molecular cloning, a laboratory manual. 2nd edn. Cold Spring Harbor, NY: Cold Spring Harbor, Laboratory.

Sambrook, J. & Russel, D. W. (2001) Molecular Cloning: A Laboratory Manual. 3rd edn. Cold Spring Harbor, NY: Cold Spring Harbor Laboratory.

Sambrook, J. & Russel, D.W. (2006). Molecular cloning: a laboratory manual. 2nd edn. Cold Spring Harbor, NY; Cold Spring Harbor Laboratory.

Sanada, N. & Sanada, Y. (2000). The sensitivities of various erythrocytes in a

haemagglutination assay for the detection of psittacine *beak and feather disease virus*. *J Vet Med B* **47**, 441-443.

Schoemaker, N. J., Dorrestein, G. M., Latimer, K. S., Lumeij, J. T., Kik, M. J. L., van der Hage, M. H. & Campagnoli, R. P. (2000). Severe leukopenia and liver necrosis in young African grey parrots (*Psittacus erithacus erithacus*) infected with psittacine circovirus. *Avian Dis* **44**, 470-478.

Schutten, M., van den Hoogen, B., van der Ende, M. E., Grunters, R. A., Osterhaus, A. D. M. E. & Niesters, H. G. M. (2000). Development of a real-time quantitative RT-PCR for the detection of HIV-2 RNA in plasma. *J Virol Methods* **88**, 81-87.

Sharp, P. M., Bailes, E., Grocock, R. J., Peden, J. F. & Sockett, R. E. (2005). Variation in the strength of selected codon bias usage among bacteria. *Nucleic Acids Res* **33**, 1141-1153.

Shearer, P. L., Bonne, N., Clark, P., Sharp, M. & Raidal, S. R. (2007). Development and applications of a monoclonal antibody to a recombinant *beak and feather disease virus* (*BFDV*) capsid protein. *J Virol Methods* **147**, 206-212.

Shearer, P. L. (2008). Development of novel diagnostic and vaccine options for *beak and feather disease virus* (*BFDV*). Ph.D. Thesis, Murdoch University, Perth.

Shearer, P. L., Bonne, N., Clark, P., Sharp, M. & Raidal, S. R. (2008). *Beak and feather disease virus* infection in cockatiels (*Nymphicus hollandicus*). *Avian Pathol* **37**, 75-81.

Shearer, P. L., Sharp, M., Bonne, N., Clark, P. & Raidal, S. R. (2009a). A quantitative real-time polymerase chain reation assay for *beak and feather disease virus* (*BFDV*). *J Virol Methods* **159**, 98-104.

Shearer, P. L., Sharp, M., Bonne, N., Clark, P. & Raidal, S. R. (2009b). A blocking ELISA for the detection of antibodies to psittacine beak and feather disease virus (*BFDV)*. *J Virol Methods* **158**, 136-140.

Sompuram, S. R. Vani, K., Hafer, L. J. & Bogen, S. A. (2006). Antibodies immunoreactive with formalin-fixed tissue antigens recognize linear protein epitopes. *Am J Clin Pathol* **125**, 82-90.

Sree, K. V., Rao, M. V. S., Malathy, V. B. & Reddy, Y. N. (1998). Development of a latex agglutination test for detection of egg drop syndrome-76 virus (EDS-76). *Indian Vet J* **7**, 870-872.

SPSS, IBM Corp. (2012). IBM SPSS Statistics for Windows, Version 21.0 Armonk, NY: IBM Corp.

Stanley, J. (2002). Essentials of Immunology and Serology. Albany, NY: Thomson Delmar Learning.

Stewart, M., Bonne, N., Shearer, P., Khalesi, B., Sharp, M. & Raidal, S. (2007). Baculovirus expression of *beak and feather disease virus* (*BFDV*) capsid protein capable of self assembly and haemagglutination. *J Virol Methods* **141**, 181-187.

Studdert, M. J. (1993). *Circoviridae*: new viruses of pigs, parrots and chickens. *Aust Vet J* **70,** 121-122.

Tamura, K., Nei, M. & Kumar, S. (2004). Prospects for inferring very large phylogenies by using the neighbor-joining method. *Proc Natl Acad Sci USA* **101**, 11030-11035.

Tamura, K., Peterson, D., Peterson, N., Stecher, G., Nei, M. & Kumar, S. (2011). MEGA5: Molecular Evolutionary Genetics Analysis using Maximum Likelihood, Evolutionary Distance, and Maximum Parsimony Methods. *Mol Biol Evol* **28**, 2731-2739.

Thavarajah, R., Mudimbaimannar, V. K., Elizabeth, J., Krishnamohan Rao, U. & Ranganathan, K. (2012). Chemical and physical basics of routine formaldehyde fixation. *J Oral Maxillofac Pathol* **16**, 400-405.

Todd, D., Mawhinney, K., Graham, D. A. & Scott, A. N. J. (1999). Development of a blocking enzyme-linked immunosorbent assay for the serological diagnosis of chicken anaemia virus. *J Virol. Methods* **82**, 177-184.

Todd, D. (2000). Circoviruses: immunosuppressive threats to avian species: a review. *Avian Pathol* **29**, 373-394

Todd, D., Weston, J. H., Soike, D. & Smyth, J. A. (2001). Genome sequence determinations and analyses of novel Circoviruses from Goose and Pigeon. *Virology* **286**, 354-362.

Todd, D., Bendinelli, M., Biagini, P., Hino, S., Mankertz, A., Mishiro, S., Niel, C., Okamoto, H., Raidal, S., Ritchie, B. W. *et al.* (2005). *Circoviridae*.In *Virus taxonomy:*

Eighth report of the international Committee on Taxonomy of Viruses, pp. 327-334. Edited by C. M. Fauquet, M. A. Mayo, J. Maniloff, U. Desselberger & L.A. Ball, San Diego: Elsevier Academic Press.

Tree of Life Web Project. (2008). *Agapornis nigrigenis.* Black-cheeked Lovebird. Retrieved from http://tolweb.org/Agapornis_nigrigenis/91575/2008.11.14.

University of Rochester Proteomics Center. 4/29/09 Silver Staining Gel Protocol Compatible with Mass Spectrometry Analysis. Retrieved from http://www.urmc.rochester.edu/proteomics/documents/SilverStainGelsforMS.pdf.

Van Wyk, P. W. J. & Wingfield, M. J. (1991). Ascospore ultrastructure and development of *Ophiostoma cucullatum*. *Mycologia* **83**, 698-707.

Varsani, A., de Villiers, G. K., Regnard, G. L., Bragg, R. R., Kondiah, K., Hitzeroth, I. I., Rybicki, E. P. (2010). A unique isolate of *beak and feather disease virus* isolated from budgerigars (*Melopsittacus undulatus*) in South Africa. *Arch Virol* **155**, 435-439.

Wissman, M. A. (2006). Avian Plasma Proteins. Retrieved from http://www.exoticpetvet.net/avian/proteins.html

Wylie, S. L. & Pass, D. A. (1987). Experimental reproduction of Psittacine beak and feather disease/French moult. *Avian Pathol* **16**, 269-281.

Yang, S. & Rothman, R. E. (2004). PCR-based diagnostics for infectious diseases: uses, limitations, and future applications in acute-care settings. *Lancet Infect Dis* **4**, 337-348.

Yang, X., Chen, F., Cao, Y., Pang, D., Ouyang, H. & Ren, L. (2012). Complete genome sequence of porcine circovirus 2b strain CC1. *J Virol* 86, 9536.

Yano, J., Rachochy, V. & van Houten, J. L. (2003). Glycosyl phosphatidylinositol-anchored proteins in chemosensory signalling: antisense manipulation of *Paramecium tetraurelia* PIG-A gene expression. *Eukaryot Cell* **2**, 1211-1219.

Ypelaar, I., Bassami, M. R., Wilcox, G. E. & Raidal, S. R. (1999). A universal polymerase chain reaction for the detection of Psittacine beak and feather disease virus. *Vet Microbiol* **68**, 141-148.

Zhang, B., Chen, H., Li, M., Gu, Z., Song, Y., Ratledge, C., Chen, Y. Q., Zhang, H. & Chen, W. (2013). Genetic engineering of *Yarrowia lipolytica* for enhanced production of *trans*-10, *cis*-12 conjugated linoleic acid. *Microb Cell Fact* **70**, 2-8.

APPENDIX A

Table 1. Table indicating sequence names and accession numbers used in real-time primer design in Chapter 3.

	Sequence Name	**GenBank Accession Number**
1.	NC_001944_Beak_and_feather_disease_virus_complete_genome	AF071878
2.	DQ384622_UFS1_rep_protein_gene	DQ384622
3.	DQ384621_UFS2_rep_protein_gene	DQ384621
4.	DQ384623_UFS3_rep_protein_gene	DQ384623
5.	DQ384624_UFS4_rep_protein_gene	DQ384624
6.	DQ384625_UFS5_rep_protein_gene	DQ384625
7.	HM748938_BFDV_ZA_PR_41a_2008_complete_genome	HM748938
8.	HM748936_BFDV_ZA_PR_45A_2008_complete_genome	HM748936
9.	HM748924_BFDV_ZA_Am_83e_2008_complete_genome	HM748924
10.	HM748926_BFDV_ZA_ER_78a_2008_complete_genome	HM748926
11.	HM748928_BFDV_ZA_PK_75A_2008_complete_genome	HM748928
12.	HM748930_BFDV_ZA_PR_61A_2008_complete_genome	HM748930
13.	HM748932_BFDV_ZA_PR_54b_2008_complete_genome	HM748932
14.	HM748934_BFDV_ZA_PR_51A_2008_complete_genome	HM748934
15.	HM748922_BFDV_ZA_PGM_69A_2008_complete_genome	HM748922
16.	HM748923_BFDV_ZA_PGM_68A_2008_complete_genome	HM748923
17.	HM748921:_BFDV_ZA_PGM_70A_2008_complete_genome	HM748921
18.	HM748921:_BFDV_ZA_PGM_70A_2008_complete_genome	HM748921
19.	HM748919_BFDV_ZA_PGM_81A_2008_complete_genome	HM748919
20.	HM748925_BFDV_ZA_Am_83a_2008_complete_genome	HM748925
21.	HM748927_BFDV_ZA_PK_76f_2008_complete_genome	HM748927
22.	HM748929_BFDV_ZA_PK_74d_2008_complete_genome	HM748929
23.	HM748931_BFDV_ZA_PE_55A_2008_complete_genome	HM748931
24.	HM748933_BFDV_ZA_PR_54A_2008_complete_genome	HM748933
25.	HM748935_BFDV_ZA_PR_50A_2008_complete_genome	HM748935
26.	HM748937_BFDV_ZA_PR_42A_2008_complete_genome	HM748937
27.	HM748939_BFDV_ZA_38A_PR_2008_complete_genome	HM748939
28.	HM748918_BFDV_ZA_PR_60A_2008_complete_genome	HM748918
29.	HM748920_BFDV_ZA_PGM_80A_2008_complete_genome	HM748920
30.	GU936296_BFDV_NZ_CN_B127_2008_complete_genome	GU936296

APPENDIX B

Figure 1: Clustal O Multiple sequence alignment of qPCR (BFDV rep F and R) primers (Table 3.1.) with *BFDV* whole genome; Accession number: AF071878.1 (Niagro *et al*., 1998).

```
CLUSTAL O(1.2.1) multiple sequence alignment


BFDV_repR           ------------------------------------------------------------
BFDV_AF071878.1     ttagtattacccgccgcctggggcaccggggcaccgcagctattggctgccttgcggagg
BFDV_repF           ------------------------------------------------------------


BFDV_repR           ------------------------------------------------------------
BFDV_AF071878.1     tgcccgcccctagggaggagtaaatggcgccgttaggcgcccgttaatctccggaggatc
BFDV_repF           ------------------------------------------------------------


BFDV_repR           ------------------------------------------------------------
BFDV_AF071878.1     acactcgtccgggaaccatcccgtccaaggagggctctggctgtcgccgttggtgtttca
BFDV_repF           ------------------------------------------------------------


BFDV_repR           ------------------------------------------------------------
BFDV_AF071878.1     ctcttaacaaccctacagacggcgaaatcgaattcgtccgttctctcgggcctgacgaat
BFDV_repF           ------------------------------------------------------------


BFDV_repR           ------------------------------------------------------------
BFDV_AF071878.1     tctactatgccatcgttggacgggaaaagggtgagcaaggcactccccatttgcaaggct
BFDV_repF           ------------------------------------------------------------


BFDV_repR           ------------------------------------------------------------
BFDV_AF071878.1     actttcattttaaaaataagaagcgactgagcgcgcttaagaaaatgctgccgcgaggtc
BFDV_repF           ------------------------------------------------------------


BFDV_repR           ------------------------------------------------------------
BFDV_AF071878.1     attttgagcgcgctaaagggagcgacgcggataacgagaagtattgcagtaaagaggggg
BFDV_repF           ------------------------------------------------------------


BFDV_repR           ------------------------------------------------------------
BFDV_AF071878.1     acgtcatacttaccctgggcattgtggcgagagacggtcaccgcgctttcgatggagctg
BFDV_repF           ------------------------------------------------------------


BFDV_repR           ------------------------------------------------------------
BFDV_AF071878.1     ttgctgccgtgatgtccggacccaaaatgaaggaagtcgcgcgagagttcccagatatct
BFDV_repF           ------------------------------------------------------------
```

```
BFDV_repR           ------------------------------------------------------------
BFDV_AF071878.1     acgtcaggcatgggcggggcttgcatagcctctcgctattggttggttcccgcccgcgtg
BFDV_repF           ------------------------------TGTCGCTATTGGTCGGTTC-----------

BFDV_repR           ------------------------------------------------------------
BFDV_AF071878.1     attttaagactgaggttgacgtcatttacgggccaccggggtgtggcaagagtcgatggg
BFDV_repF           ------------------------------------------------------------

BFDV_repR           ------------------------------------------------------------
BFDV_AF071878.1     ccaatgagcagcctgggaccaaatattataaaatgcgcggtgaatggtgggatggatatg
BFDV_repF           ------------------------------------------------------------

BFDV_repR           ------------------------------------------TATTTAGTTCCGGGCTGC
BFDV_AF071878.1     atggggaagatgtcgtcatcttggacgacttttatgggtggctaccttattgcgagatgc
BFDV_repF           ------------------------------------------------------------

BFDV_repR           TC----------------------------------------------------------
BFDV_AF071878.1     tccgcctctgcgaccgttacccacataaagtgccagttaagggcgcttttgtggagttta
BFDV_repF           ------------------------------------------------------------

BFDV_repR           ------------------------------------------------------------
BFDV_AF071878.1     cgagcaagaggatcattatcacgagcaataaggccccggagacctggtacaaggaggact
BFDV_repF           ------------------------------------------------------------

BFDV_repR           ------------------------------------------------------------
BFDV_AF071878.1     gtgacccgaagccactgttccggagattcactcgtgtttggtggtacaacattgacaagt
BFDV_repF           ------------------------------------------------------------

BFDV_repR           ------------------------------------------------------------
BFDV_AF071878.1     tggaacaagtccggcctgatttcctcgcccaccccatcaatttttgatagtctcggtgat
BFDV_repF           ------------------------------------------------------------

BFDV_repR           ------------------------------------------------------------
BFDV_AF071878.1     gtttaataaagttaggcgtcgggccgaaggcccgatgccgcaggggggggacccccctgccg
BFDV_repF           ------------------------------------------------------------

BFDV_repR           ------------------------------------------------------------
BFDV_AF071878.1     gagggttcgcagggccgtcaggcccgagaacccgaccagcccggagggcctagtctgtat
BFDV_repF           ------------------------------------------------------------

BFDV_repR           ------------------------------------------------------------
BFDV_AF071878.1     cgggggggggcccccgggggggtccccccgacacgacgaacacggtagcgacgaaggcgcc
BFDV_repF           ------------------------------------------------------------

BFDV_repR           ------------------------------------------------------------
BFDV_AF071878.1     aataaacactcaaaaaggtatttgctgcttgagtctttattaagtactgggattgttagg
BFDV_repF           ------------------------------------------------------------

BFDV_repR           ------------------------------------------------------------
BFDV_AF071878.1     ggcaaactgacggaattgaacatatatagtgagcttggttacataagtgatcgtttgttc
BFDV_repF           ------------------------------------------------------------

BFDV_repR           ------------------------------------------------------------
BFDV_AF071878.1     tggctgagggaagctgaagccaatgccgtagtgcctgactttcgctcctgctgcgttggg
BFDV_repF           ------------------------------------------------------------
```

```
BFDV_repR           ------------------------------------------------------------
BFDV_AF071878.1     tcctccttgtagtgggatccagccggttctggcgctgtttagccacaatgctgcagactg
BFDV_repF           ------------------------------------------------------------

BFDV_repR           ------------------------------------------------------------
BFDV_AF071878.1     gttcgctgtggtgaggtcgtttatcgttatttgtggttttggtctgaggagacgtttgaa
BFDV_repF           ------------------------------------------------------------

BFDV_repR           ------------------------------------------------------------
BFDV_AF071878.1     tcccctgctaacataccattttctggcaccgtcgaaaggtgccagtgggtcttgtgtttg
BFDV_repF           ------------------------------------------------------------

BFDV_repR           ------------------------------------------------------------
BFDV_AF071878.1     gtctgcaacagttttaaatttacttatcctggagtcttggattacggccgtgtggccgaa
BFDV_repF           ------------------------------------------------------------

BFDV_repR           ------------------------------------------------------------
BFDV_AF071878.1     tccgtctccttgtatggtgtagtgtccccatgtgggcctcatttccattttagctaactt
BFDV_repF           ------------------------------------------------------------

BFDV_repR           ------------------------------------------------------------
BFDV_AF071878.1     aatccggtagttttcgaaattcagtgtttgtgggtttggtgtgtttgttatgaagtctga
BFDV_repF           ------------------------------------------------------------

BFDV_repR           ------------------------------------------------------------
BFDV_AF071878.1     caatgcaaaggttacaaagtcggagctaaaaattaggttgccagtactggtggtttgttt
BFDV_repF           ------------------------------------------------------------

BFDV_repR           ------------------------------------------------------------
BFDV_AF071878.1     ttgaatttggaatttgaattggcgtgtgagtctgagagtgtaaaccctattggttgagaa
BFDV_repF           ------------------------------------------------------------

BFDV_repR           ------------------------------------------------------------
BFDV_AF071878.1     acggcgtctgcggaagtgtctacgtcgccggcggtatcgcctgatgtgacgtctgcggta
BFDV_repF           ------------------------------------------------------------

BFDV_repR           ------------------------------------------------------------
BFDV_AF071878.1     gtatgggcgggcataccgtcgtctaacctgaaatatagcgcatgcgtagttagaggtgcc
BFDV_repF           ------------------------------------------------------------

BFDV_repR           -------------
BFDV_AF071878.1     ccataggcggcgg
BFDV_repF           -------------

BFDV_repR           ------------------------------------------------------------
BFDV_AF071878.1     aataaacactcaaaaaggtatttgctgcttgagtctttattaagtactgggattgttagg
BFDV_repF           ------------------------------------------------------------

BFDV_repR           ------------------------------------------------------------
BFDV_AF071878.1     ggcaaactgacggaattgaacatatatagtgagcttggttacataagtgatcgtttgttc
BFDV_repF           ------------------------------------------------------------

BFDV_repR           ------------------------------------------------------------
BFDV_AF071878.1     tggctgagggaagctgaagccaatgccgtagtgcctgactttcgctcctgctgcgttggg
BFDV_repF           ------------------------------------------------------------
```

Figure 2: Graphic representation of position of BFDV rep F primer binding in *BFDV* genome.

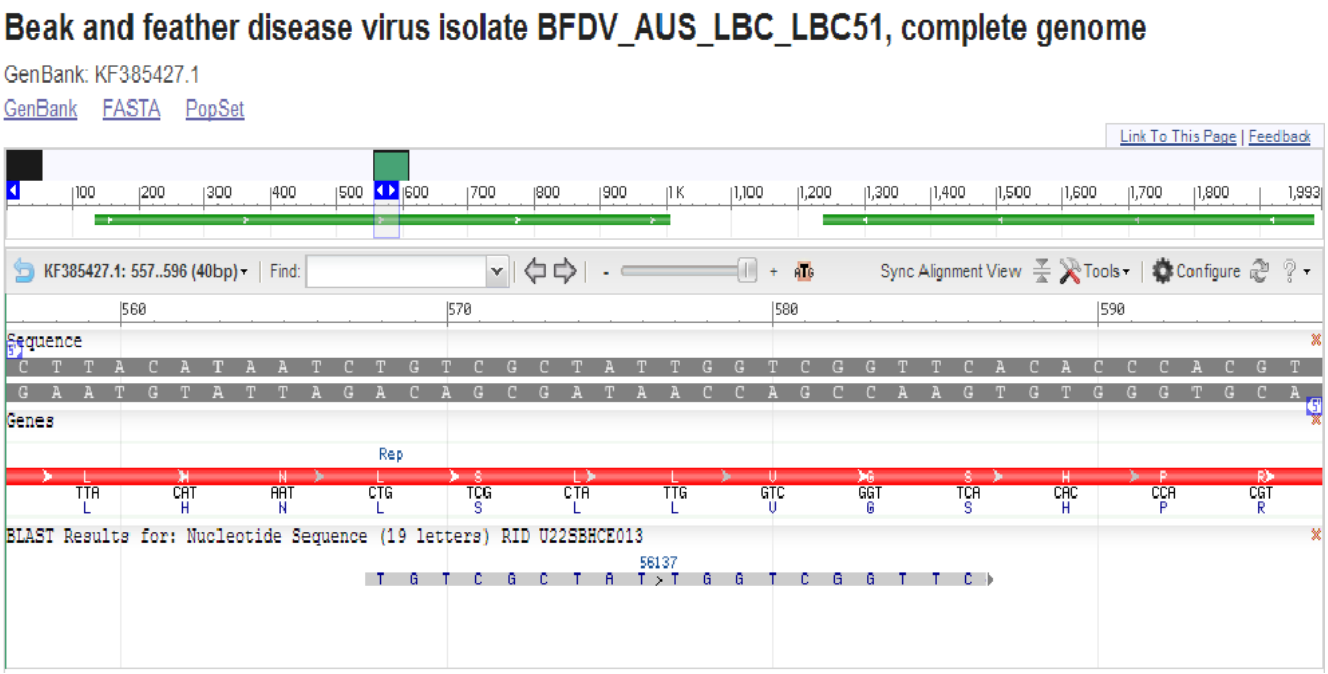

Figure 3: Graphic representation of position of BFDV rep R primer binding in *BFDV* genome.

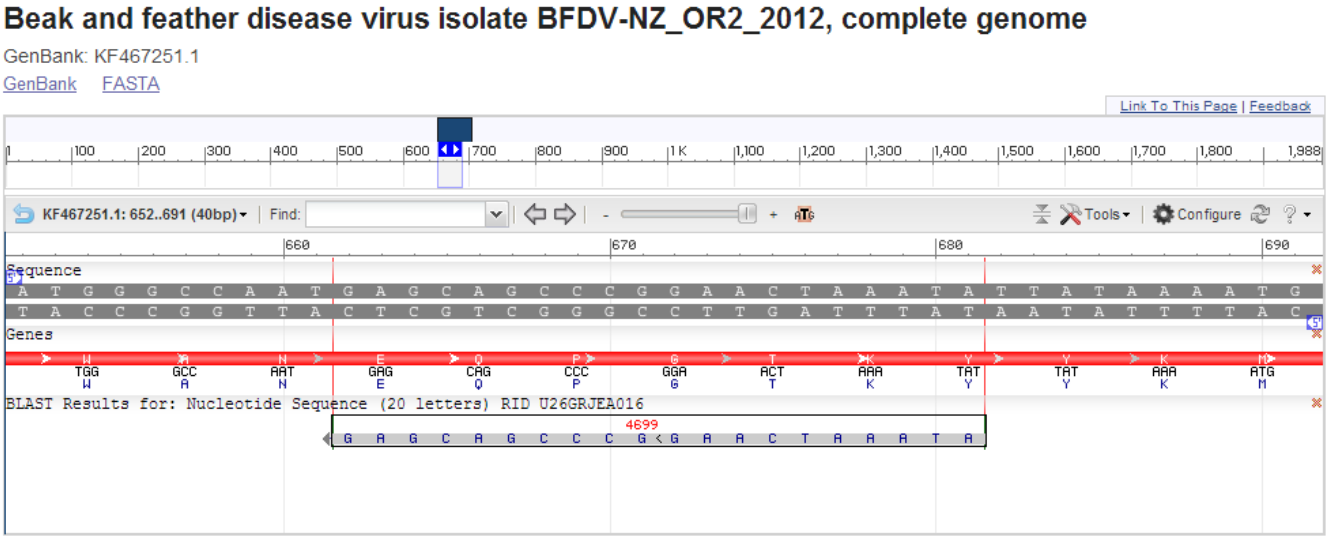

APPENDIX C

Figure 4: BLAST results showing specificity of BFDV rep F primer.

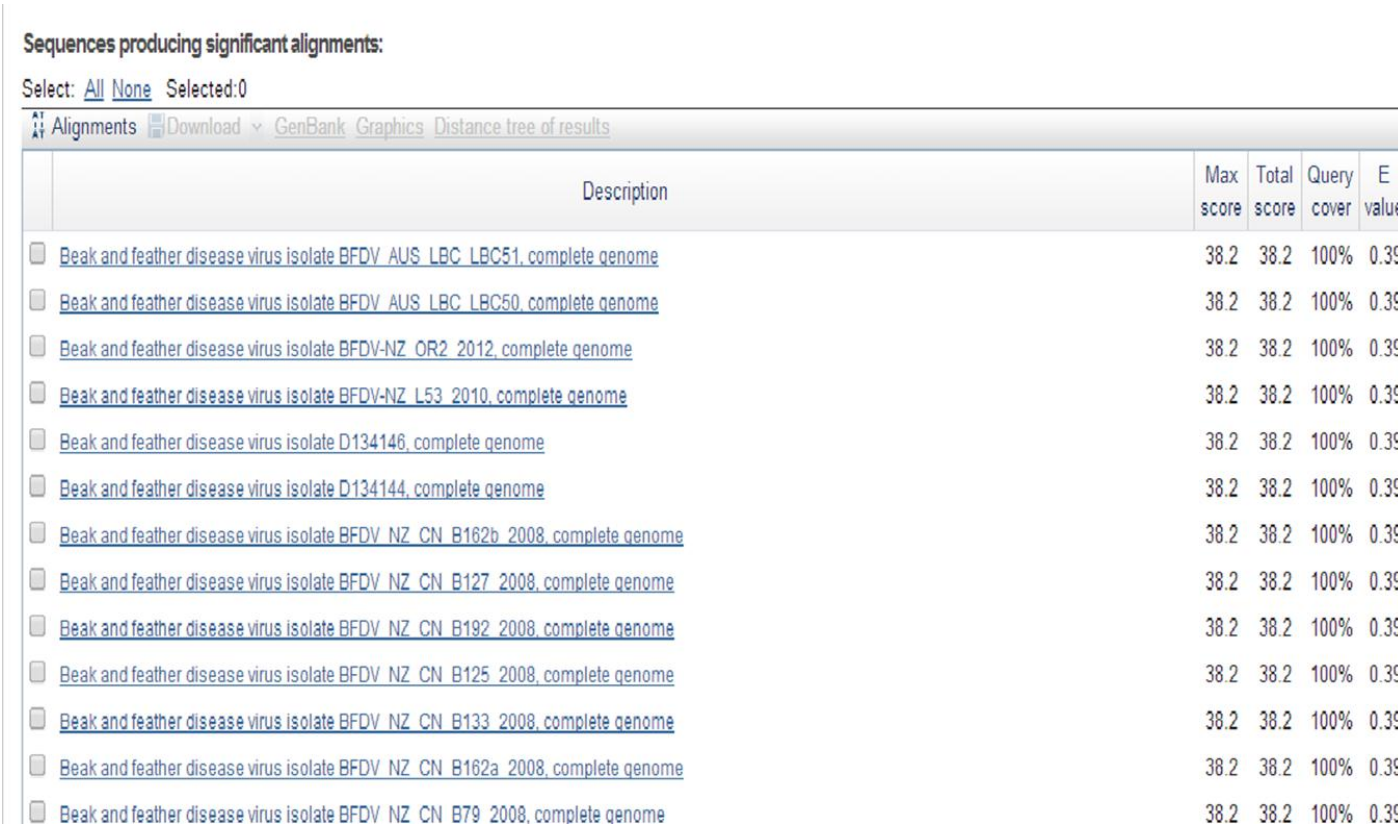

Sequences producing significant alignments:

Select: All None Selected:0

Alignments Download GenBank Graphics Distance tree of results

Description	Max score	Total score	Query cover	E value
Beak and feather disease virus isolate BFDV_AUS_LBC_LBC51, complete genome	38.2	38.2	100%	0.3
Beak and feather disease virus isolate BFDV_AUS_LBC_LBC50, complete genome	38.2	38.2	100%	0.3
Beak and feather disease virus isolate BFDV-NZ_OR2_2012, complete genome	38.2	38.2	100%	0.3
Beak and feather disease virus isolate BFDV-NZ_L53_2010, complete genome	38.2	38.2	100%	0.3
Beak and feather disease virus isolate D134146, complete genome	38.2	38.2	100%	0.3
Beak and feather disease virus isolate D134144, complete genome	38.2	38.2	100%	0.3
Beak and feather disease virus isolate BFDV_NZ_CN_B162b_2008, complete genome	38.2	38.2	100%	0.3
Beak and feather disease virus isolate BFDV_NZ_CN_B127_2008, complete genome	38.2	38.2	100%	0.3
Beak and feather disease virus isolate BFDV_NZ_CN_B192_2008, complete genome	38.2	38.2	100%	0.3
Beak and feather disease virus isolate BFDV_NZ_CN_B125_2008, complete genome	38.2	38.2	100%	0.3
Beak and feather disease virus isolate BFDV_NZ_CN_B133_2008, complete genome	38.2	38.2	100%	0.3
Beak and feather disease virus isolate BFDV_NZ_CN_B162a_2008, complete genome	38.2	38.2	100%	0.3
Beak and feather disease virus isolate BFDV_NZ_CN_B79_2008, complete genome	38.2	38.2	100%	0.3

Figure 5: BLAST results showing specificity of BFDV rep R primer.

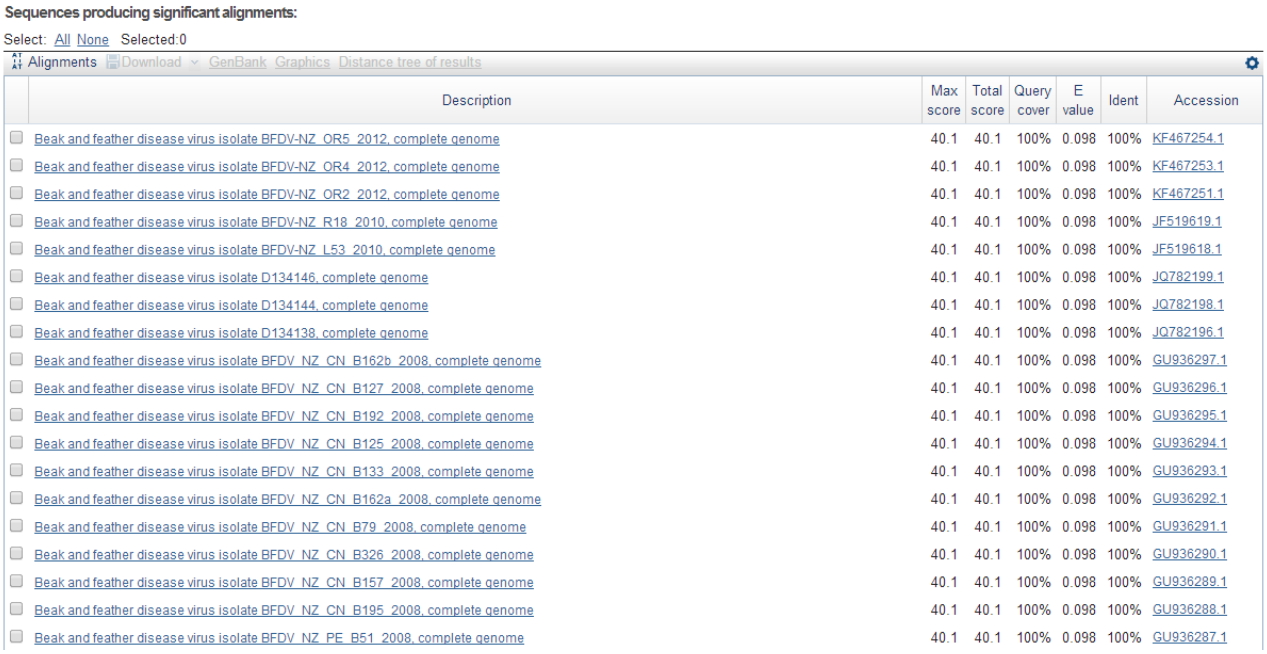

Sequences producing significant alignments:

Select: All None Selected:0

Alignments Download GenBank Graphics Distance tree of results

Description	Max score	Total score	Query cover	E value	Ident	Accession
Beak and feather disease virus isolate BFDV-NZ_OR5_2012, complete genome	40.1	40.1	100%	0.098	100%	KF467254.1
Beak and feather disease virus isolate BFDV-NZ_OR4_2012, complete genome	40.1	40.1	100%	0.098	100%	KF467253.1
Beak and feather disease virus isolate BFDV-NZ_OR2_2012, complete genome	40.1	40.1	100%	0.098	100%	KF467251.1
Beak and feather disease virus isolate BFDV-NZ_R18_2010, complete genome	40.1	40.1	100%	0.098	100%	JF519619.1
Beak and feather disease virus isolate BFDV-NZ_L53_2010, complete genome	40.1	40.1	100%	0.098	100%	JF519618.1
Beak and feather disease virus isolate D134146, complete genome	40.1	40.1	100%	0.098	100%	JQ782199.1
Beak and feather disease virus isolate D134144, complete genome	40.1	40.1	100%	0.098	100%	JQ782198.1
Beak and feather disease virus isolate D134138, complete genome	40.1	40.1	100%	0.098	100%	JQ782196.1
Beak and feather disease virus isolate BFDV_NZ_CN_B162b_2008, complete genome	40.1	40.1	100%	0.098	100%	GU936297.1
Beak and feather disease virus isolate BFDV_NZ_CN_B127_2008, complete genome	40.1	40.1	100%	0.098	100%	GU936296.1
Beak and feather disease virus isolate BFDV_NZ_CN_B192_2008, complete genome	40.1	40.1	100%	0.098	100%	GU936295.1
Beak and feather disease virus isolate BFDV_NZ_CN_B125_2008, complete genome	40.1	40.1	100%	0.098	100%	GU936294.1
Beak and feather disease virus isolate BFDV_NZ_CN_B133_2008, complete genome	40.1	40.1	100%	0.098	100%	GU936293.1
Beak and feather disease virus isolate BFDV_NZ_CN_B162a_2008, complete genome	40.1	40.1	100%	0.098	100%	GU936292.1
Beak and feather disease virus isolate BFDV_NZ_CN_B79_2008, complete genome	40.1	40.1	100%	0.098	100%	GU936291.1
Beak and feather disease virus isolate BFDV_NZ_CN_B326_2008, complete genome	40.1	40.1	100%	0.098	100%	GU936290.1
Beak and feather disease virus isolate BFDV_NZ_CN_B157_2008, complete genome	40.1	40.1	100%	0.098	100%	GU936289.1
Beak and feather disease virus isolate BFDV_NZ_CN_B195_2008, complete genome	40.1	40.1	100%	0.098	100%	GU936288.1
Beak and feather disease virus isolate BFDV_NZ_PE_B51_2008, complete genome	40.1	40.1	100%	0.098	100%	GU936287.1

APPENDIX D

Table 2. Full table indicating the PCR results, species and location (if known) of parrots tested by conventional PCR in Chapter 3.

Sample identity	PCR results	Species	Location
001/12	+		Wolmaranstad
002/12	+		Wolmaranstad
003/12	+		Wolmaranstad
004/12	+		Wolmaranstad
005/12	-		Wolmaranstad
006/12	+		Wolmaranstad
007/12	+		Wolmaranstad
008/12	+		Wolmaranstad
009/12	+		Wolmaranstad
010/12	-		Wolmaranstad
011/12	+		Wolmaranstad
012/12	+		Wolmaranstad
013/12	-		Wolmaranstad
014/12	+		Wolmaranstad
015/12	+		Wolmaranstad
016/12	+		Wolmaranstad
017/12	+		Wolmaranstad
018/12	+		Wolmaranstad
019/12	+		Wolmaranstad
020/12	+		Wolmaranstad

021/12	+	Wolmaranstad
	+	Wolmaranstad
022/12	+	Wolmaranstad
023/12	+	Wolmaranstad
024/12	+	Wolmaranstad
025/12	+	Wolmaranstad
026/12	-	Wolmaranstad
027/12	+	Wolmaranstad
028/12	+	Wolmaranstad
029/12	+	Wolmaranstad
030/12	+	Wolmaranstad
031/12	+	Wolmaranstad
032/12	+	Wolmaranstad
033/12	-	Wolmaranstad
034/12	-	Wolmaranstad
035/12	-	Wolmaranstad
036/12	-	Wolmaranstad
037/12	-	Wolmaranstad
038/12	+	Wolmaranstad
039/12	+	Wolmaranstad
040/12	+	Wolmaranstad
041/12	+	Wolmaranstad
042/12	+	Wolmaranstad
043/12	+	Wolmaranstad
044/12	-	Wolmaranstad
045/12	+	Wolmaranstad
046/12	+	Wolmaranstad
047/12	+	Wolmaranstad

048/12	+	Wolmaranstad
049/12	+	Wolmaranstad
050/12	+	Wolmaranstad
051/12	+	Wolmaranstad
052/12	-	Wolmaranstad
053/12	-	Wolmaranstad
054/12	+	Wolmaranstad
055/12	-	Wolmaranstad
056/12	+	Wolmaranstad
057/12	+	Wolmaranstad
058/12	+	Wolmaranstad
059/12	+	Wolmaranstad
060/12	+	Wolmaranstad
061/12	+	Wolmaranstad
062/12	+	Wolmaranstad
063/12	+	Wolmaranstad
064/12	-	Wolmaranstad
065/12	-	Wolmaranstad
066/12	-	Wolmaranstad
067/12	-	Wolmaranstad
068/12	-	Wolmaranstad
069/12	-	Wolmaranstad
070/12	-	Wolmaranstad
071/12	-	Wolmaranstad
072/12	-	Wolmaranstad
073/12	-	Wolmaranstad
074/12	-	Wolmaranstad
075/12	-	Wolmaranstad

076/12	-		Wolmaranstad
077/12	-		Wolmaranstad
078/12	-		Wolmaranstad
079/12	-		Wolmaranstad
080/12	+		
081/12	+		
082/12	+		
083/12	+		
084/12	+		
085/12	+		
086/12	+		
087/12	+		
088/12	+		
089/12	+		
090/12	+		Kimberley
091/12	+		Worcester
092/12	+		Worcester
093/12	+	Indian ringneck	Worcester
094/12	+		Worcester
095/12	+	Alexandrine Parakeet	Worcester
096/12	+	Alexandrine Parakeet	Worcester
097/12	+	Indian Ringneck	Bloemfontein
098/12	+	Cape Parrot	Bloemfontein (Birds are from all over SA)
099/12	+		Bloemfontein (Birds are from all over SA)
100/12	+	Cape Parrot	Bloemfontein (Birds are from all

		over SA)
101/12	+	Bloemfontein (Birds are from all over SA)
104/12	+	Bloemfontein (Birds are from all over SA)
105/12	+	Bloemfontein (Birds are from all over SA)
106/12	+	Bloemfontein (Birds are from all over SA)
107/12	+	Bloemfontein (Birds are from all over SA)
108/12	+	Bloemfontein (Birds are from all over SA)
109/12	+	Bloemfontein (Birds are from all over SA)

APPENDIX E

3. Raw data from real-time PCR was exported to draw a standard curve in Microsoft Excel, to determine the standard curve equation.

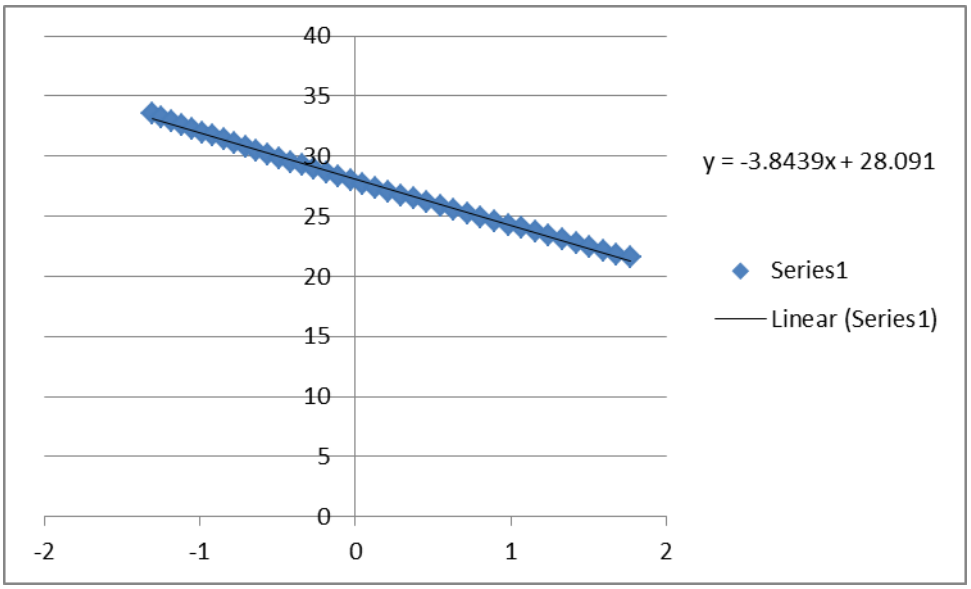

$$DNA\ amount\,(\mathrm{g}) = 10^{(\mathrm{Cp}\,-\,\text{Y-intercept})/\text{slope}}$$

Equation 1:

$$DNA\ (copy\ number) = \frac{6.02\times10^{23}\,(\mathrm{copy/mol}) \times \text{DNA amount (g)}}{\text{Length (bp)} \times 660\ (\mathrm{g/mol/bp})}$$

Equation 2:

Table 4. Calculation of copy number of DNA standards used in real-time PCR viral quantification

Sample Identity	**A**	**B**	**C**	**D**	**E**
	Mean C_p of standard samples	**(C_p – Y-intercept)/ slope** **(Column A – 28.091)/-3.8439**	**DNA amount** **$10^{\text{Column B}}$**	**6.02×10^{23} × Column C**	**Column D / (length x 660)** **= Column D/ 75900**
1, 7, 13	21.85	1.623	41.975	2.53×10^{25}	3.33×10^{20} copies
2, 8, 14	25.43	0.6922	4.922	2.96×10^{24}	3.89×10^{19} copies
3, 9, 15	29.12	-0.267	0.541	3.25×10^{23}	4.28×10^{18} copies
4, 10, 16	33.37	-1.37	0.0427	2.57×10^{22}	3.38×10^{17} copies

Table 5. Calculation of copy number used in real-time PCR viral quantification

Sample Identity	**A**	**B**	**C**	**D**	**E**
	C_p	**(C_p – Y-intercept)/ slope** **(Column A – 28.091)/-3.8439**	**DNA amount** **$10^{\text{Column B}}$**	**6.02×10^{23} × Column C**	**Column D / (length x 660)** **= Column D/ 75900**
090/12	22.26	1.517	32.88	1.98×10^{25}	2.609×10^{20} copies
097/13	26.93	0.302	2.00	1.201×10^{24}	1.59×10^{19} copies
212/12	23.89	1.09	12.385	7.456×10^{24}	9.823×10^{19}
213/12	23.01	1.32	20.98	1.263×10^{25}	1.66×10^{20}
051/13	25.63	0.64	4.36	2.63×10^{24}	3.46×10^{19}
052/13	25.93	-0.56	0.27	1.65×10^{23}	2.17×10^{18}
127/13	24.20	1.01	10.286	6.19×10^{24}	8.16×10^{19}
128/13	24.90	0.83	6.76	4.07×10^{24}	5.36×10^{19}
131/13	24.11	1.04	10.86	6.54×10^{24}	8.61×10^{19}